NATIONAL COOPERATIVE HIGHWAY RESEARCH PROGRAM

NCHRP Report 384

Plasma Arc Cutting of Bridge Steels

Transportation Research Board
National Research Council

NATIONAL COOPERATIVE HIGHWAY RESEARCH PROGRAM

Report 384

Plasma Arc Cutting of Bridge Steels

IAN D. HARRIS
Edison Welding Institute
Columbus, OH

Subject Areas

Bridges, Other Structures, and Hydraulics and Hydrology

Research Sponsored by the American Association of State Highway and Transportation Officials in Cooperation with the Federal Highway Administration

TRANSPORTATION RESEARCH BOARD
NATIONAL RESEARCH COUNCIL

NATIONAL ACADEMY PRESS
Washington, D.C. 1997

NATIONAL COOPERATIVE HIGHWAY RESEARCH PROGRAM

Systematic, well-designed research provides the most effective approach to the solution of many problems facing highway administrators and engineers. Often, highway problems are of local interest and can best be studied by highway departments individually or in cooperation with their state universities and others. However, the accelerating growth of highway transportation develops increasingly complex problems of wide interest to highway authorities. These problems are best studied through a coordinated program of cooperative research.

In recognition of these needs, the highway administrators of the American Association of State Highway and Transportation Officials initiated in 1962 an objective national highway research program employing modern scientific techniques. This program is supported on a continuing basis by funds from participating member states of the Association and it receives the full cooperation and support of the Federal Highway Administration, United States Department of Transportation.

The Transportation Research Board of the National Research Council was requested by the Association to administer the research program because of the Board's recognized objectivity and understanding of modern research practices. The Board is uniquely suited for this purpose as it maintains an extensive committee structure from which authorities on any highway transportation subject may be drawn; it possesses avenues of communications and cooperation with federal, state and local governmental agencies, universities, and industry; its relationship to the National Research Council is an insurance of objectivity; it maintains a full-time research correlation staff of specialists in highway transportation matters to bring the findings of research directly to those who are in a position to use them.

The program is developed on the basis of research needs identified by chief administrators of the highway and transportation departments and by committees of AASHTO. Each year, specific areas of research needs to be included in the program are proposed to the National Research Council and the Board by the American Association of State Highway and Transportation Officials. Research projects to fulfill these needs are defined by the Board, and qualified research agencies are selected from those that have submitted proposals. Administration and surveillance of research contracts are the responsibilities of the National Research Council and the Transportation Research Board.

The needs for highway research are many, and the National Cooperative Highway Research Program can make significant contributions to the solution of highway transportation problems of mutual concern to many responsible groups. The program, however, is intended to complement rather than to substitute for or duplicate other highway research programs.

Note: The Transportation Research Board, the National Research Council, the Federal Highway Administration, the American Association of State Highway and Transportation Officials, and the individual states participating in the National Cooperative Highway Research Program do not endorse products or manufacturers. Trade or manufacturers' names appear herein solely because they are considered essential to the object of this report.

NCHRP REPORT 384

Project D10-40 FY'93

ISSN 0077-5614

ISBN 0-309-06052-4

L. C. Catalog Card No. 96-61802

Price $27.00

NOTICE

The project that is the subject of this report was a part of the National Cooperative Highway Research Program conducted by the Transportation Research Board with the approval of the Governing Board of the National Research Council. Such approval reflects the Governing Board's judgment that the program concerned is of national importance and appropriate with respect to both the purposes and resources of the National Research Council.

The members of the technical committee selected to monitor this project and to review this report were chosen for recognized scholarly competence and with due consideration for the balance of disciplines appropriate to the project. The opinions and conclusions expressed or implied are those of the research agency that performed the research, and, while they have been accepted as appropriate by the technical committee, they are not necessarily those of the Transportation Research Board, the National Research Council, the American Association of State Highway and Transportation Officials, or the Federal Highway Administration, U.S. Department of Transportation.

Each report is reviewed and accepted for publication by the technical committee according to procedures established and monitored by the Transportation Research Board Executive Committee and the Governing Board of the National Research Council.

Published reports of the

NATIONAL COOPERATIVE HIGHWAY RESEARCH PROGRAM

are available from:

Transportation Research Board
National Research Council
2101 Constitution Avenue, N.W.
Washington, D.C. 20418

Printed in the United States of America

FOREWORD

By Staff
Transportation Research Board

This report contains the findings of a study that was performed to provide guidance for the use of the plasma arc cutting process for steel bridge fabrication. The report provides a comprehensive description of the research including a User's Guide to help bridge engineers, fabricators, and inspectors ensure proper use of the process. The contents of this report will be of immediate interest to bridge engineers, researchers, and others concerned with design, construction, and rehabilitation of steel bridge structures.

The plasma arc cutting process for steel plates can offer substantial advantages in terms of speed and economy when compared with the traditional oxyfuel cutting process for plates that are 25-mm (1-in.) or less in thickness. However, current standards do not offer sufficient guidance for engineers, fabricators, and inspectors on the use of plasma arc cutting process and related issues.

Under NCHRP Project 10-40, "Plasma Arc Cutting of Bridge Steels," Edison Welding Institute was assigned the tasks of evaluating the effectiveness of plasma arc cutting for bridge fabrication and recommending guidelines for its use. To accomplish these objectives, the researchers reviewed relevant domestic and foreign literature and performed laboratory tests to evaluate the effects of this steel cutting process on the performance of cut and welded steels. The report documents the work performed under project 10-40 and discusses the primary parameters of the plasma arc cutting process and their effects on the performance of cut steel.

The recommended User's Guide, included in this report, contains information on the types of plasma arc cutting systems, equipment operation, typical cutting speeds, factors effecting edge quality, and causes and remedies of cutting problems. The User's Guide includes specific recommendations for the use of the plasma arc cutting process.

CONTENTS

ACKNOWLEDGMENTS

The work reported herein was performed under NCHRP Project 10-40 by the Edison Welding Institute (EWI). EWI was the main contractor for this study.

Ian D. Harris, Senior Research Engineer, Arc Welding and Automation Section, Technical Division, was the principal investigator. The portion of the work concerning the mechanical testing was conducted under the supervision of Fabian Orth, Senior Research Engineer, Structural Integrity Section, Technical Division. The work was done under the general supervision of Ian D. Harris.

PLASMA ARC CUTTING OF BRIDGE STEELS

SUMMARY

This work was conducted to determine the effectiveness of plasma arc cutting for bridge fabrication. The study involved development of plasma cutting procedures, characterization of the cut edges, welding trials on as-cut edges, determination of the tensile and impact properties of welded plasma-cut edges, and fatigue properties of welded and as-cut edges. The overall conclusion to this study is that plasma cutting should be applied to bridge fabrication as an effective thermal cutting tool to increase overall productivity. The User's Guide, Appendix A, describes the recommended practices for plasma arc cutting.

A comprehensive review of current practice and research findings in the literature has been undertaken to establish the state of the art in plasma arc cutting in the bridge industry. Information has also been gathered in areas such as shipbuilding and general fabrication where it relates to plasma arc cutting of plate. The information gathered from the literature search and unpublished experiences of engineers, fabricators, and plasma arc cutting equipment manufacturers was evaluated and summarized to determine current practice and the state of knowledge.

The plasma arc cutting process is not widely used in the bridge fabrication industry, with barely a dozen companies identified from the survey of fabricators and state departments of transportation (DOTs) as using the process in this country. Internationally, use of plasma cutting in the bridge industry is not much higher, although its use in shipbuilding is. This factor is largely related to the range of thickness in shipbuilding material, which is lower than that for bridge construction. In the bridge industry, a lot of work is carried out for coping I-beams and stripping plate with multiple oxyfuel torches, and where triple bevelling heads are used for edge bevelling for weld preparations, use of three plasma torches would be cost prohibitive. In practice, much plate stripping is carried out with only two oxyfuel torches, and cutting speed could be considerably increased by using one or two plasma cutting torches. Use of plasma cutting for webs, stiffeners, and gusset plates in the thickness range of 6 mm to 19 mm ($^1/_4$ to $^3/_4$ in.) can make significant improvements in productivity with good cut edge quality. In many cases, the absence of guidelines for plasma cutting in the Bridge Welding Code prohibits or severely limits its application.

The conditions and parameters affecting the performance of free edges and edges affected by welding were identified. The primary parameters of the plasma arc cutting process are arc current, cutting speed, and the plasma gas employed. The current voltage and cutting speed determine the heat input of the cutting process and the edge quality with respect to the combination of cutting speed and material thickness. The plasma cutting gas has significant impact on the composition of the cut edge in terms of nitrogen pick-up and potential for porosity in subsequent welds. Review of the literature revealed that the resid-

ual stress in a plasma-cut edge was found to be compressive in many cases and reduction in fatigue life was experienced if the edge was ground. The presence or absence of cutting defects controls the performance of free edges, particularly in fatigue. Residual stress, surface roughness, and hardness play a lesser role. The primary parameters affecting welded edges are presence of any welding defects, the composition and microstructure of the plasma-cut edge and the heat input of the welding process.

A User's Guide, containing basic information on the types of plasma cutting systems, equipment operation, typical cutting speeds, factors affecting edge quality, and causes and remedies of cutting problems, was drafted. Data from the experimental program and comments from state DOT personnel, U.S. Department of Transportation personnel, a consultant in the bridge industry, and fabricators using the plasma arc cutting process were incorporated into the final User's Guide.

A number of individual conclusions resulting from this study are described below. The dross-free range of cutting speeds is much wider for cutting with oxygen and air than that of nitrogen plasma cutting. Cutting under water reduces the range of dross-free cutting speeds compared with cutting in air. The range of dross-free cutting conditions is important as it directly affects the tolerance of the cutting process. In economic terms, dross-free cuts require no further preparation, while removal of dross is labor-intensive and therefore expensive. Oxygen plasma cutting produces a heavily oxidized, easily removable dross, similar to that for oxyfuel cutting. Nitrogen plasma cutting and, to a substantial extent, air plasma cutting rely almost completely on melting, and so any dross is mostly resolidified metal. If the dross is adherent, it has to be removed by grinding. Cutting underwater can be carried out at the same speed using 260 A with oxygen plasma or 400 A with nitrogen plasma. Considerable power savings can be made using oxygen when cutting under water. Cutting with nitrogen and air plasma causes nitriding of the plasma-cut edge. This causes edge hardening, and can result in rejectable porosity when welding over edges cut with nitrogen in air (rather than under water). Oxygen plasma cutting does not cause nitriding, and thus the weldability of the edge is better.

Flux-cored arc welding (FCAW) and submerged arc welding (SAW) can be successfully carried out to radiographic quality standards on as-cut edges of all plasma cutting variants (except nitrogen cutting in air). The cross-weld tensile properties of weldments produced by FCAW and SAW processes meet or exceed those of the parent material specifications. The Charpy impact toughness of weldments produced by FCAW and SAW on plasma-cut edges meets or exceeds the properties of the base material for all plasma cutting techniques. The fatigue properties of unrounded as-cut plasma-cut edges exceeded those of oxyfuel-cut specimens, which had been edge rounded. Testing of primed plate using ASTM salt fog and cross-cut adhesion testing showed no significant difference in performance between edges rounded to Bridge Welding Code specifications and unrounded edges.

CHAPTER 1

INTRODUCTION AND RESEARCH APPROACH

RESEARCH PROBLEM STATEMENT

The use of plasma arc cutting for steel plates can offer substantial advantages in terms of cutting speed and cost when compared with oxyfuel cutting on plate thicknesses below 25 mm (1 in.). However, existing standards do not offer sufficient guidance to engineers, fabricators, and inspectors on plasma arc cutting or on the need for edge treatment. Therefore, there is a reluctance to use plasma arc cutting during fabrication of steel bridges.

Some of the concerns regarding the use of plasma arc cutting techniques and procedures are (1) the effects of process variables such as speed, current and voltage, gases, pre- and postheat, and water quenching; (2) the effects of material variables such as steel grade and surface condition; (3) the characteristics of the free edge including hardness, toughness, fatigue resistance, edge profile, and paint adhesion; (4) the characteristics of edges affected by welding, including porosity and heat-affected zone (HAZ), and fusion boundary properties; and (5) the need for or extent of edge treatment.

Research was needed to assess the characteristics and performance of plasma-cut edges and to develop specifications and guidelines that encourage the use of this process in steel bridge fabrication.

RESEARCH OBJECTIVES AND SCOPE

The main objective of the research was to develop a User's Guide and recommended specifications for plasma arc cutting of bridge steels. Recommendations are based on test results of representative grades of AASHTO M270 (ASTM A709) steels in the thickness range of 9.5 mm to 19 mm ($^3/_8$ to $^3/_4$ in.). The User's Guide and recommended specifications address the performance of both free edges and edges affected by welding. The research included the following tasks:

Task 1: Review relevant current domestic and foreign practice, performance data and research findings. This information will be assembled from both technical literature and unpublished experiences of engineers, fabricators and bridge owners, as well as plasma arc and flame cutting equipment manufacturers and suppliers.

Task 2: Evaluate and summarize the information generated in Task 1 in order to determine current practice and the state of knowledge. Identify all conditions and parameters that may affect the performance of free edges and edges affected by welding. Identify and rank those areas where research is required to assess existing plasma arc cutting procedures and develop rational specifications.

Task 3: Propose preliminary test procedures and criteria for evaluating the acceptability of plasma arc-cut edges. Develop a detailed test plan for laboratory work.

Task 4: From the Task 2 findings, develop a draft guide for designers, fabricators and inspectors providing specific recommendations for the use of plasma arc cutting. The guide should provide appropriate precautions and limitations, and also address repair of defects.

Task 5: Prepare and submit an interim report summarizing the findings from Tasks 1 through 4.

Task 6: Conduct laboratory tests in accordance with the approved test plan from Task 5. An extensive series of tests, including plasma arc cutting, arc welding, and mechanical testing will be carried out to evaluate cut edges and welds made on plasma-cut edges.

Task 7: Analyze the results of the tests performed in Task 6 and summarize the findings. On the basis of these findings, develop recommended specifications and commentary for plasma arc cutting in a format suitable for adoption by AASHTO and AWS. Revise the draft User's Guide to reflect the test findings.

Task 8: Prepare and submit a final report documenting all research findings and provide recommendations for further research.

CURRENT KNOWLEDGE AND RESEARCH APPROACH

Introduction

The use of plasma arc cutting for steel plates can offer significant advantages in terms of cutting speed and cost when compared with OFC on plate thickness below 25 mm (1 in.). This has been well demonstrated in the general fabrication and shipbuilding industries but has not been exploited in the bridge fabrication industry. A significant reason for this is that existing standards do not contain sufficient guidance on plasma arc cutting or on the need for edge treatment. Research is therefore required to assess the characteristics and the performance of free and welded plasma-cut edges, and to develop specifications and guidelines that will eliminate barriers to the use of this process in steel bridge fabrication.

This introduction includes an overview of the research approach and a discussion of the principal investigator's perspective on conditions and parameters that influence the

performance of plasma-cut free edges and edges affected by welding.

There are two types of plasma cutting equipment: (1) those using a dry plasma gas for cutting in air and (2) those which make use of a secondary water shield or underwater cutting. There are two distinct types of water shield systems: (1) water injection into the plasma within the torch and (2) a secondary shield or water muffler that is outside the arc area. The former will increase the quality of the cut by increased arc constriction; the latter is only effective in reducing particulate fume and noise levels. These systems are used with a water table, which is used to submerge the plate up to 3 in. Submerging the plate reduces noise, fume, and arc glare. The project plan will include cutting both in air and under water to assess the effect of water quenching and to assess the general effects of different plasma gases including air, nitrogen and oxygen.

As the cutting speed is increased from the optimum value (for a particular combination of material thickness and cutting power), the drag angle of the striations on the cut face increases, the bevel angle increases and "high-speed" dross on the bottom edge of the cut appears. High-speed dross tends to adhere to the bottom surface of the plate and can be difficult to remove. Eventually, a cutting speed will be reached where the material is not completely severed. As the cutting speed is reduced from optimum speed and reaches the lower limit of the dross-free condition, the most common feature is excessive dross. This "low-speed" dross is often much less adherent than the high-speed variety, but can still present problems in postcut operations. Thus, there is a window of dross-free cutting speeds for a particular power setting. For a particular material type and thickness, this tolerance box will vary depending on a number of factors, particularly plasma gas type, the cutting power, the torch stand-off, and condition of the cutting torch consumables.

Thermal Cutting Guidelines and International Perspective

The requirements for dressing of the plasma-cut edge are not adequately defined in existing standards, specifications, or recommendations. When doubts exist concerning the performance of a free edge or of an edge to be welded, material is routinely removed by grinding. This is usually accomplished manually using an angle grinder. An example is access holes for on-site welding of bridge sections, where $^1/_{32}$ to $^1/_{16}$ in. of material is removed from the free edge of the cut hole. This practice is labor intensive, may well be unnecessary for plasma-cut edges, and, if applied incorrectly, may lead to other problems such as excessive local hardening of the edge in some grades of steel.

The American Welding Society (AWS) has published guidelines for both oxyfuel cutting (AWS C4.1-77: "Criteria for Describing Oxygen-Cut Surfaces") and plasma cutting (AWS C5.2-83: "Recommended Practices for Plasma Arc Cutting") but the latter does not include specific guidelines on the assessment of edges or the need for postcut dressing. The German Standard DIN 8518 gives a comprehensive description of faults, definitions, and terms for flame, and plasma-cut edges. DIN Standard 2310, Part 4, gives a useful description of the assessment of plasma-cut edges. Other standards are available from Sweden and Japan, and there is a draft International Standard, ISO/TC 44/SC 8 407, which classifies cut edges in terms of surface smoothness, flatness (squareness), and edge rounding. The principal investigator is a U.S. representative on the International Institute of Welding's (IIW) Subcommittee 1E (Thermal Cutting). The experience and perspective gained from this subcommittee have been used in this project, particularly in the review phase of the program and in defining the assessment criteria to be used in laboratory work.

Assessment of the Cut Edge

The arc energy input of the plasma cutting process will largely determine the maximum thickness of plate that can be cut and the maximum cutting speed. The quality of the cut edge is of primary importance as this will determine the necessity or extent of any further preparation that may be required before welding or use as a free edge. In assessing the cut quality, four main criteria should be considered: (1) edge smoothness, (2) squareness, (3) amount and adherence of dross where present, and (4) metallurgical effects such as surface oxide, hardness, and the possibility of microcracking. In many cases, dross is easily removed so attention is focused on the other three criteria. The angle of striation and any top edge rounding also are indicators of cut edge quality and are easily assessed visually. These criteria have been used by the principal investigator in previous research projects and will also be used in this project.

The cutting technique and plasma cutting gas, the type and thickness of the base material, the microstructure and thickness of the heat-affected zone (HAZ), the joint preparation, the welding process, the heat input, the surface condition, and any pick-up of porosity-forming gases in the cut edge all affect the performance of a welded edge. The performance of an as-cut free edge is largely dependent on the surface roughness of the edge, the presence or absence of any edge notches or imperfections (such as microcracks), and the presence of residual stresses. The major concern with the structural performance of plasma-cut free edges and plasma-cut welded joints is the avoidance of fatigue cracks and brittle fractures.

In oxyfuel cutting, the reactions with oxygen result in increases in carbon in the cut edge becasue of depletion of iron and a hard martensitic layer, which may contain microcracks. The hardened layer can produce cracking when the edge is subsequently welded. In plasma cutting, there is no fuel gas and the hardness of the martensitic-cut edge is increased by nitrogen pick-up from the plasma gas.

When welding on a plasma-cut edge, the part of the plasma-induced HAZ that will be subsequently absorbed into the weld metal is important. The grain structure and the toughness properties of the HAZ are determined by the chemical composition of the parent plate and the thermal cycle of the cutting process. Also significant is the degree to which this region is affected by the cutting and shielding gases used in the plasma cutting process. This interaction can cause porosity or oxide entrapment, which may be associated with sidewall fusion discontinuities when the material is subsequently welded. These discontinuities may extend in service by fatigue or propagate in a brittle manner if the toughness is low and the applied stress is sufficiently high. Nitrogen pick-up in the plasma-cut edge, which may be 10 to 15 times higher than in the parent plate, causes an increase in edge hardness, and may result in porosity if the edge is subsequently welded. Nitrogen picked up in the cutting operation will generally be released into the weld pool if the edge is part of a joint that is welded. The increased level of nitrogen can lead to porosity if the threshold solubility of nitrogen is exceeded. Low-heat input welding processes such as short-circuit gas metal arc welding (GMAW) are prone to low penetration and sidewall fusion discontinuities; therefore, plasma-cut edges welded with this process are most prone to nitrogen porosity. There is a synergistic relationship between nitrogen and oxygen, since it has been found that plates cut with air plasma are more susceptible to this effect that those cut with nitrogen. The higher hardness of a nitrogen-enriched free edge would influence the susceptibility to microcracking and, therefore, the fatigue performance of the plasma-cut free edge. Gas analysis for nitrogen and oxygen absorption in plasma-cut edges will be carried out in the experimental plan.

The quality of an unwelded plasma-cut edge may affect the adhesion of paint. The amount and adhesion of any surface oxide on the plasma-cut edge would directly affect paint adhesion on an otherwise unprepared edge. However, surface cleaning is carried out to a finish of Sa 2.5 according to ASTM D2200 or SSPC-SP10. This achieves a near white metal finish on the steel. In addition, a corner radius of $^1/_{16}$ in. is usually specified for free edges for good paint adhesion. Therefore, the postcut operations required before painting would minimize any differences in the performance of plasma-cut edges compared to oxyfuel or machined edges.

Although most plasma cutting is carried out to produce square edges, it can also be used for bevel cutting and for use as a joint preparation as part of a welded joint. This can be achieved by simply employing a torch clamped at an angle to the plate, or by using a special bevelling head. Work will be carried out in this project to develop cutting procedures for both square edges and bevelled edges, both of which will be used for weld edge preparations. The effective thickness of the cut will, of course, be greater when bevel cutting compared with cutting square edges. Work carried out on carbon steels by the principal investigator has established that the tolerance box for cutting speed, producing dross-free, good-quality cut edges, is increased when bevel cutting. This is because the efflux plasma ejects the molten material from the kerf in a direction away from the bevelled part (i.e., any adherent dross tends to be on the left hand, scrap side of the cut when angling the torch in that direction).

Cut quality is important in both minimizing prewelding operations and for unwelded (free) cut edges, reducing the sensitivity to fatigue loading through minimizing areas of stress concentration. To produce a high-quality cut, the plasma gas must form a narrow columnar arc, which enables the part to separate from the scrap material with a minimum of dross attached to the edge or underside of the plate. The clockwise swirl ring, present in most plasma cutting torches, will produce the highest quality, squarest edge on the right-hand side of the kerf because of the arc action with the workpiece material. It should be noted that the maximum cutting speed is normally limited to the minimum level of cut quality that can be accepted while maintaining a substantially dross-free cut. A high-quality plasma-cut edge will have a minimum bevel angle (unless this is intentionally applied for a weld edge preparation), will have a smooth surface, will be free from dross on the bottom edge of the cut, and will not exhibit any microcracking of the edge.

Structural Performance of Plasma-Cut Edges

During service, fatigue cracks that might start from the plasma-cut edge are caused by the presence of three things: (1) microcracks or other crack-like features, (2) local stress concentrations resulting from the striations on the cut surface, and (3) residual stresses. As discussed in the previous sections, the microstructure and the high hardness levels of the HAZ can lead to low toughness in that region, and the presence of any microcracking might lead to the initiation of brittle fracture. In general, there are few cases of brittle fractures occurring from thermally cut edges. In plasma-cut free edges, the occurrence of microcracks or crack-like features decreases as the quality of the cut increases. The risk of brittle fracture from free edges is therefore minimized with higher quality cuts.

The structural performance of plasma-cut edges needs to be assessed from two perspectives. The first is the fatigue and fracture behavior of the free-cut surface, and the second is the fatigue and fracture behavior of a welded plasma-cut edge. The fatigue behavior of welded and free plasma-cut edges will be assessed using a series of stress-life (S-N) fatigue tests. The fracture behavior will be assessed by performing a series of Charpy V-notch tests on the welded specimens only. The measurement of the toughness of the HAZ of the free edge is very complex. Nevertheless, the risk of brittle fracture can be assessed on the basis of the quality of the cut, microstructural and hardness data, and the level of microcracking in the HAZ.

In the case of welded plasma-cut edges, the HAZ of the cut will be altered by each weld pass. There is a potential for low toughness zones to occur in the different regions of the HAZ and a fatigue crack growing into this zone might potentially trigger brittle fracture. Consequently, the toughness of the fusion-line and the various regions of the HAZ require assessment.

Another parameter that plays a major role in the structural performance of thermally cut free edges is residual stress in the HAZ. Residual stress significantly affects both the fatigue and brittle fracture behavior of a structural component. A number of studies have been reported in the literature where residual stresses have been determined in the HAZ of flame- and plasma-cut edges. Generally, it is found that in approximately the outer $^1/_2$ mm, the residual stresses are compressive and this is beneficial from both fatigue and brittle fracture perspectives. However, tensile residual stresses approaching two-thirds of the yield strength of material can be present in the remaining HAZ. In this project, limited residual stress measurements will be made on the free edge using the hole-drilling technique. The objective of these measurements will be to confirm that compressive residual stresses are indeed present on the outer surface as reported in the literature. The static strength of welded plasma-cut edges will be assessed by carrying out a series of tensile tests.

Industrial Exploitation of Plasma Cutting

In the industrial sector involved with plate profiling, the nitrogen water injection and oxygen plasma cutting systems have the potential for enhancing cut-edge squareness compared with other plasma systems, and producing lower levels of nitrogen in the cut edge compared with air plasma cutting. However, the quality of the cut edges has been somewhat inconsistent in practice. Problems associated with nitrogen porosity in welds made on undressed air plasma-cut edges have contributed to the increased use of these other process variants. The use of nitrogen water injection, oxygen, and air plasma cutting processes under water reduces the width of the HAZ of the cut edge, reduces distortion and improves the working environment. Therefore, underwater plasma cutting is being used increasingly for larger mechanized profiling installations. This will be reflected in the test plan, which will involve cutting in air with air, nitrogen, and oxygen plasma gases, and underwater cutting with nitrogen water injection and oxygen plasma systems.

Plasma cutting is being increasingly used in the general fabrication, manufacturing, automotive, chemical, and materials reclamation industries. When compared with oxyfuel cutting, plasma cutting shows particular advantages in that it can cut any metal and, in thicknesses below an inch, it can do so considerably faster and more economically than oxyfuel cutting.

CHAPTER 2

FINDINGS

INTRODUCTION

This chapter presents the results of the literature review, followed by the results of the laboratory test program. The User's Guide, a draft document produced for AASHTO Code authorities and the Bridge Welding Code Committee, appears in Appendix A.

LITERATURE REVIEW

The literature review includes over 100 references concerning plasma arc cutting, including general process operation and plasma cutting variants; research results for thermal cut edges regarding metallographic studies, weldability and mechanical performance of free edges and welded edges; applications in the general fabrication, shipbuilding, offshore and bridge fabricating industries; international standards on plasma arc cutting and other thermal cutting processes such as oxyfuel cutting. References are included in Appendix B.

Also included are general views and experiences of the bridge fabricating industry in the United States and abroad, materials producers and plasma cutting equipment producers. A nationwide survey of AISC Category III fabricators and state DOTs was also carried out to gain a comprehensive view of the state of the art of thermal cutting in the bridge fabricating industry.

PRINCIPLES OF PLASMA CUTTING AND ITS OPERATION

In plasma cutting, gas is transformed into plasma when it is heated, and comprises positive ions, neutral atoms and negative electrons, which results in extremely high temperatures being generated (i.e., up to 27,000°C)(*1*). The plasma arc cutting process severs metal by means of this highly concentrated arc jet, which has sufficient energy and force not only to melt the metal but also to eject the molten material (Figure 1). The action of the arc forms a keyhole in the material to be cut, and in traversing the arc across the workpiece using the transferred arc mode, the keyhole becomes a slot, which is called the kerf. Because melting rather than oxidation produces the cut, plasma cutting can be used to cut any metallic material, including many impossible to cut with the oxyfuel gas process. The plasma arc cutting process requires no preheat and produces minimal distortion in the material being cut.

In operation, a pilot arc is initiated by a high-voltage discharge between the electrode and the constricting copper nozzle. This is called nontransferred arc because it is not transferred to the workpiece material to be cut. The arc then transfers automatically to the workpiece through the cutting machine program cycle, or on pressing a start button that initiates a higher current level for cutting. This transferred arc that is directly between the electrode tip and the workpiece is confined by the nozzle orifice. The torch electrode has negative polarity and the workpiece has positive polarity. Most torches use a vortex flow of gas, which substantially raises the operating voltage and improves cut quality and electrode life by rotating the arc roots on the electrode and workpiece.

Plasma cutting power supplies can be of a traditional drooping characteristic transformer type or, more recently, of a switchmode transistor design that makes increased use of power electronics to vary the output, resulting in a unit that has full-range current output control and a higher electrical efficiency (*2*). Both switchmode types of power supply control current through pulse width modulation, and are known as choppers or inverters, according to the internal switching designs. These power supply types are more complex and expensive than the conventionally designed transformers, but they have several advantages.

The chopper power supply design involves two smaller power supplies linked together. For example, a 200 A cutting capacity machine will have two nominally 100 A power packs. The open circuit voltage of plasma cutting power supplies is often 200 to 300 V, while the cutting arc voltage is usually 100 to 150 V for a power supply delivering 200 A. The inverter design has additional advantages in that it achieves a smaller and lighter power source with higher efficiency and weight reduction resulting from the high frequency switching, which reduces the size of the transformer core.

TYPES OF PLASMA SYSTEMS AND PLASMA GASES

Broadly speaking, there are two types of equipment: those using a dry gas (Figures 1 and 2), and those that make use of a secondary water shield either as a shroud or in the form of a water bed. The water is beneficial for two reasons; it improves the quality of the cut, and reduces noise levels and the amount of particulate fume produced, which can be quite copious. In shroud-type systems, there are two different kinds

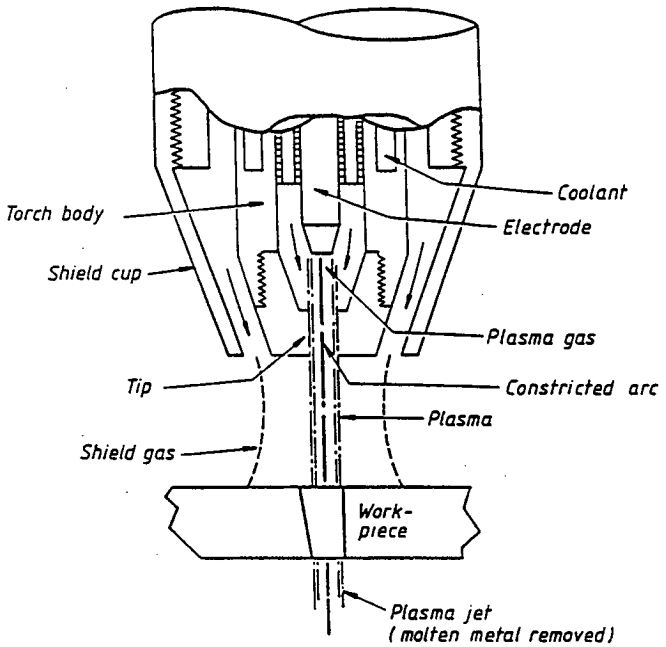

Figure 1. Schematic of a gas plasma cutting torch in operation.

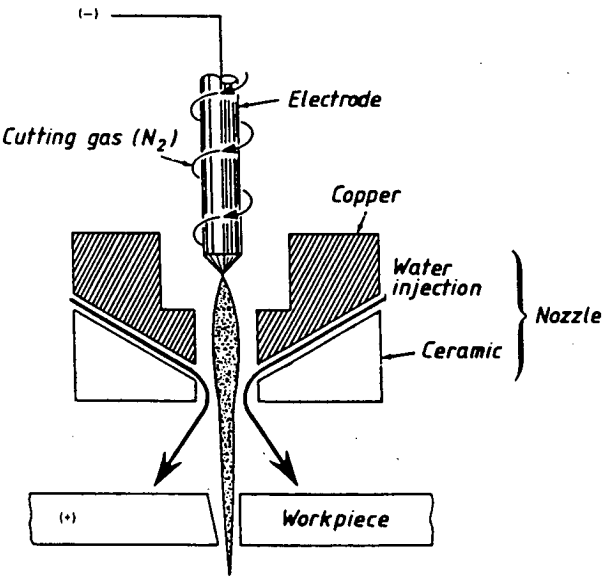

Figure 3. Use of water in plasma arc cutting—water injection plasma arc cutting.

of equipment: water injection into the plasma within the torch (*3,4*) (Figure 3) and the use of a secondary shield, which is outside the arc area (*4*) (Figure 4). The former will increase the quality of the cut by increased arc constriction, but the latter is only effective in reducing particulate fume and noise levels. All types of water injection plasma arc cutting systems require the use of a water table (*5*). Submerging the plate reduces noise, fume, and arc glare (*6,7*), and the workpiece is often submerged to a depth of 50 to 75 mm (2 to 3 in.). The water table is used to collect the water.

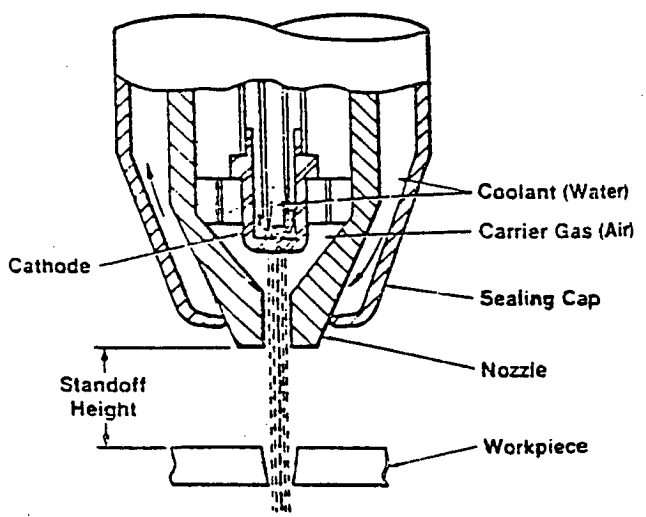

Figure 2. Schematic of an air plasma cutting torch in operation.

Plasma cutting using a transferred arc was developed by Union Carbide in the late 1950s. European companies such as AGA, BOC, and Messer Griesheim were the dominant market for plasma gases. The shortage and general unavailability of cylinder gas supplies in Russia and Eastern Europe led to the development of air plasma cutting, particularly in Russia and East Germany in the mid 1960s. Outside Eastern Europe, Japan was one of the first countries to use air plasma cutting on a large scale, especially for profile cutting for shipbuilding applications.

In the first 20 years of its existence, plasma cutting using argon, hydrogen and nitrogen, and gas mixtures became recognized as an efficient method of thermal cutting for nonferrous metals such as aluminum alloys and stainless steels. However, in spite of its high-cutting-speed advantage, the plasma cutting process could not compete with oxy-gas cutting costwise when applied to carbon and low-alloy steels.

Its second 20 years have been characterized by development of plasma cutting variants suitable for cutting low-alloy and carbon steels at competitive cost. Among these process variants are nitrogen water injection (*4*), oxygen (*8,9*), oxygen water injection, nitrogen with oxygen injection (*10*) and air plasma cutting (*11*). Air plasma offers the advantage of operating from compressed air rather than cylinder or bulk gas supply; however, a compressor is required. Most of these systems are also suitable for cutting nonferrous materials and stainless steels.

Growth in the use of air plasma in Western Europe was very slow, but by the late 1970s improved reliability and competitive cost made it more attractive. Recent developments in torch design have extended the capabilities of air-cooled plasma cutting torches considerably (*12*).

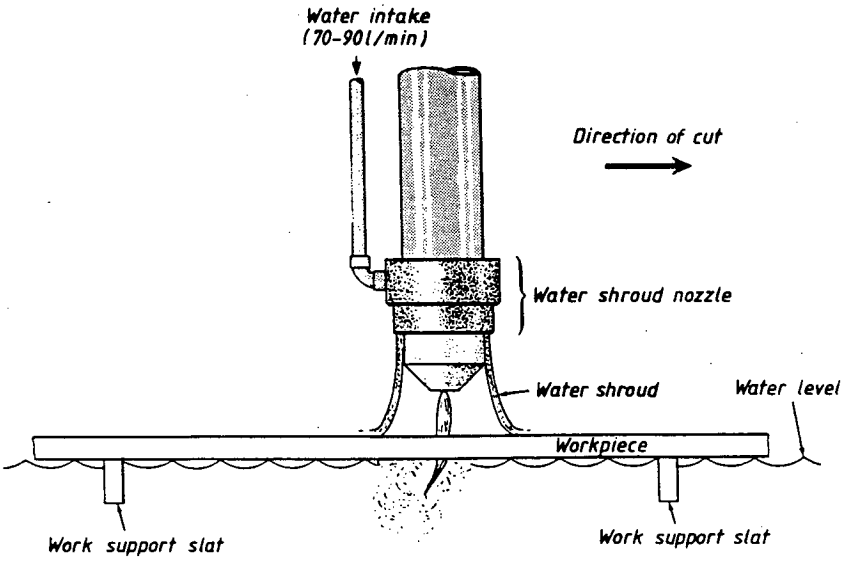

Figure 4. Use of water in plasma arc cutting—pollution control using a water shroud.

GENERAL CUTTING—OXYFUEL AND PLASMA

The development of oxyfuel cutting started around the turn of the century. The process itself has not changed significantly in many years; developments have occurred in fuel gases and cutting tip design. The most significant changes are in the equipment that is used to manipulate the torch; this is discussed in the section on cutting automation in this chapter. In oxyfuel cutting, the exothermic oxidation reaction (*13*) of steel with cutting oxygen produces a very effective cutting action. With the correct parameters, the cut edge can be very square (i.e., 90 deg to the plate surface), have a smooth finish, and be dross-free. The oxidation reaction usually produces a type of dross that is easily detachable from the plate being cut. In terms of its ability to produce good quality edges, the process is very effective for carbon and structural steel. However, a significant drawback of the oxyfuel cutting process is the slow cutting speed, particularly on thinner material of 19 mm ($^3/_4$ in.) or less. It is generally accepted that the economic cutoff point between oxyfuel cutting and plasma cutting is between 19 mm ($^3/_4$ in.) and 25 mm (1 in.). Plasma arc cutting is typically four to five times faster than oxyfuel cutting, although this factor depends to a large extent on material thickness and the power of the plasma cutting system (Table 1). In other words, it is more economical to cut using the plasma arc process below this thickness. This will naturally vary according to the specific production environment and the mix of materials in terms of type, quantity, and thickness (*14*).

Most new cutting capacity installed involves plasma cutting equipment, either alone or in conjunction with oxyfuel cutting equipment. A common configuration is one plasma cutting torch and two or more oxyfuel torches. The plasma cutting system is used for high-speed cutting of material up to 25 mm thick, while the oxyfuel equipment is employed for cutting smaller parts in thicker materials. The improvements in reliability and accuracy of plasma arc cutting and in the traverse speed capabilities of cutting machines have been a major driving force in the increased use of plasma arc cutting (*15*). Precise planning of the cutting operation is very important to the economic viability of the process. The faster cutting speeds obtainable with plasma cutting require that the duty cycle of the cutting operation be able to keep pace with plate materials and/or parts and scrap removal needs of the cutting operations. This can be done by alternating cutting between two cutting tables, so that cutting can be continued on one while loading/unloading is carried out on the other (*16*). The lower duty cycle results in the effective economic cross-over point being at 25 mm between plasma cutting and oxyfuel cutting (*17*).

GENERAL PLATE PREPARATION

Both oxyfuel and plasma cutting can be used for plate edge preparation, either for a nominally square edge or bevelled edges for weld preparations. A single torch is usually used in the vertical position for cutting vertical edges, but can be equipped with an adjustable angled support bracket to cut various bevel angles. Bevels can be cut for single- and double-vee joint preparations, both with and without root faces (*18,19,20*). A double bevel with a root face can be prepared in a single pass with a triple-torch system. The cutting heads can be adjusted manually, but for large-scale cutting operations this would be impractical. By arranging the bevel

torches on guide bars, it is possible to provide automatic bevel angle adjustment (*18*). Rotating head arrangements are available to cut bevel angles while simultaneously following a profile path for shape cutting. Continuous rotation is possible through annular chambers for cutting gas distribution and transmission of electrical power via sliprings. The fact that each plasma cutting torch needs its own power supply means that triple bevel heads for plasma cutting are less common than those for oxyfuel cutting.

Torch height control can be achieved by mechanical means, but a more effective method is capacitive height sensing or voltage height control, both of which are noncontact methods of maintaining the optimum torch height above the workpiece.

The ends of structural I-beams can be cut using oxyfuel and plasma cutting. However, as these machines typically have two or four cutting torches, it is more economical to use oxyfuel cutting. The cost of separate power supplies for multiple torches would be prohibitive in this instance, although it would be possible to complete the work with a single plasma arc cutting torch. Separate torches are used to cut each of the flanges and to cope webs. Typically, this equipment is operated under computer numerical control (CNC) using torch sensing to locate potentially misaligned webs and flanges (*21*).

CUTTING MECHANIZATION, AUTOMATION, AND CNC

The manual cutting process can be mechanized or automated to a wide range of degrees. At the simplest level, a radius bar can be used for circle cutting and straight-line cutting can be achieved by a guide rail. The torch can be mounted on a mobile, track-mounted cutting machine to make straight-line cuts with simple mechanization. Such equipment is suitable for the mechanized preparation of joint preparations for flange splices (*22*). This type of guidance is more suitable to the slow travel speeds used for oxyfuel cutting, although it can also be used for plasma arc cutting with low-current machines of 100 to 150 A. This equipment was seen in use for production of split tees from structural I-beams using low-current plasma cutting.

TABLE 1 Typical cutting speeds for various plasma arc cutting (PAC) systems compared with oxyfuel cutting

Material Thickness		Cutting Process	Cutting Current (A)	Cutting Speed	
(mm)	(in)			(mm/min)	(in/min)
6	¼	Oxyfuel Gas	N/A	685	27
6	¼	NWI	350	3810	150
6	¼	Air	200	3050	120
6	¼	Oxygen	200	4060	160
10	⅜	Oxyfuel Gas	N/A	610	24
10	⅜	NWI	350	3175	125
10	⅜	Air	200	2030	80
10	⅜	Oxygen	200	2540	100
13	½	Oxyfuel Gas	N/A	560	22
13	½	NWI	400	2540	100
13	½	Air	200	1520	60
13	½	Oxygen	200	2030	80
19	¾	Oxyfuel Gas	N/A	480	19
19	¾	NWI	400	1270	50
19	¾	Air	200	1010	40
19	¾	Oxygen	200	1400	55
25	1	Oxyfuel Gas	N/A	405	16
25	1	NWI	400	760	30
25	1	Air	200	635	25
25	1	Oxygen	200	890	35

NWI = Nitrogen water injection

For most plate cutting operations, a stationary guiding machine with X-Y coordinate axes is used. The oldest type of machine uses pantograph tracing from steel templates with a magnetic follower, although it is limited in both size and flexibility. Photoelectric tracing from line drawings, dating from the 1950s, is a commonly used technique, even today. The line drawings are scanned by a photoelectric head travelling tangentially to the line drawing. This technique has the advantage of requiring no programming and is effective for one-time use of parts and for operations involving up to eight oxyfuel cutting torches for cutting large numbers of small repetitive parts. The photoelectric system is capable of accuracy up to ±0.4 mm (*23*). The technique relies on accurately produced drawings on distortion resistant media. The large scale of many parts in the structural steel, bridge, and shipbuilding industries makes this technique impractical for the storage and handling of the drawings. Therefore, as technology has progressed, such users have turned to numerical control, initially using punch tape, pioneered in the 1960s (*24*) and used on a wide scale in the 1970s (*25,26*) and early 1980s (*27–31*). This was followed by full computer numerical control (CNC) without tape (*32*). State of the art today is direct or distributed numerical control (DNC) (*33*). The latter technique allows remote parts programming and nesting of parts off-line for subsequent direct downloading into the CNC mounted on the profiling machine. Sophisticated software is now available for generating cutting programs and nesting routines in conjunction with computer aided design (CAD) workstations. This technique is becoming more and more common, and systems are available for large and small fabricators.

The particular benefit of DNC is that the cutting machine can be in operation while new part programs are being prepared. This allows the productivity of the cutting machine to be maximized. The nesting software optimizes the arrangement of individual parts on a plate, minimizing scrap rates from the "skeleton" of material left after cutting.

Modern cutting machine control can be programmed for corner slowdown routines to maintain square corners on profiled parts when using high-speed plasma cutting. Work has been conducted in real-time control of the plasma cutting process by using intensity measurements of the efflux plasma jet (*34*). While still at the experimental stage, this technique would be appropriate for fixed-head machines such as flexible manufacturing centers [e.g., plasma punch presses manufactured by W.A. Whitney (*35*), Amada, Trumpf, and Pullmax].

The cutting machine itself can be one of several types, the most common of which are cantilever and portal type machines. Cantilever types are used for smaller cutting areas, while the portal type machines are larger and more accurate. Dual drives, one for each side of the portal or bridge, are used to increase accuracy. Today's coordinate drive profiling machines are capable of high travel speeds, typically up to 6 m/min, to cater to the faster travel speeds of plasma arc cutting. Some of the lighter machines can traverse as fast as 12 or even 20 m/min.

For cutting long narrow strips, two torches cutting simultaneously offer the best control of lateral distortion. This kind of distortion results partly from stress relieving from the original plate, but mostly from the unbalanced heat input caused by cutting only one side. The overall distortion caused by plasma cutting is considerably lower than that resulting from oxyfuel cutting. This is due to the high heat density and the faster cutting speed of the plasma cutting process.

In the industrial sector involved with plate profiling (i.e. cutting of shapes from plate), the nitrogen water injection and oxygen plasma systems have greater potential for enhanced cut edge squareness than other plasma systems, and lower levels of nitrogen in the cut edge compared with air plasma cutting. However, in practice, the quality of the cut edge has been found to be somewhat inconsistent when cutting underwater. Problems associated with nitrogen porosity in welds made on undressed air plasma cut edges have contributed to the increased use of these other process variants. The use of underwater cutting with nitrogen water injection, oxygen, and air plasma cutting reduces the width of the HAZ of the cut edge, reduces distortion and improves the working environment by reducing particulate and noise levels. Therefore, there is an increase in underwater plasma cutting for larger mechanized plate profiling installations.

Cutting operations are becoming increasingly mechanized, with the use of profiling machines of various types for cutting materials from sheet for ductwork, through to large plate profiling installations and fabricating centers. Use of dedicated computer systems for CNC and DNC of profiling operations is also on the rise.

METALLURGICAL PROPERTIES AND WELDABILITY

Microstructure of Plasma-Cut Surfaces

General characteristics of thermal cuts include melting of the removed material, surface roughness of the cut as the arc or torch wavers, the possibility of dross on the exit surface, and the possibility of crack-like defects from fast quenching at the edges of the cut. The cutting mechanism can also chemically modify the cut edges by addition or removal of chemical components, such as absorption of nitrogen in plasma-cut edges, and carburization of surfaces in oxygen gas cutting from preferential removal of iron (*36*).

The microstructures extending from the plasma-cut edge surface into the base metal are found to be:

- A thin layer of resolidified molten material
- A layer of martensite with peak hardness of 450–700 VHN
- A partially transformed layer of martensite, bainite, and ferrite
- A ferrite pearlite heat tempered zone
- The original ferrite pearlite base steel.

These layers are shown in Figure 5 after one from Goldberg (*37*), with corresponding hardness results for plasma and oxyfuel cut edges shown in Figure 6 and Figure 7, respectively. The thickness of these layers will vary with steel chemistry and process parameters. For instance, Nibbering et al. (*38*) report a martensite layer of only 0.05 to 0.06 mm thick with a partially transformed zone to 0.5 mm.

Plasma cuts do not induce carburization of the cut surface as oxygen flame cuts do. Instead, the resolidified zone is low in carbon (*39*) and has a limit in hardness of approximately 500 VHN (*37*). The rapid solidification of this layer leaves a martensitic structure.

Adjacent to the resolidified zone, a low-carbon martensite is formed that ranges in hardness from 350–700 VHN (*37*) based on the steel chemistry, heat input, and travel speed. Tempering of the martensite from heat after the arc has passed will reduce the hardness and increase the toughness of this layer. The transformation to martensite limits the possible tensile residual stresses at the cut surface, often creating a region of compressive residual stress.

Cut Quality

The arc energy input will largely determine the maximum thickness of plate that can be cut and the maximum cutting speed. The quality of the cut edge is of primary importance as this will determine the extent of any further preparation required before welding. In assessing the cut quality, four main criteria should be considered; namely, smoothness, squareness, amount of dross, and metallurgical effects such as surface oxide, hardness values, and the possibility of microcracking in the case of some heat sensitive alloys (*37*). In many cases dross is easily removed and so attention is focused on the other three criteria. The angle of striations and any top edge rounding are also important indicators of edge quality.

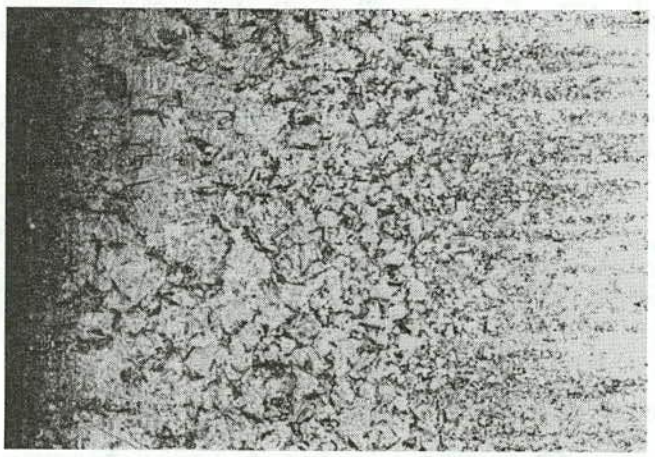

Figure 5. The microstructure of a plasma-cut edge. From left: The fully transformed zone and the partially transformed zone.

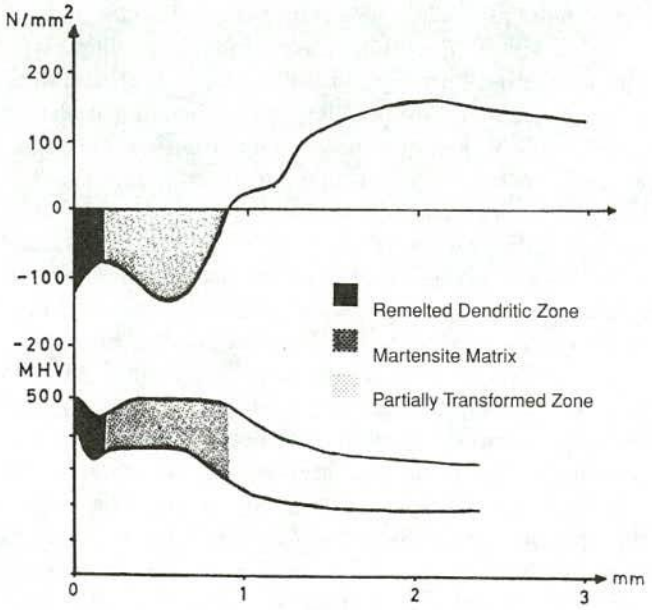

Figure 6. The relation between microstructure, microhardness, and residual stress at a plasma-cut surface in ST 52-3 steel.

Cut quality is important with regard to both minimizing prewelding operations and, for unwelded cut edges, reducing the sensitivity to fatigue loading. To produce a high-quality cut edge, the plasma gas must form a narrow columnar arc, which enables the part to separate from the scrap material with a minimum of dross attached to the edge or underside of the plate. It should be noted that the maximum cutting speed is normally limited by the minimum level of cut quality that can be accepted.

Metallurgical Effects of Air Plasma Cutting

Cutting with air as the plasma gas is associated with nitrogen pick-up in the resolidified region on the extreme edge of the cut (*40,41,42*). Increased nitrogen levels are associated with increases in arc length, cutting speed and flow rate of cutting air. The maximum nitrogen content of the cut edge is 50 times that of the parent metal, and is more than ten times

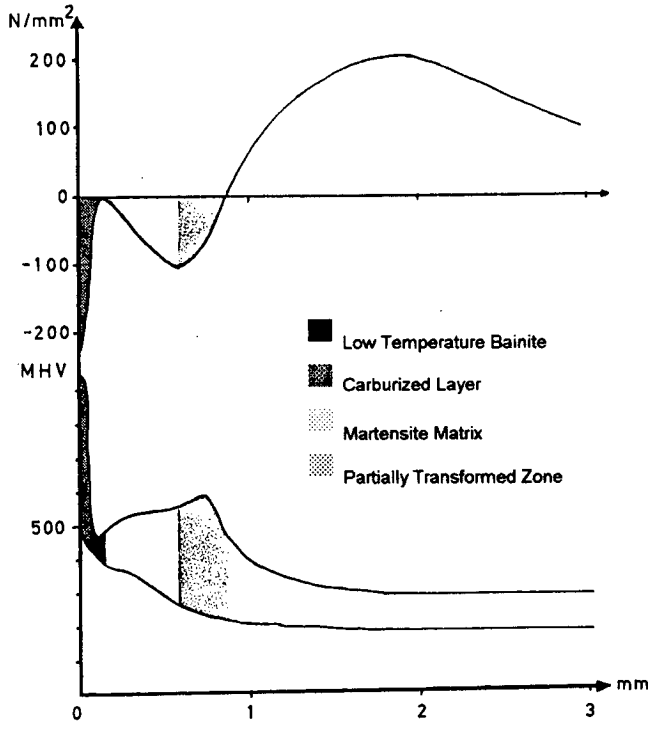

Figure 7. The microhardness, microstructure, and residual stress at a gas-cut surface in ST 52-3 steel.

the ultimate solubility of nitrogen in steel (*41*). When cuts are made in nitrogen, the maximum nitrogen content of the cut edge is higher than that for oxyfuel cutting, but in most cases it is lower than when cuts are made in air.

The increased absorption of nitrogen in an oxidizing air atmosphere is associated with the combination of nitrogen and oxygen, present in air plasma in an atomic active state, to form the oxide NO. The NO in the arc is dissociated and dissolved in the molten metal at the edge of the cut, increasing the nitrogen content in this area. Welding on the cut edge, even with a high-heat input process such as SAW, can result in porosity in the weld metal. This effect can be minimized by reducing the thickness of the resolidified layer. This is achieved by decreasing the arc voltage and increasing the cutting speed, consistent with achieving good edge squareness. The thickness of the affected layer is rarely greater than 0.07 mm (0.003 in.).

The nitrogen content has been found to be associated with the carbon content of the steel; the higher the carbon content, the higher the nitrogen content of the resolidified "cast" zone (*42*). The amount of nitrogen in the edges also increases with a reduction in the thickness of the steel. This trend is consistent with the author's experience; more problems with porosity have been found with porosity in low-heat input welding of thinner plate material. Often, this is also associated with lack of sidewall fusion defects.

Research work comparing gas plasma cutting with air plasma cutting (*43*) at similar current levels determined that optimum cut quality for air plasma was achieved at a speed double that for gas plasma cutting, when cutting 13 mm and 25 mm C-Mn structural steel. The maximum edge hardness for plasma cutting was 400 VHN to 500 VHN, depending on the cutting gas employed. Measurements for oxyfuel cutting yielded maximum edge hardness of 500 VHN, with the total HAZ being wider in the case of the oxyfuel-cut edge. No microcracking was observed on any of the edges. Given that surface hardness levels are similar to oxyfuel and plasma-cut HAZs are narrower, these results indicate that plasma arc cutting is an acceptable method of plate cutting without special considerations for further edge treatment.

Metallurgical Effects of Oxygen Plasma Cutting

One method of overcoming the effect of nitrogen in air plasma cutting is to increase the percentage of oxygen in the plasma gas. Investigations of this type led to the development of plasma cutting systems operating with air/oxygen mixtures and then systems capable of operating with 100 percent oxygen. Increasing the oxygen content of the plasma cutting gas reduces the effect of nitrogen absorption and porosity. It also allows higher cutting speeds to be employed when cutting steel because of the additional thermal energy from the exothermic reaction of oxygen with iron in the steel (the cutting mechanism used for oxyfuel cutting).

Work by Shinada et al. (*44*) indicated that the rate of porosity formation decreased sharply when the oxygen content of the plasma gas exceeded 80 percent. Similar results were reported by Williamson (*45*) using oxygen/nitrogen gas mixtures ranging from 100 percent nitrogen to 100 percent oxygen. Work by Koike Europe (*46*) compared oxyfuel cutting with oxygen plasma arc cutting for high strength structural steel 10 mm and 18 mm thick. The study concluded that the nitrogen levels in the plate were the same for both processes, while the carbon levels were higher in the oxyfuel cut edges. This resulted in hardness levels being lower for the 10-mm-thick plate cut by the oxyfuel process, but the same for both processes on the 18-mm-thick steel. The HAZ was reported to be of an even thickness from top to bottom for the oxygen plasma-cut edge; the HAZ for the oxyfuel-cut edge was generally wider and much wider at the top surface of the cut because of the effect of the preheating flame.

Effects of Water Injection and Underwater Cutting

The addition of water to the plasma cutting system, either in the form of an addition to the plasma gas (*47*) or in the form of water injection (*4*), results in improved cutting performance. Simple addition of moisture to the plasma gas can reduce top edge rounding for nitrogen plasma cut-ting of structural steel (*47*). True water injection, by tangential injection into the plasma gas stream downstream of the cutting electrode, causes arc constriction through

creation of a steam boundary layer between the nozzle bore and the plasma arc column. The increased arc constriction results in a higher density plasma which cuts with a squarer edge. When cutting under water, the dross created can be more adherent when cutting with nitrogen than when cutting with oxygen as the plasma gas, presumably because of the higher oxidation of the dross in oxygen plasma cutting (*48*).

Underwater oxygen plasma cutting of 16-mm-thick, BS4360-50D steel, a structural steel (*49*), resulted in hardness levels as follows: as-cast material at the edge 350 to 440 VHN; martensitic layer 410 to 500 VHN at 80 μm from the edge; 220 to 250 VHN at 0.4 mm from the edge (Figure 8). Underwater nitrogen plasma cutting of the same material resulted in edge hardness of 490 to 515 VHN, with a martensitic layer to a depth of 0.4 mm (Figure 9). By comparison, cutting the same structural steel with air plasma resulted in surface hardness in the range 645 to 780 VHN. This is a result of a narrow nonetching nitrided layer on the surface (Figure 10). Behind this layer was a large-grained martensitic structure about 0.3 mm wide with a microhardness range of 425 to 540 VHN. Away from the cut edge, the structure changed progressively to partially transformed martensite and ferrite, and finally to ferrite and pearlite at about 0.8 mm. Hardness values fell progressively to 170 to 190 VHN at 2 mm from the cut edge.

Welding on Edges Prepared by Plasma Cutting

A study of the effects of air plasma arc cutting on the strength of welds made by shielded metal arc welding (SMAW) was conducted using 16-mm-thick structural steel (*50*). The performance of edges prepared by air plasma cutting was compared to edges produced by oxyfuel cutting and also by machining. The study concluded that there were no cracks, pores, subcutaneous blowholes, or nonmetallic inclusions in welds prepared by air plasma cutting. The results of mechanical testing by tensile, impact, and bend testing showed that the mechanical properties of joints produced with as-cut edges produced by air plasma cutting were the same as for edges prepared by oxyfuel cutting or machining.

A Czech study (*51*) of bainitic and quenched and tempered high-strength steels compared the tensile properties and impact toughness of butt joints in three steels, with edges prepared by oxyfuel cutting (both with and without preheat), plasma arc cutting, and mechanical machining. The method of edge preparation was found to have no effect on the tensile properties of the joints. The impact properties for joints made on thermally cut edges were the same or higher in all cases than those produced from machined edges. Cross weld hardness measurements showed that peak hardness was the same irrespective of the preparation technique for one steel, and that peak hardness for the other two steels was higher for oxyfuel-cut and machined edges compared with edges prepared by plasma cutting.

Work conducted to evaluate the effect of plasma cutting on the weldability of 16-mm-thick BS4360-50D structural steel (*52*) employed air plasma, underwater oxygen plasma, and underwater nitrogen plasma cutting to prepare joint edges and fillet and butt joints, with an intentionally severe single bevel butt joint (i.e. with one cut face vertical). Cutting with air plasma resulted in increased root porosity associated with nitrogen pick-up in the cut edge. Cross weld tensile testing results showed parent metal failure for welds made on edges cut with both the underwater plasma cutting processes. The welds made on air plasma-cut edges had lower strength and failed in the weld metal as a result of the porosity in the root region of the joint. The proportion of joint edge relative to weld pool size is highest in the root region, and explains why this region showed the highest porosity from nitrogen in the remelted cut edges.

Charpy impact tests on weld metal (*52*) at −40°C showed a strong influence on toughness resulting from nitrogen levels in the cut edge. The average value of 16J (Joules) for the weld metal in an air plasma-cut joint preparation was appreciably lower than the underwater nitrogen and underwater oxygen results at 41J and 48J, respectively. Full transition curves were not obtained, but the data for the last two processes were good.

An investigation of the weldability of plasma-cut edges (*53*) using gas metal arc welding (GMAW) concluded that there was an effect of the nitrogen level in the plasma gas, and consequently in the cut edge, on the weldability of 6-mm-thick carbon-manganese steel. Engblom and Williamson (*53*) report that plasma cutting with nitrogen or nitrogen oxygen mixtures can cause pick-up of nitrogen on the cut surface. These nitride layers can cause mechanical pore formation as the nitrogen gas escapes during subsequent MAG welding. These pores can act as initiation sites for cracking and weld defects. However, the pores, with their smoothly curved surfaces, are generally much weaker initiation sites than weld toes. Acceptance standards have allowed 3 percent or more of the area in radiographs to show pores without downrating of the weld.

In one recent publication, Mutnansky and Handl (*54*) examined mechanical properties of welds with varying initial bevel preparation. They report no loss of tensile or impact toughness properties from converting bevels from machined surfaces to nitrogen plasma-cut edges. The cut edges did show surface microcracking and other defects, but these were consumed by the semi-automatic GMAW CO_2 welds. The HAZ microstructure changes noted did not have a noticeable effect on the measured properties. These results were consistent across the four steels tested.

As described by Mutnansky and Handl (*54*), the cut-surface features such as roughness and microcracks will be erased by remelting during subsequent welding. The HAZ

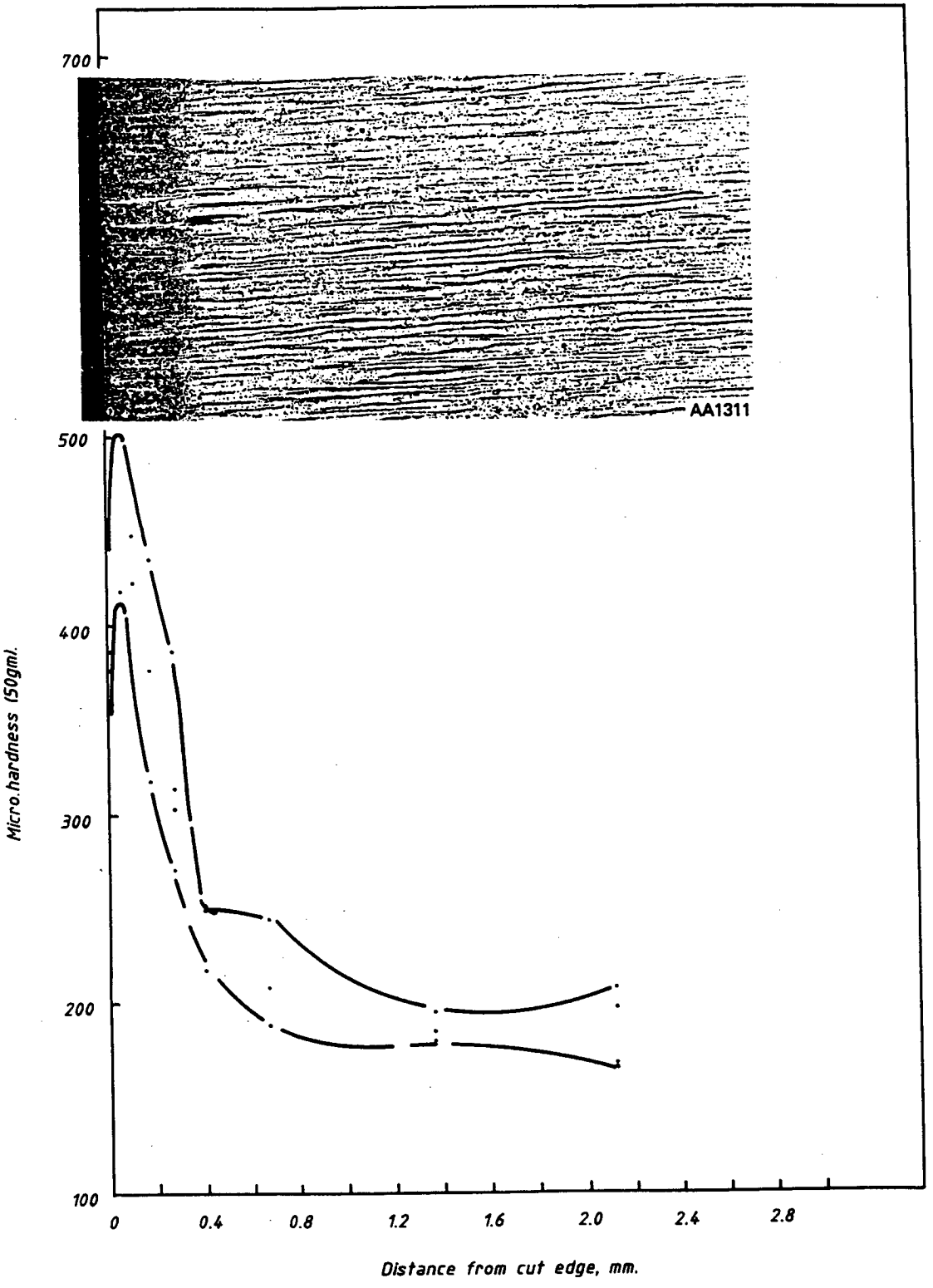

Figure 8. Microhardness plot across underwater oxygen plasma produced HAZ–BS4360:50D.

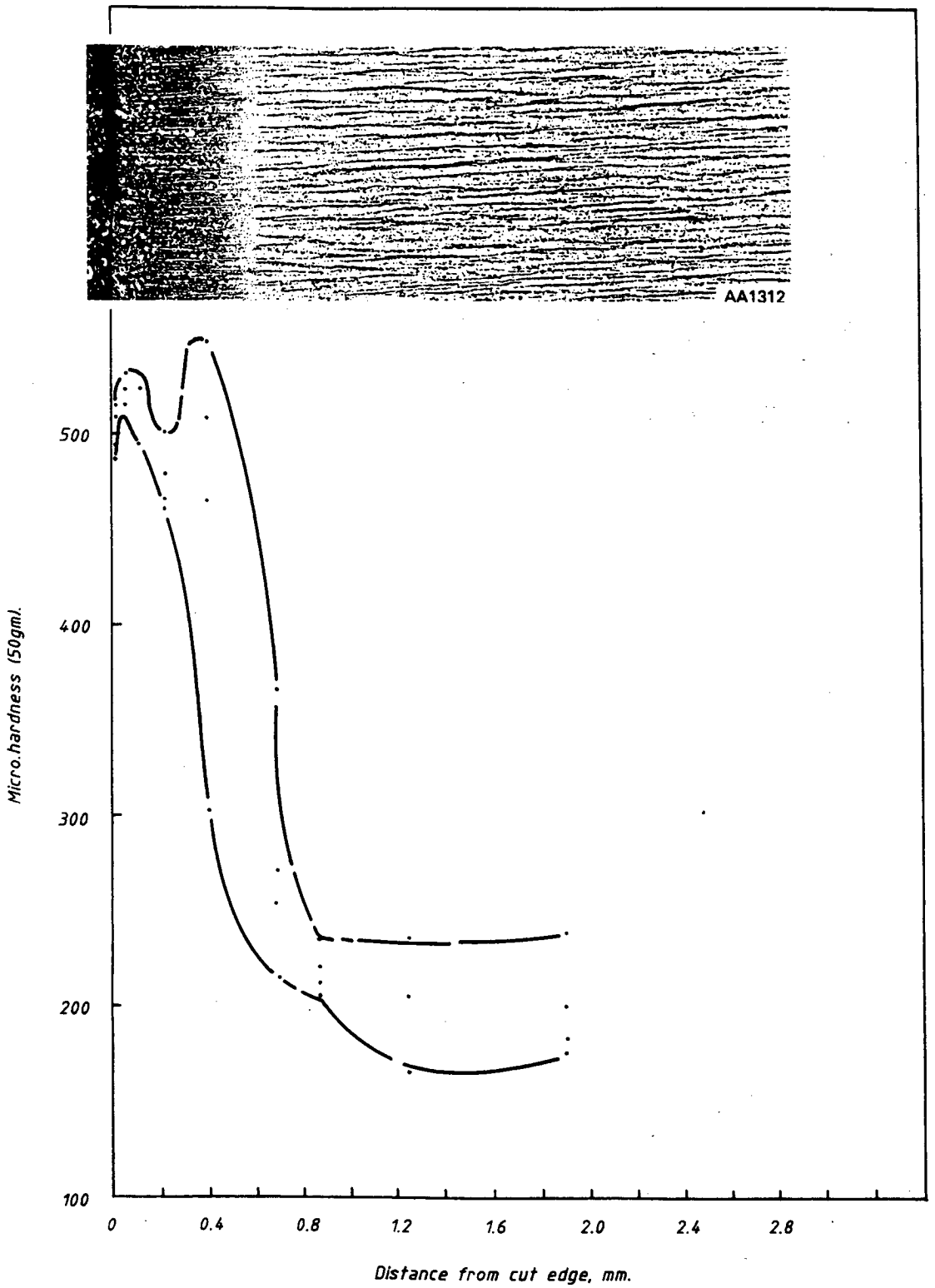

Figure 9. Microhardness plot across underwater nitrogen plasma produced HAZ—BSR4360:50D.

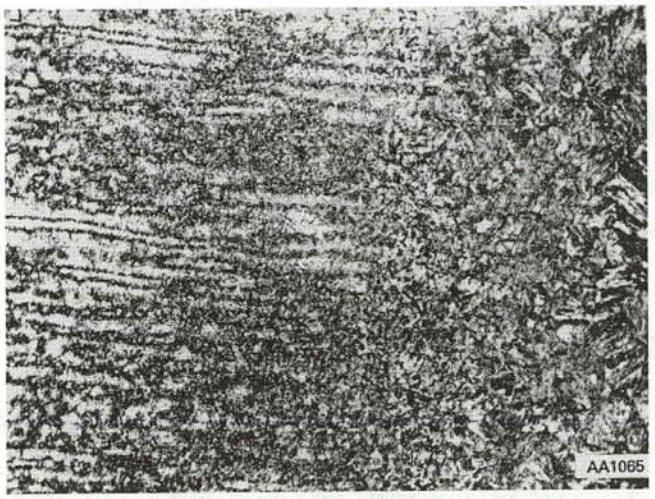

Figure 10. Microstructure of HAZ produced by air plasma cutting of C-MN steel—BS4360:50D. Original mag. ×200, as shown ×114.

will not be remelted, rather it will be altered by re-heating with each weld pass. There is a potential for low toughness zones where the two HAZs interact, but their results did not detect any such zones.

MECHANICAL PROPERTIES

The mechanical issues of interest for plasma-cut edges in bridge steels are fatigue performance, static strength, and brittle fracture risk. Both cut edges and welded cut pieces are of interest.

The reported hardness of plasma-cut surface resolidified layer of 350–500 VHN (*55,56*) will exceed the requirement of BS 5400 Part 6 (*57*) for flame-cut surfaces under stress, which specifies a hardness of no more than 350 VHN. If plasma cuts have the surface layers removed by grinding to meet this hardness requirement, the surface residual stresses will most likely be tensile since both the resolidified layer and the martensite layer would need to be ground away. Such a treatment will result in poorer fatigue performance, as was found by Sabelström (*58*) for normalized plasma cuts, and Khil'chevskii et al. (*59*) for air plasma-cut edges. This type of hardness limitation for plasma cuts would severely limit the use of as-cut surfaces, without obvious benefit noted in the literature reviewed here.

The HAZ for plasma cutting is smaller than the HAZ for oxygen cutting due to the higher cutting speeds allowed by plasma cutting. Goldberg (*55*) notes that the larger energy density of the plasma torch would create a wider HAZ if run at the same speed as an oxyfuel cut. However, as plasma arc cutting speeds are generally much higher than those for oxyfuel cutting, the HAZ is narrower. The zone of tensile residual stresses will generally correspond to the HAZ that has not transformed to martensite to a significant extent. Thus, the zone of tensile residual stress will also be deeper for oxyfuel cuts than for plasma arc cuts.

In plasma cutting, the surface roughness of the cut edge is usually well controlled, but Goldberg (*55*) notes that poor process conditions can increase the surface roughness to one similar to that which normally appears in oxyfuel cutting. The discussion of surface roughness must be further defined, however, since the method of measurement can greatly change the ratings. The peak-to-peak roughness for plasma cuts generally has been seen to be much smaller than normal for oxyfuel cutting. The notch valleys, on the other hand, tend to be sharper and occur at closer intervals in plasma cuts as discussed by Krüger (*60*).

Under examination, the position of fatigue crack initiation has preferentially been found to be the front surface of the cut, at small cracks or intrusions within the heat-affected zone. Ho et al. (*61*) found fatigue crack origin preferentially on the unground hot rolled surface of ASTM A572 Grade 42 steel in preference to the ground surface, as a result of surface defects or possibly unfavorable residual stresses. When both plate surfaces were ground, the fatigue crack origins were preferentially on the upper edge of the cut.

The locations of initiation of cracks considered by other investigators are as follows:

- Microcracks at the front face of the cut edge
- Defects on as-rolled surface adjacent to cut
- Zones of high hardness in HAZ
- Zones of high tensile residual stress
- Cut edge surfaces.

Wilson (*62*) studied the microstructure, hardness, and bend characteristics of thermal-cut bridge steels (A572 Grade 50, A588 and A36), including a small section on plasma cutting. No thermal cuts showed optically detectable cracking. Intergranular microcracking of the cut edge material was observed by scanning electron microscopy on each specimen examined. This microcracking was found to be the initiation site for cracking in the bend tests, although three of four bend tests of plasma-cut samples did not grow macroscopic cracks. The hardness measurements for plasma-cut specimens exhibited less scatter than for the flame-cut edges.

Residual Stress

Residual stresses will be created by cutting adjacent to the cut edge, due to constraint during cooling and the transformation to martensite, with its associated volume expansion. The constraint of the plate away from the cut will tend to create tensile residual stress in the cut edge as the edge cools and contracts after the arc has passed. The transformation to the higher volume martensite will create compressive residual stresses as a higher volume phase replaces a microstructure of lower volume. The competition

between these effects establishes the distribution of residual stress of a cut edge.

Transformation to martensite requires a rapid cooling from above approximately 1550°F to 600°F, which can only occur in close proximity to the cut edge. Alloy additions which increase the hardenability and promote martensite formation will expand this band of martensite near the cut edge. The volume expansion of 5 percent on transformation to martensite will be resisted by the surrounding material causing compressive residual stresses. These compressive residual stresses will be larger and cover a greater volume where a large percentage of the edge material is transformed to greater depths into the plate. Compared with air-cooled cuts, water-cooled or water-immersed cuts will have greater quenching rates with thinner heat-affected zone sizes but relatively larger martensite layers, thus modifying the distribution of residual stresses.

Most measurements find compressive residual stresses within 1 mm of the cut surface. The compressive residual stress will inhibit initiation of fatigue cracks at geometrical defects. Sabelström (*6*) reported that normalization of the cut edge decreases fatigue life, due to reductions in the surface compressive residual stress. However, the tensile residual stresses expected within the HAZ away from the cut edge can increase the fatigue crack growth rate. The HAZ is larger on the upper surface and tensile residual stresses can be expected to be higher and cover a greater region into the surrounding plate. Goldberg (*55*) measured tensile residual stresses at depths beyond 1 mm with a maximum at 2 mm from the cut surface. While Ho (*61*) did not measure residual stress, the martensite layer was only 0.3 to 0.5 mm deep. Goldberg (*55*) noted that the zone of compressive residual stresses nearly matches the martensite zone.

The far-field effects of plasma cutting were measured by Johnson et al. (*63*) on ship steel plates, with much less distortion in underwater oxygen plasma-cut plates than in oxy-propane-cut plates. This effect on far-field residual stress was laid partly to the much higher cutting speeds for plasma, 200 mm/sec as opposed to 20 mm/sec for the oxy-fuel cut on 9.5-mm-thick plate. No deviation in temperature was measured on surface thermocouples placed within 1 mm of the plasma-cut surface. The investigators reported that similar results were obtained with nitrogen plasma cutting.

Toughness of Plasma-Cut Edges

Toughness is a measure of the material resistance to fracture. Higher toughness, fewer and smaller initial discontinuities, and less tensile residual stresses will provide increased resistance to brittle fracture. The cut edge toughness is difficult to measure directly, since the microstructural layers of interest are often less than 1 mm thick. Additionally, toughness values are desired for cracks transverse to the cut edge. Thus, as a crack progresses, it will sample microstructures expected to have varying toughness. Under these conditions, Charpy impact tests or other common toughness measurement techniques will not give unambiguous results. The situation should be at least slightly improved over flame cuts based on the lower scatter in hardness for plasma cuts.

Lower toughness than machined edges at extremely low temperatures (−90°C) has been measured on unnotched impact bend specimens (*64*). This is an extremely severe test for crack initiation, since the resistance to brittle fracture will be extremely low at these temperatures. The microcracking detected by Wilson (*62*) could cause this drop in cryogenic temperature impact toughness.

At ambient temperatures, the risk of brittle fracture can be assessed on the basis of quality of cut, microstructural and hardness data, and the level of microcracking in the HAZ. This qualitative method has been applied widely and successfully in the absence of standardized measurement techniques for edge toughness. EWI has participated in research designed to create standard toughness tests for shallow cracks, but as yet these techniques have not been validated for nonhomogeneous, layered materials, such as thermal cut edges.

Fatigue of Plasma-Cut Edges

Tests on fatigue performance have generally shown plasma-cut surfaces as equivalent or nearly equivalent to machined edges (*55,60,61,65*). Those tests which compare plasma-cut edges to flame-cut edges regularly find longer lives and higher allowable stresses for plasma cuts. Isolated cases have been observed, as in the case of Krüger's tests (*60*), where plasma-cut edges are only equivalent to flame cuts.

Graphs of performance from Goldberg (*55*) on steel equivalent to ASTM A572 Grade 55 show a drop of 10 N/mm^2 in stress at all endurance levels for plasma-cut surfaces compared to machined surfaces as shown in Figure 11. One sample, cut with a defective nozzle, failed at 2×10^5 cycles rather than the expected 1.2×10^6 cycles, suggesting to Goldberg that a roughened surface will reduce fatigue strength in plasma cutting as well as other thermal cutting. The range of fatigue performance for flame cuts extends from 10 N/mm^2 below the plasma-cut line for high-quality cuts to 90 N/mm^2 below for low-quality flame cuts. The points on Ho's graphical representation (*61*) suggest that plasma-cut surfaces of ASTM A572 Grade 42 gave higher fatigue stresses than machine cuts at endurance levels above 10^5 cycles, but these differences were reported to be not statistically significant.

The Dutch Ship Structure Committee (*38,66*) results give lower values of fatigue performance for both normal quality and cuts with defects in Fe51 ship construction steel. The defects were created by arc travel stops of 2 sec. These results appear to be based on lower heat input and thus thin-

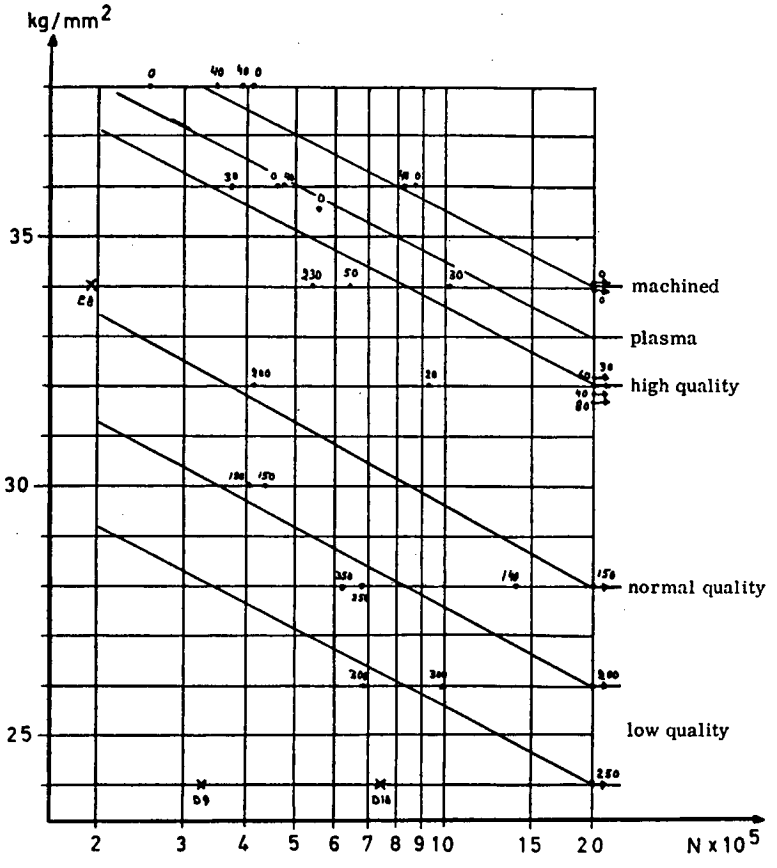

Figure 11. Results of fatigue tests plotted as S vs. Log N curves showing the relation among the five quality levels tested.

ner HAZ and less transformation to martensite, which caused less compressive, even slightly tensile, residual stress at the cut surface. The hardness measured far below the lower bounds of the plate center line hardness measured by Goldberg (*55,56*). The effect of the defects was much less severe than similar defects in flame-cut surfaces. It should also be noted that the machined surface fatigue results also fall into the same range as the plasma-cut surfaces without defects from these researchers.

Krüger (*60*) describes bending fatigue tests for an ST37-2 carbon steel where the gas-cut and plasma-cut edges had nearly equivalent fatigue performance at 185 Ma. The 50 percent probability of failure was at 271,700 cycles for oxy-acetylene cuts and 229,100 cycles for plasma cuts. The surface roughness of the two cuts was equivalent, but the drag lines on the plasma-cut surface were closer together (1 mm vs. 3.5 mm). The notch effect of the drag lines was mentioned, although the location of crack origin was not noted.

Prokopenko et al. (*65*) reported approximately the same fatigue strength for machined and plasma-cut surfaces for a high strength bainitic steel designated 14KhGNMDAFBRT (0.14%C 0.36%Si 1.15%Cr 1.25%Mn 1.12%Ni 0.27%Mo 0.5%Cu 0.0028%N 0.16%V 0.036%Nb 0.05%Al 0.09%Ti). Bend tests were used to characterize the fatigue of plasma-cut surfaces, since initial tensile fatigue tests failed preferentially at machined surfaces. The overall rate of fatigue crack propagation was also found to be unchanged.

Surface roughness of the edge seems to have less effect on plasma-cut edges than on oxygen-cut edges. The toughness of the resolidified metal at the cut surface appears to limit crack formation from plasma-cut surface defects. The surface compressive residual stresses may also be limiting crack formation on the cut surface. Prokopenko (*65*) noted an order of magnitude increase in surface roughness without decrease in fatigue life.

Static Strength of Plasma-Cut Edges

Prokopenko et al. (*65*) measured the static strength of the cut-edge region in 12-mm-diameter tensile bars machined so one specimen was tangent to the plasma-cut edge surface. Compared with the same type of specimen without the plasma-cut edge, the ultimate tensile strength increased by 6 percent to 881.5 Ma while the elongation decreased by 5 percent and the reduction in area by 4.5 percent. The limit of

proportional loading also decreased, suggesting a softer zone at some position in the heat-affected zone.

While the steel used by Prokopenko et al. was a high-strength and complex alloyed grade, the same type of tensile property changes would be expected for bridge steels. The ultimate tensile strength can be expected to increase in the presence of a cut edge, while the elongation and reduction in area will both decrease slightly.

Summary of the Effect of Plasma Cutting on Mechanical Properties

The performance of plasma-cut edges in engineering tests has generally fallen between that of flame-cut edges and machined edges, with behavior often indistinguishable from the machined edge. This is true for fatigue performance, tensile results, and bend tests. The structure of the plasma-cut edge, with low carbon martensite adjacent to the cut, causes compressive residual stresses which limit the propagation of microcracks at the cut edge. Stop-and-start defects and larger surface roughness have not been noted to reduce properties of plasma-cut edges below those for normal quality flame-cut edges. Thus to a first approximation, the quality requirements set for flame-cut edges (*67,68*) could be conservatively applied to plasma-cut edges. However, the defects in flame-cut edges have caused more severe reductions in properties (notably fatigue properties), so less restrictive standards could safely be applied to plasma-cut edges, with no loss of properties below those of normal flame-cut surfaces. Alternatively, restrictive standards placed on plasma-cut quality could allow performance nearly equal to machined surfaces and well above flame-cut edges.

SHIPBUILDING—OFFSHORE AND GENERAL FABRICATION

The shipbuilding industry fabricates very large tonnages of steel plate for hulls, decks, bulkheads and numerous other assemblies. Significant advantage has been taken of the productivity improvements available from plasma cutting compared to oxyfuel cutting. Most of the largest plate profiling operations take place in the shipbuilding industry, usually with numerous large portal-frame cutting machines and several water bed cutting tables. Nitrogen water injection plasma arc cutting equipment was installed at the Lindo shipyard of the Odense Steel Shipyard Company, Denmark, in 1976 (*69*). The process quickly replaced many of the oxyfuel torches for cutting plate and several plasma cutting torches are used, sometimes two or three to each of the ten cutting machines.

Developments in the U.S. shipbuilding industry use of plasma cutting occurred on a similar time scale. The San Pedro yard of Todd Shipyards installed plasma arc cutting equipment in the late 1970s (*70*). Originally, the oxyfuel cutting was replaced with plasma on the same machine. Although the cutting speed increased significantly, the overall productivity was not increased. The reason for this was that the production bottleneck moved from the cutting operation itself to the loading and unloading of plate, parts, and scrap. This was overcome by using separate plate supports which are shuttled backwards and forwards to the cutting machine. The production rate was tripled compared to the original oxyfuel cutting system. Bath Iron Works (*71*) is equipped with plasma arc cutting equipment for profiling of carbon steel, high-strength steel, stainless steel, and aluminum alloys. The aluminum alloys are used for the ship superstructures. HBC Barge (*72*) installed plasma cutting equipment in 1979 as part of a change of emphasis in production capacity for nonmarine markets. The full-size lofting operation involved 3,000 sq ft, with a 90 × 40 ft cutting area and a cutting template area of equal size. This was all replaced by a numerically controlled system operating two plasma cutting torches and four oxyfuel cutting torches. The extra space was used to increase floor space for other productive fabricating work.

In 1982, Steiner Shipyard (*73*) installed CNC profiling equipment to replace manual and simple mechanized cutting operations. Two shape-cutting machines were purchased with plasma cutting, oxyfuel cutting, and punch marking stations. Installation of this equipment reduced cutting time for parts for boat production by 75 percent.

An overview of the equipment available for cutting operations in shipbuilding (*74*) stated that significant increases in the use of water injection plasma cutting were taking place at the expense of oxyfuel cutting. Depending on the plate thickness, cutting speeds of up to four times faster than oxyfuel can be achieved. Much of the cutting is carried out under water, as this achieves reduction in noise levels, arc glare, and particulate levels. However, provision is still required for fume extraction. At this time, most NC or CNC shape-cutting machines used punch tape for the machine control. DNC was slow to be adopted; this may have been partly associated with the unknown nature of the incoming data. The advent of CRT screens on the machine mounted CNC allows visual verification of parts and part nests to be cut.

An interesting study of plate distortion resulting from thermal cutting of typical compositions and part configurations used in shipbuilding showed that the thermal cutting operation is largely responsible for the distortion (*63*), rather than the release of residual stresses resulting from initial plate production. The study, by U.K. shipbuilder Harland and Wolff, found a much larger distortion resulting from oxyfuel cutting compared to that caused by plasma arc cutting. Although it is fairly common knowledge that plasma cutting results in lower distortion, it is commonly believed that much of the distortion results from relief of "locked in" stresses. DNC plasma cutting with oxygen plasma gas was employed for the study, with oxypropane as the benchmark for comparison. Calculations

of heat input showed that the heat input for oxypropane cutting was 2 to 3 kJ/mm, and less than 1 kJ/mm for oxygen plasma cutting. The lower heat input is largely responsible for the reduced distortion.

While it is true to say that the plate cutting operation is only a small part of the overall manufacturing operation, the effect of distortion in ship manufacture is considerable, and improvements are welcome. Since distortion during fabrication can lead to poor fit-up and higher fabrication costs, use of oxygen plasma cutting can result in significant improvements in economy of fabrication. Harland and Wolff experienced useful improvements from using oxygen plasma cutting, resulting from the very low distortion achieved with this process.

In the decision-making process of considering plasma cutting to replace oxyfuel cutting, the differences in cutting rate, manning costs, consumable costs, and depreciation are usually compared. Although the oxygen plasma cutting process is capable of cutting speeds about six times that of oxyfuel cutting, when comparisons are based simply on retrofitting a plasma cutting torch to an existing oxyfuel cutting machine, the advantage is reduced to about twice the throughput as the parts removal process becomes the bottleneck to increased productivity. Increased throughput is dependent on the timely availability of accurate technical information, machine instructions, and material delivery and scheduling, particularly unloading of cut parts.

While plasma, oxyfuel, and mechanical cutting methods are used for naval shipbuilding in the United Kingdom, a recent overview (*75*) of the welding and cutting operations indicated that oxyfuel cutting was used more widely because it is more adaptable for applying bevelled edge preparations for butt welds in decks, bulkheads, and in the hull. The viewpoint on the general use of plasma cutting is certainly different from that of the U.K. commercial or merchant ship fabricators. Since comments were specific to weld joint preparation and largely for submarine construction where material thicknesses are greater than for surface ships, it is assumed that greater use of plasma cutting is made for cutting plates with nominally square edges and for thinner plate.

The implementation of two CAD/CAM production lines with robots at the Turku Shipyard in Finland (*76*) in 1987 successfully introduced a computer-integrated manufacturing (CIM) approach to shipbuilding. This CIM approach represents the state of the art in thermal cutting and welding in the shipbuilding industry. The project was initiated in 1984 to improve production of ship hulls. The shipyard typically produced luxury cruise liners, arctic vessels, and gas tankers. A robotized DNC profile cutting line, Figure 12, was established using a 6-axis robot mounted in the overhead position. The cutting equipment selected was an oxyacetylene cutting torch. No explanation was given for the selection of oxyfuel cutting over plasma cutting, although it may have related to high-frequency arc initiation of the plasma cutting system interfering with the robot control. However, plasma cutting equipment has been successfully mounted to a robot before and since.

A CAD/CAM "micro panel" fabrication line (*76*) was established for the cutting and welding of stiffened subassemblies of the ship's inner hull. The stiffeners are first fitted and welded onto the plates using automatic welding, and then finished parts are cut using CNC underwater plasma arc cutting on a conventional cutting machine (Figure 13).

Future trends in cutting in the shipbuilding industry may result in the use of lasers for thinner materials, especially with the development of high power Nd:YAG lasers which can be used in conjunction with robotics and fiber optic beam delivery (*77*).

The offshore industry uses large tonnages of steel, with increasing amounts of high-strength steels. Thermal cutting of an offshore steel with a yield strength of 355 N/mm^2 causes hard heat-affected zones despite a low carbon content. However, the high ductility of the material (20%) means that this is not a significant concern (*78*). Face bend tests were conducted with 25 percent deformation in the tensile zone and no cracks were produced.

The majority of structural components on an offshore fabrication are delivered as a plate that has to be cut, rolled, and fabricated into tubular leg and brace members, and beam sections. Cutting for fabrication of offshore jacket structures at Highlands Fabricators, Scotland (*79*) involves oxypropane cutting, usually of a mechanized or automated nature, to increase the accuracy, reproducibility, and productivity of the cutting process. An example of some of the specialized equipment used is the pipe flame cutting unit used for producing complex profiles for intersecting tubular nodes. The cutting involves making the cut for the intersection locus or footprint, and also making the cut for the weld preparation. The weld preparation can be external or internal and all the requirements can be programmed into the computer controlling the cutting machine. Plasma cutting is restricted to pipework applications, mainly involving austenitic and duplex stainless steels and nickel alloys. Both 100 A and 450 A plasma cutting power supplies are employed in cutting and weld preparation on tube diameters up to 400 mm and thicknesses up to 25 mm.

Application of plasma arc cutting in the general fabrication industry is widespread, with automated CNC systems installed in the late 1970s for cutting steels (*80,81,82*), and considerably earlier for stainless steels and non-ferrous alloys. Reducing scrap levels and increasing productivity in profile cutting operations was the goal of Fiat-Allis UK (*80*), a former manufacturer of earth-moving equipment. The solution was installation of a cutting machine equipped with nitrogen water injection plasma arc cutting. The cutting machine was an ESAB Telerex TXB 8500, a portal type machine with synchronous drive to each side carriage for traverse speeds up to 12 m/min; the first in the U.K. It was fitted with six oxypropane torches, three zinc oxide powder marking torches and three Hypertherm nitrogen water injec-

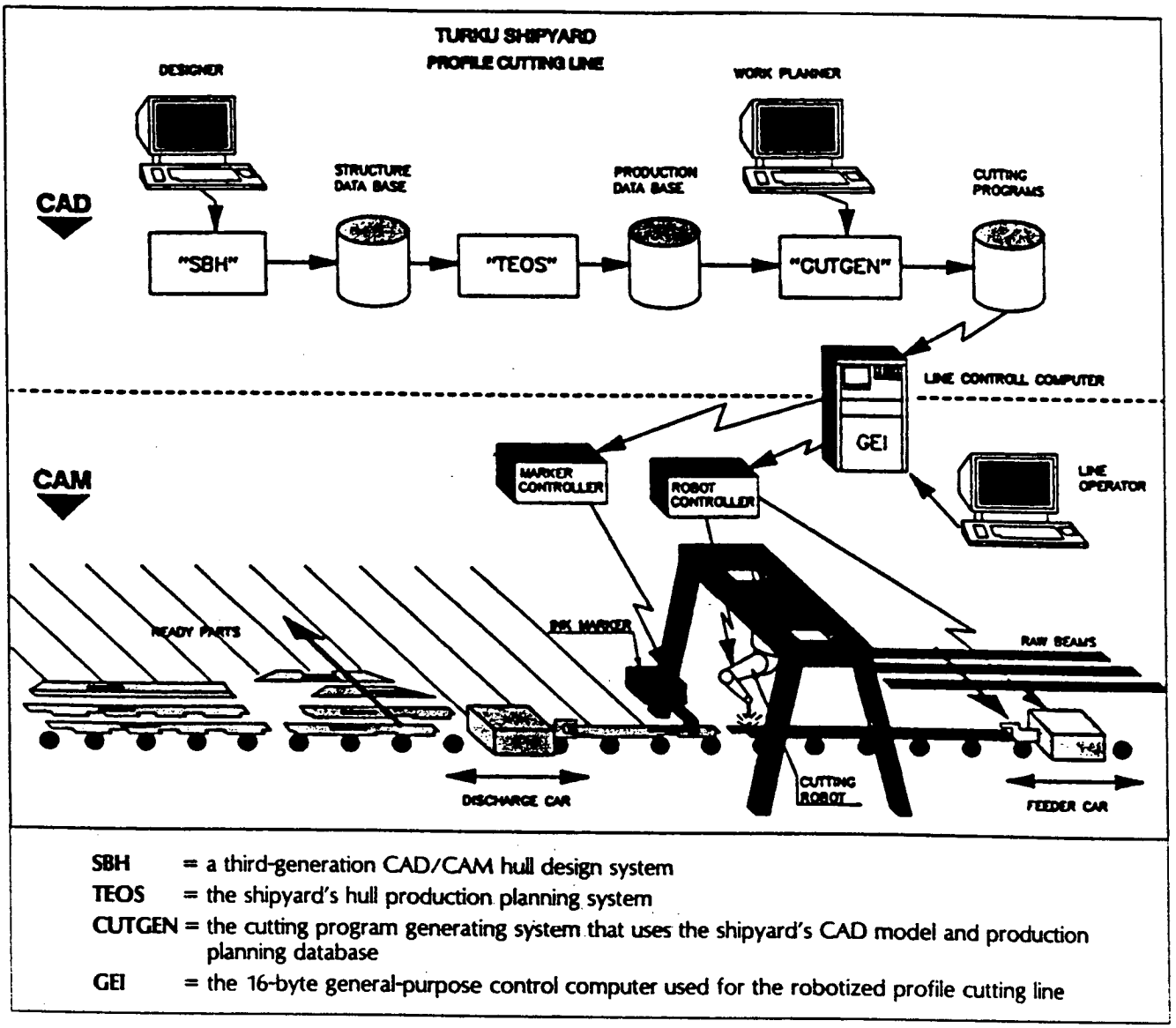

Figure 12. The CIM concept of profile cutting and marking.

tion plasma cutting torches. The plasma cutting torches were used on plate thicknesses up to 25 mm while thicker material was cut using the oxypropane torches. Cutting was performed under water on three water tables, with the plate surface submerged 50 to 75 mm. (Use of a water table significantly reduces arc noise, arc glare, and particulate levels.) Three cutting tables were used to maintain cutting efficiency using a simultaneous loading, cutting, and unloading cycle. Interactive nesting software reduced scrap significantly and a rationalization program reduced the combinations of plate thickness and composition. With the above economies, a return-on-investment period of less than two years was expected.

Overall costs for plasma cutting compared to oxyfuel cutting will vary depending on a large number of factors specific to a particular fabricator. Using the cost to cut a linear meter of plate as the basis for comparing the two, the plasma torch operating costs are higher, but the labor costs are much lower because of the higher cutting speeds. Comparing the overall operating costs for one nitrogen water injection plasma torch with one oxyfuel torch, the cost of the plasma torch is 30 percent that of the oxyfuel torch for 6-mm plate and 65 percent at 25 mm (*81*).

Plasma arc cutting is used extensively by fabricators of construction equipment in the United States, particularly Caterpillar and J.I. Case. One installation on a large CNC plasma punch press uses air and air/oxygen plasma cutting to profile the side frames for large 4 × 4 tractors, typically in plate thicknesses of 12 mm. This machine is equipped with automatic plate loading and parts unloading to further enhance productivity. CNC plasma punch presses combine plasma cutting and mechanical punching operations in one

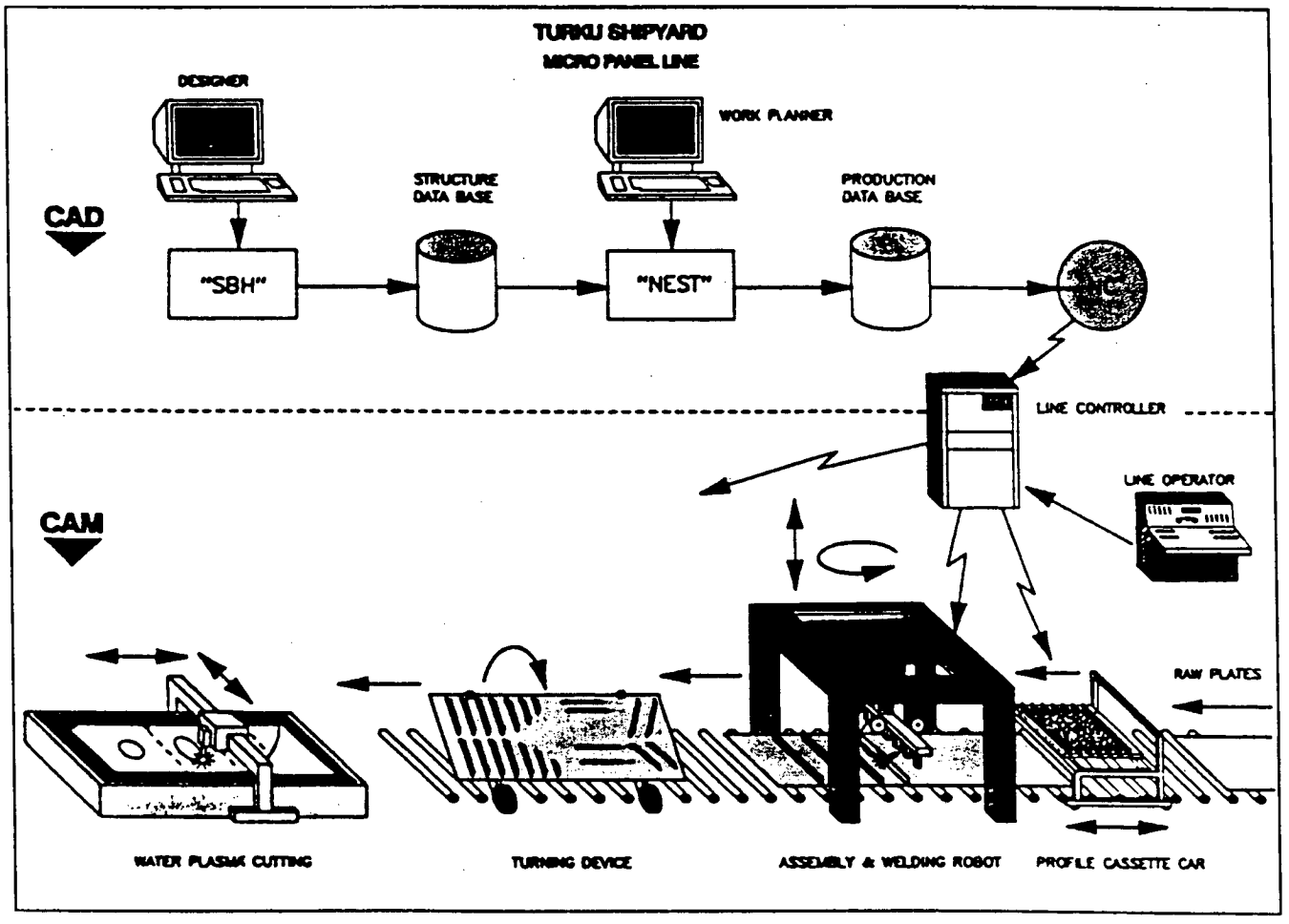

SBH = a third-generation CAD/CAM hull design system

Figure 13. The CIM concept for small, stiffened, irregularly shaped panels.

machine and can significantly increase productivity by this dual operation on one machine (*35*).

BRIDGE FABRICATION

Oxyfuel cutting was and, to a considerable extent, still is the predominant process used for plate profiling and joint preparation of bridge steels. While the oxyfuel process is still most efficient and cost-effective for cutting square and bevelled edges in plate thicknesses over 25 mm, the use of plasma cutting in bridge fabrication is increasing. A number of structural fabricators that use plasma cutting for structural building work also contract for bridge work. The plasma cutting process has also been used for bridge work by some of these fabricators.

Typical use of oxyfuel cutting in the past was for square and bevel cutting of beam flanges and webs; for example, square butt or T-butt joints for web splices up to 19 mm, or web to flange joints where the web does not exceed 19 mm, also double-vee and single-vee joint preparations, and double-J preparations for plate girder flange splices. This was accomplished through the operator's attentive use of simple mechanized equipment such as a linear tractor, and the accurate control of process gases (*83*). While this is labor-intensive, for material thicknesses typically involved with flange splices, oxyfuel cutting is still the most effective process to use.

The developments in plasma cutting have produced savings in time and labor costs by using faster plasma cutting process on material thicknesses up to 25 mm. The savings are realized when the process is applied to cutting large lengths of plate. In bridge structures, this applies primarily to the webs of fabricated beams. Repeat cutting of other parts, notably web stiffeners, would also be appropriate for plasma cutting as the stiffeners are often in the thickness range of 9 to 12 mm ($^3/_8$ to $^1/_2$ in.) and are cut with nominally square edges. Multiple torch cutting with oxyfuel would rival the productivity of a single plasma cutting torch, and shearing becomes a possibility for simple rectangular shapes.

The construction of the Oshima bridge in Japan (*84*) involved 5359 tons of steel. At the time of completion in 1976, it was the second largest continuous truss bridge in the world at 1020 m long. Much of the construction involved plate and section in thicknesses of 30 to 50 mm, with expansion joints made from plate 135 mm thick. Consequently, most of the cutting was performed by the oxyfuel process and NC cutting and marking was employed via design data input.

Construction of an arched steel railway bridge over the Brisbane River (*85*) involved fabrication of three steel sections for the main part of the bridge, two 36-m-long end sections and a 60-m central span. Fabrication consisted of two inwardly inclined arches comprising an angled box-like design from plate material. Thermal cutting of plate thicknesses up to 89 mm (3.5 in.) was achieved using oxyfuel cutting, including profiles for the arches, flanges, and gusset plates.

A partially collapsed bridge in New Zealand (*86*), brought about by river water undermining of one of the piers, was replaced by a new bridge of box girder construction. Flanges were 12 in. × $^3/_4$ in. with 10-in. × $^1/_2$-in. doubling plate with bracing by 3.5-in. × 3.5-in. × 0.5-in. angle. All cutting was carried out by oxyfuel cutting.

Redpath Dorman Long, a major U.K. structural steel and bridge fabricator, installed nitrogen water-injection plasma arc cutting equipment in the late 1970s (*87*). The gantry-type cutting machine was equipped with two plasma cutting torches and two triple-contour bevel cutting heads, each with three oxyfuel cutting torches. A 19-m × 4-m water table was installed for underwater cutting to reduce fume and noise levels. CNC via punched tape is used to control the machine. One of the first jobs for this equipment was cutting 500 castellas. This involves cutting an I-beam about its centerline into a shape ready to be rewelded to produce a castellated beam. Previously, this job was completed using a web crawling tractor with an oxyfuel cutting torch, taking 40 to 50 min. Using the two plasma arc cutting torches, six beams were loaded into each of two jigs. The second jig was unloaded and reloaded while the first batch was cut, thus maximizing productivity. The two torches travelled at 2.3 m/min, equivalent to a total cutting speed of 4.6 m/min, enabling two castellas (from one beam) to be cut in 5 to 6 min, and all six in only 20 min; less than half the time for one castella using the old method. This is a classic illustration of how significant improvements in productivity can be achieved through the thermal cutting process, by maximizing use of the cutting equipment and the latest cutting guidance machines. This is the usual result of the change from mechanized oxyfuel cutting to CNC/DNC plasma cutting.

A fabricator of steel beams in Finland (*88*) manufactures beams for construction and shipbuilding applications. The beams range in size from 250 to 2,700 mm deep, with flanges from 50 to 800 mm wide and up to 50 mm thick. Welded beams have 30 to 50 percent weight savings compared with rolled beams of similar width and flange width. Standard products produced include I-sections for roof girders and columns; H-sections for columns; asymmetrical sections for crane and bridge beams; box sections for pillars, supports and steel frames; and L- and T-sections for shipbuilding. Cutting of hot rolled steel plate is carried out using two oxyfuel cutting machines that have a total of 48 torches. The large number of torches, used for stripping of the plate, would presumably provide higher productivity compared with a smaller number of plasma cutting torches. However, there was no discussion on the number of torches used simultaneously. All welding is carried out using the submerged arc process, making two web-to-flange welds simultaneously on one side. The beam is turned over for similar welds on the other side of the web.

Cleveland Bridge, a major U.K. fabricator of bridges and structural steel, opened a new facility in 1982 on a green field site (*89*). Factory capacity is 33,000 tons of heavy fabricated steelwork, based on single shift operation with a workforce of 500. Much of the output is exported around the world, an example being a bridge for Cairo, Egypt. Plate cutting is carried out using the oxyfuel process, using optical and CNC cutting machines. One CNC machine controls cutting, marking, and punching heads, while another operates a flame planing unit with four heads, each carrying three oxyfuel torches for bevel cutting. A flame stripping machine with nine torches is also used for stripping plate. Water tables are used to control fume and reduce distortion.

A large numerically controlled, gantry-type, high-speed drilling machine is used for tasks such as hole drilling of 27-m plate girders. Edge and end planes and milling cutters with a bed length of 10 m can be used for mechanical edge preparation. This is often found to be an economical alternative to grinding where hardness requirements must be met after flame cutting. Plasma arc cutting was not used, and this is assumed partly due to the significant use of triple bevelling heads for plate edge preparation.

Significant improvements in productivity can be achieved by the installation of automated beam lines for general structural steelwork and bridge fabrication lines. CNC drilling and coping centers and lift-and-carry material handling systems can be combined to maximize productivity (*90*). Automated coping systems usually operate with three or four cutting torches and are capable of bevel cutting of flanges up to 45 deg for weld preparations. Consequently, the preferred cutting process is oxyfuel cutting, both for the number of torches and the effective cutting thickness on beam flanges. Comparing man-hour estimates for coping at a variety of structural fabricators, the benefits of a CNC coping center translate into a 10-to-1 gain in productivity over manual cutting (*90*).

The latest state-of-the-art techniques have been incorporated into a new bridge production line at NKK in Japan (*91*). The line employs 14 articulated-arm welding robots and a plasma cutting system capable of cutting 25-mm-thick steel

plate at 3 m/min. The line also includes a laser beam cutting head that cuts steel plate for bridge fabrication; two 3 Kw CO_2 lasers, each capable of cutting plate at 1 m/min. The panel line includes assembling, welding, straightening, drilling, and finishing operations. Total investment was $17 million and the cost of an associated production control system to be integrated with the computer integrated manufacturing (CIM) program is expected to cost a further $68 million. NKK is Japan's second largest steelmaker and also a diversified engineering company.

General Observations from Visiting Bridge Fabricators

Three bridge plants were visited, representing a cross section of the types of fabrication facilities. These ranged from small family-run businesses to large nationally based fabricators. The mix of technologies and degree to which the latest technologies were applied varied widely. This makes it difficult to generalize on the level of technology presently used. At one end of the scale is mechanized cutting with a tractor on rail unit; at the other end, automated cutting with direct numerical control (DNC) on a large profiling table.

The structural steel business is very competitive, and "good-enough" technology reigns in many cases. Where throughput requirements did not demand high speeds, the thermal cutting technology seen was crude; greater efficiency in cutting operations did not result in improved overall efficiency.

In terms of automated beam handling, even the smaller plants had state-of-the-art equipment for CNC cutting and drilling of beam ends. CNC coping equipment for structural I-beams involves the use of three or four cutting torches. The capital equipment cost of plasma cutting torches in this case is prohibitive and, in any case, the thickness of flanges, especially the effective thickness when bevelling, makes the oxyfuel process the natural choice.

One of the issues affecting the more widespread use of plasma cutting is the need for totally 90-deg edges on some parts, such as breakaways for overhead sign supports. As plasma cutting can often produce a slight bevel angle on cut edges of a few degrees, the need to refinish the parts by grinding makes oxyfuel cutting more attractive. However, when cutting plate for webs of fabricated I-beams, the plasma cutting process is faster than oxyfuel cutting and introduces less heat into the plate, lowering distortion. Thus, not only are productivity improvements readily obtainable through increased cutting speed, but improved fit-up resulting from reduced distortion can be achieved. In turn, the improved fit-up can reduce the cost of welding operations by minimizing joint gaps and reducing fit-up time.

Welding mechanization was generally of a high level, from simultaneous double sided submerged arc welding (SAW) of flange-to-web joints to flux cored arc welding (FCAW) of stiffeners.

The highly competitive, small-profit-margin nature of steelwork fabrication and the conservatism of the bridge fabrication industry produce a climate that precludes investment in new cutting technology. Companies compensate for OFC steel plate distortion in their cutting procedures. One large fabricator uses angle iron tacked alongside the cutting machine to guide a cutting head, a simple but effective method that counteracts distortion and achieves the desired camber in the beam web. Other companies use standard structural sections and have the limited amount of profiled plate they use cut at job shops or steel service centers. Hence, the requirement for faster and more productive cutting equipment in-house is minimal.

INTERNATIONAL STANDARDS AFFECTING PLASMA ARC CUTTING

A comprehensive standard on classification, terms, and definitions for flame and plasma cutting, DIN 8518, was produced in Germany in 1974 (*92*). While this gave a very good description of various faults and defects, they were not quantified and no recommendations were included on defect tolerance limits. In 1977, the American Welding Society (AWS) published AWS C4.1-77, "Criteria for Describing Oxygen-Cut Surfaces" (*93*), although this was not as comprehensive as the German standard. This standard has been updated and combined with other information into ANSI/AWS C4.2-90 Operator's Manual for Oxyfuel Gas Cutting (*94*). This describes general procedures for setting up and operating oxyfuel gas cutting equipment as well as pointers on achieving good cut quality. AWS first published recommended practices for plasma arc cutting in 1973. This document was superseded by AWS C5.2-83 "Recommended Practice for Plasma Arc Cutting" in 1983 (*95*). Although this document gives some typical values for heat-affected zone width for plasma-cut edges for steel, stainless steel, and aluminum, they are generic in nature. Little or no guidance is given in areas such as classification of edge defects or recommendations to improve cut quality. This document is presently in the revision stage (*96*); it may take an additional two years before the document is published as an official ANSI/AWS document.

The German standard DIN 2310 is the most comprehensive available for the description, classification and quantification of thermal cutting (*97,98,99*). Divided into six parts, it includes specific sections on oxyfuel (*100*), plasma (*101*), and laser (*102*) cutting.

In 1990, Engblom and Falck (*103*) published a comprehensive review of international standards dealing with the classification of thermally cut surfaces. More than half of this work was based on DIN 2310, but it also included AWS C4.1-77 and a number of other standards from France, Russia, Sweden, Japan, and Hungary.

The British Railways Board standard, BR 539:1983, on thermal cutting quality classifications is an acceptance standard for oxygen- and plasma-cut exposed edges on steel plates (*104*). This standard quotes two quality levels, the first requiring removal of at least 1 mm from the entire cut edge, the second referring to acceptance with reference to a comparison sample. AWS provides an oxygen cutting surface roughness gauge (AWS C4.1-G) in the form of four surface replicas (*105*) and a wall chart, "Criteria for Describing Oxygen-Cut Surfaces" AWS C4.1-WC (*106*). It is suggested that these could be used to judge plasma-cut edges as well, although replicas of plasma-cut edges would presumably be preferred.

The British Bridge Welding Code, BS 5400, covers steel, concrete and composite bridges, with Part 6 covering specifications for materials and workmanship for steel (*57*). The revised requirements concerning flame cutting permit edges and ends to be flame cut (providing at least one of several alternative requirements are satisfied), and are as follows:

1. Hardness of the cut edge does not exceed 350 VHN.
2. The cut edge is not subjected to applied stress.
3. The cut edge is wholly incorporated in a weld.
4. Material from the edge is removed by grinding or machining to the extent of either 2 mm or the minimum necessary to demonstrate that the hardness on the edge does not exceed 350 VHN.
5. The edge is softened by a suitable heat treatment approved by the engineer and is shown by dye penetrant or magnetic detection procedure to be free from cracks.
6. Material is Grade 43 and is not greater than 40 mm thick, and edge preparation is by machine flame cutting.

It should be noted that BS 5400 Part 6 does not specifically mention plasma cutting as distinct from oxyfuel cutting. However, thermal cutting is taken to include both oxyfuel and plasma cutting, and edges cut by either process are considered to be subject to the above requirements. Discussions with British Steel indicated that bridge fabricators use plasma cutting widely, applying the same criteria for cut edge quality whether using plasma cutting or oxyfuel cutting.

The ANSI/AASHTO/AWS D1.5-88 Bridge Welding Code (*107*) specifies maximum surface roughness for oxygen cutting (i.e., oxyfuel cutting, of 1000 microinches for material thicknesses up to 4 in.). The Bridge Welding Code does not mention plasma arc cutting specifically. This is interpreted by some state highway departments to mean that the plasma cutting process shall not be employed. However, other departments interpret the Code to allow plasma arc cutting, applying the same criteria for plasma-cut and oxyfuel-cut edges. AASHTO Commentary on the Bridge Welding Code (*108*) refers to the use of thermal cutting and thermal cut edge (TCE) as generic terms to describe both plasma- and oxyfuel-cut edges in welding specifications.

Unlike BS 5400, the Bridge Welding Code does not specify a particular maximum hardness for the cut edge. The Commentary on the Code mentions that thermal cut edges (both from oxyfuel and plasma cutting) can frequently have surface hardnesses in excess of the equivalent of HR_c50 to HR_c60 and that this localized region can be removed by shallow grinding of the surface. Some states in AASHTO Region 1 specify a maximum surface hardness of HR_c30 for plasma-cut edges based ostensibly on work for the New York State DOT to avoid hydrogen cracking in welds in structural steel buildings. The HR_c30 maximum edge hardness requirement is written in the Steel Construction Manual for NYDOT. While the overly conservative nature of this requirement is recognized, and is not incorporated in the Bridge Welding Code, it is employed in daily practice by several state DOTs including several in Region 1, and also in Colorado and Oregon, according the results of the survey carried out for this project.

SUMMARY

Plasma cutting is being increasingly utilized throughout the fabrication, construction, shipbuilding, and general manufacturing industries. Use of the process in the bridge fabrication industry is fairly low. There are a number of reasons for this, including its relatively high capital costs compared with oxyfuel cutting equipment, and economic factors limiting the cutting thickness, making the process suitable for bridge steels (up to 19 or 25 mm). It should be noted that for an automated cutting machine with CNC/DNC, the cost of the cutting equipment itself is a small portion of the system's total cost. The present lack of specific guidelines for plasma arc cutting in the Bridge Welding Code is a significant deterrent factor to its application in many states.

Compared with oxyfuel cutting, plasma cutting shows particular advantages in that it can cut any metal, not just carbon and low-alloy steels, and it can do so at a much faster speed, particularly at thicknesses below 15 mm, which covers the majority of cutting applications. The thinner the material, the greater the advantage in cutting speed for plasma cutting. This potential can best be exploited in mechanized profile cutting operations for shape cutting of steel plate, where speeds of several meters per minute can be employed, depending on cutting power and material thickness. Since a fair amount of plate cutting for fabricated plate girder webs in the bridge industry involves single torch operation, plasma cutting would serve its needs well.

RESULTS OF THE PLASMA CUTTING SURVEY OF STATE DOTs AND AISC CATEGORY III BRIDGE FABRICATORS

Two surveys were carried out to ascertain the use of plasma arc cutting in the bridge fabrication industry; one was sent to state departments of transportation (DOTs) and one to bridge and general American Institute for Steel Construction (AISC) fabricators. Copies of the surveys are presented in Appendix C.

Survey Results for State DOTs

Surveys were sent to the state DOTs in the fifty states and the District of Columbia. Twenty-nine replies were received as follows:

Arkansas	Massachusetts	Oregon
California	Michigan	Pennsylvania
Colorado	Minnesota	Texas
Florida	Mississippi	Utah
Georgia	Missouri	Vermont
Idaho	Nebraska	Virginia
Illinois	Nevada	Washington
Iowa	New Mexico	Wyoming
Louisiana	Ohio	District of Columbia
Maine	Oklahoma	

Of the 29 replies, 21 state DOTs indicated that they allow plasma cutting, 6 noted that they did not, and 2 noted that there were no specifications and none of the fabricators used it. Plasma cutting is not allowed in work performed for California, Iowa (except webs on a case-by-case basis), Mississippi, New Mexico, Oklahoma, or Pennsylvania. Florida and Idaho stated that the Code did not discuss the process and that, therefore, there were no specifications to cover it (presumably meaning that they did not allow its use). It is interesting to note that most of the states allowing use of plasma cutting do so on the basis that its use is not excluded, or apply similar criteria to plasma cutting as they do to oxyfuel cutting. At least three states (Colorado, New York, and Oregon) apply the additional criterion that the plasma-cut edge shall not exceed a hardness of HR_c30. The additional requirement is written into the state construction and material specifications. Although 21 states allow its use, only 14 states noted that any of the fabricators building bridges for the state actually used the plasma cutting process; more specifically, 9 indicated that none of the fabricators they routinely use to perform state work use the process.

Twelve of the 14 respondents indicated that they experienced no problems in the use of plasma cutting. Of the other two, Virginia indicated that surface profile was a problem when painting or galvanizing, and Michigan stated that noise levels were high, a lot of fumes were generated, the process was expensive, and it was limited to a 25-mm thickness (presumably for economic rather than technical reasons). Michigan stated that water will cause quenching of the edge, although the Bridge Welding Code does not comment on edge hardness or underwater cutting since it only refers to oxyfuel (oxygen) cutting.

The thickness range cut using plasma cutting was usually quoted (7 of 15 replies) as 6 mm to 19 mm or 25 mm ($^1/_4$ to $^3/_4$ or 1 in.), although five respondents quoted upper thickness limits of 38 mm to 64 mm (1.5 to 2.5 in.). The materials cut are ASTM A36, A572 Grade 50, and A588 (i.e., A709 or AASHTO M270 G36, G50, and G50W).

Quality criteria applied to plasma-cut edges were usually quoted (11 of 15 responses) as those specified in D1.5-88 (i.e., the Bridge Welding Code). Two included the hardness limit of HR_c30, while only one said ground edges and the other quoted ANSI 1000.

The responses were mixed concerning the need for grinding of the as-cut edges. Six said yes, three said no, four stated that the requirements were the same as stated in the Bridge Welding Code. One added the additional requirement for the HR_c30 limit for edge hardness, one indicated that grinding was only required if the edge hardness exceeded the HR_c30 limit. The Bridge Welding Code requires grinding or machining to meet the specified edge roughness requirements and to repair certain edge defects in the plate from material or cutting defects (Table 3.1, page 29 of the Code). It does not specify a particular maximum hardness for the cut edge. It is interesting that many responses were simply "yes" or "no," implying different requirements for oxyfuel- and plasma-cut edges. Mention was made by one respondent of the need for grinding of corners if the edges were to be painted. This requirement is already in the Bridge Welding Code for oxyfuel cutting, Item 3.2.9, page 30, requiring a $^1/_{16}$-in. radius or equivalent flat on the corners to hold paint.

As mentioned above, the Bridge Welding Code does not specify a particular maximum hardness for the cut edge. The AASHTO Commentary on the Code mentions that thermal cut edges, both from oxyfuel and plasma cutting, can frequently have surface hardnesses in excess of the equivalent of HR_c50 to HR_c60 and that this localized region can be removed by shallow grinding of the surface. The specification of a maximum surface hardness of HR_c30 for plasma-cut edges is New York DOT based to prevent hydrogen cracking in welds in structural steel buildings. The HR_c30 maximum edge hardness requirement is written in the Steel Construction Manual for NYDOT. While this requirement is not incorporated in the Bridge Welding Code (it is seen to be overly conservative), it is employed in daily practice by several state DOTs including Colorado (AASHTO Region 8), New York (Region 1), and Oregon (Region 10).

Automation of the plasma arc cutting process is fairly high. Nine out of 12 respondents indicated that at least 50 percent of cutting is carried out by CNC or DNC shape cutting machines; five indicated that all cutting was performed in this manner. Five respondents stated that 50 percent or more of the cutting was mechanized, employing track-mounted systems such as Bug-O or Gullco tractors. Manual cutting accounted for 50 percent in 2 states and 25 percent in another, the other 8 indicating no manual cutting. No information was received in response to the question concerning knowledge of the actual equipment used (i.e., manufacturer).

The following 11 companies were mentioned in response to the question concerning fabricators' using plasma arc cutting:

- Phoenix Steel, WI (mentioned by four states)
- DeLongs Inc., MO (mentioned by two states)

- Blattner Engineering, MO
- Capital Steel, NE
- Husker Steel, NE
- Kard Bridge, OH
- Lewis Engineering, MN
- Manufab Inc., LA
- Oregon Iron Works, OR
- PDM Structural Group, IA
- Zimmerman Metals, CO

Most of these companies were contacted in the simultaneous survey of fabricators discussed below.

Survey Results for AISC Category III Fabricators

Surveys were sent to 100 fabricators across the country. Of the 30 responding companies, 11 use plasma arc cutting to a greater or lesser extent for structural steel buildings and/or bridge fabrication. The companies using plasma cutting, and the type of fabricating work for which they use it are as follows:

Phoenix Steel, Eau Claire, WI	Bridges/buildings
Drake Williams Steel, Omaha, NE	Bridges/buildings
Tampa Steel Erecting Co., Tampa, FL	Bridges (stainless steel only)/buildings
Leonard Kunkin & Associates, Line Lexington, PA	Bridges (stainless steel only)/buildings
DeLongs Inc., Jefferson City, MO	Bridges
Capital Steel, Lincoln, NE	Bridges
High Steel, Lancaster, PA	Bridges (very little use)
Cives Steel Co. Northern Div., Gouverneur, NY	Buildings
Egger Steel Co., Sioux Falls, SD	Buildings
East Coast Steel, Greenfield, NH	Buildings
PDM Structural Group, Des Moines, IA	Plate/tank work only

Of the 11 companies listed above, only 6 use plasma cutting for bridge fabrication work on a regular basis and one of these only for stainless steel tees and shims.

No problems were reported for plasma cutting by the majority (8 of 11) of these fabricators. One company reported problems obtaining a square edge, particularly on thicker material, and also in obtaining approval from Iowa and Ohio DOTs to use the process. Another reported rounded edges and fume level problems, while a third indicated dust/fume levels as a drawback.

Two companies that formerly used plasma cutting stopped using it, one because of nitrogen contamination of the cut edges and subsequent difficulties with weld quality. The other company was considering using plasma cutting again in the near future. A third company had just purchased a CNC shape cutting machine equipped with oxygen plasma arc cutting and oxyfuel torches. Oxygen plasma cutting was selected to minimize the potential for edge contamination perceived from use of nitrogen plasma cutting. However, the company will not be using the equipment for bridge fabrication because they consider that the Bridge Welding Code prohibits the use of plasma cutting by allowing only oxyfuel cutting and air carbon arc gouging.

Fabricators either were unaware of which states allowed plasma cutting or believed that all states allowed it. Only 5 companies tried to list individual states for which they had worked. The listed states were Alabama, Arkansas, Colorado, Florida, Georgia, Illinois, Indiana, Kansas, Michigan, Minnesota, Missouri, Nebraska, and Wisconsin. States that allowed plasma cutting with restrictions were Iowa, New York, and Ohio. In the cases of California, New Mexico, and Oklahoma, they were mentioned as allowing plasma cutting, but their respective state DOTs indicated that it was not allowed.

The thickness range quoted for plasma cutting of bridge steels fitted the bounds of $^3/_{16}$ to $^3/_4$ in. for six out of eight of the respondents. The other two quoted 1.25- and 2-in. upper thickness limits. For structural steel building work the thickness range fitted $^1/_8$ to $^3/_4$ in. for seven of nine respondents, the same two companies as before quoting 1.25- and 2-in. upper thickness limits.

The materials cut for bridge work are ASTM A36, A572 G50, and A588 (i.e., A709 G36, G50, and G50W), with one fabricator also cutting stainless steel. Materials for building work are mostly mild steel and A36, but include some A572, A588, and stainless steel.

The quality criteria applicable to plasma-cut edges were the same as for oxyfuel-cut edges by all nine of the respondents completing this question. Three additionally quoted the HR_c30 maximum allowable hardness required by Colorado, Connecticut, Maine (not mentioned by Maine DOT), New Hampshire, New York, and Oregon.

The answers concerning the requirements for grinding the plasma-cut edge were as diverse as those given by the state DOTs. Six said grinding was required, with three of these stating that less grinding was needed for plasma-cut edges than for oxyfuel-cut edges. Four stated that grinding was not required. Only one company responded that the same requirements as in the D1.5 Bridge Welding Code applied. The overall view was that if grinding was required at all, then less material needed to be removed to meet the surface roughness or hardness criteria.

The degree of cutting automation was fairly high; of 12 respondents, four used CNC cutting for 95 percent or more of their work, six companies using automated cutting predominantly. Five companies used mechanized cutting predominantly, and only one used manual cutting more than mechanized or automated systems.

Specific equipment employed includes the following:

Thermal Dynamics PAK 15 XC	manual (5%), mechanized (60%), CNC (35%)
Hypertherm MAX 100	mechanized (20%), CNC (80%)
Hypertherm HT 400	mechanized (5%), CNC (95%)
Hypertherm	manual (70%), mechanized (30%)
L-Tec CM250 cutting machine	CNC (100%)
Hypertherm	manual (10%), mechanized (90%)
Hypertherm on MG cutting machine	CNC (95%), mechanized (5%)
Thermal Dynamics on an L-Tec CM250 cutting machine	manual (5%), mechanized (60%), CNC (35%)
Thermal Dynamics on Whitney Panelmaster	mechanized (2%), CNC (98%)

Hypertherm, Thermal Dynamics, and L-Tec (now owned by ESAB) are the three largest manufacturers of plasma cutting equipment. L-Tec is the largest system builder, followed by Messer Griesheim (MG), integrating the cutting machine, the plasma cutting equipment, and the CNC units controls. This is reflected in the equipment listed above which is used at the various fabricators who employed plasma arc cutting for bridges and/or structural steel buildings.

SUMMARY

The interpretation of the Bridge Welding Code regarding the use of plasma arc cutting varies from one state DOT to another. As the Code does not contain any mention of plasma cutting, some states interpret this as meaning that plasma cutting is not allowed, while others state that it is not excluded from use and therefore apply the same criteria to oxyfuel- and plasma-cut edges. A number of states apply the additional requirement of a maximum edge hardness of HR_c30 for plasma-cut edges and oxyfuel-cut edges (i.e., all thermal cut edges). This inconsistency needs to be concerning the acceptability of plasma-cut edges, in terms of their metallurgical and mechanical performance. This issue is complicated somewhat by the range of plasma cutting systems available, particularly the influence of plasma gas on the characteristics and subsequent performance of welded and free edges. This will be addressed in the experimental work in Task 6 of the Working Plan for this project. The need for grinding of the plasma-cut edges varies significantly between individual states and individual fabricators and reflects the variety of plasma cutting gases and the paucity of definitive data based on metallurgical issues and mechanical performance of welded and free edges. This will also be addressed in the planned laboratory work.

The level of usage of plasma arc cutting in the bridge fabrication industry is fairly low compared to its use in other industries, and is reflected in the limited number of fabricators that use the process and responded to the survey. The present lack of definitive guidelines for use of the process in the Bridge Welding Code is certainly one reason for its limited use. However, individual fabricators mention economic reasons that may account for plasma cutting's not being more widely used. Lack of familiarity with the benefits of the process and a lack of knowledge of other issues involved also plays a part. Therefore, information concerning the basic operating principles and differences between the types of commercially available plasma cutting systems is being put in the User's Guide being produced by this project.

Steel companies routinely use plasma cutting at the steel mill to cut plate. However, these cut edges rarely end up as free edges or welded edges in the bridge structure, with the possible exception of some web splice joints.

The plasma arc cutting process is not widely used in the bridge fabrication industry, with barely a dozen companies identified in the survey of fabricators and state DOTs as using the process in this country. Internationally, use of plasma cutting in the bridge industry is not much higher, although use in shipbuilding is appreciably greater. This factor is largely related to the thickness range of material used in shipbuilding, which is lower than that for bridge fabrication. In the bridge industry, a lot of work is carried out for coping I-beams and stripping plate with multiple oxyfuel torches; when triple bevelling heads are used for edge bevelling for weld preparations, use of three plasma torches would be cost prohibitive. In practice, much plate stripping and cutting of plate girder webs is carried out with only two oxyfuel torches, and cutting speed could be considerably increased by using one or two plasma cutting torches. Use of plasma cutting for webs, stiffeners, and gusset plates in the thickness range of 6 mm to 19 mm ($^1/_4$ to $^3/_4$ in.) can realize significant improvements in productivity with good cut-edge quality. In many cases the absence of any comment and guidelines for plasma cutting in the Bridge Welding Code prohibits or severely limits the application of plasma cutting in practice.

LABORATORY TEST PROGRAM

Plate Material

The materials used in this work were AASHTO M270 steels, Grades 36, 50, and 50W in thicknesses ranging from 9.5 mm to 19 mm ($^3/_8$ to $^3/_4$ in.). The combinations of material types and thicknesses are shown in Table 2. The specifications for AASHTO M270 steels and their equivalent grades are shown in Table 3.

Plate steels were purchased direct from Bethlehem Steel and US Steel mills and work was carried out to verify the chemical composition of each material. The compositions were compared to the mill certificates and found to be within specifications. Plate material compositions are shown in Table 4.

TABLE 2 Combinations of plate material types and thicknesses

Material Type	Thickness	
AASHTO M270 Grade 36	9.5 mm	⅜ in.
AASHTO M270 Grade 36	12.7 mm	½ in.
AASHTO M270 Grade 50W	12.7 mm	½ in.
AASHTO M270 Grade 50W	19 mm	¾ in.
AASHTO M270 Grade 50	19 mm	¾ in.

TABLE 3 Specifications for AASHTO M270 steels and their equivalents

AASHTO M270 Grade	Equiv. AASHTO Grade	ASTM A709 Grade	Equiv. ASTM Grade	Min. Yield (ksi)	Min. T.S. (ksi)	Availability	
						Plates	Shapes
36	M183	36	A36	36	58	to 4" incl.	All Groups
50	M223	50	A572	50	65	to 4" incl.	All Groups
50W	M222	50W	A588	50	70	to 4" incl.	All Groups
70W	M313	70W	A852	70	90	to 4" incl.	Not Applicable
100	M244	100	A514	100 90	110 100	to 2½" incl. OV 2½-4" incl.	Not Applicable Not Applicable
100W	M244	100W	A514	100 90	110 100	to 2½" incl. OV 2½-4" incl.	Not Applicable Not Applicable

Plasma Arc Cutting Trials

Plasma cutting trials were carried out according to Table 5. This included study of air, nitrogen, and oxygen plasma cutting in air and underwater plasma cutting with oxygen and nitrogen plasma gases. AASHTO M270 steels, Grades 36, 50, and 50W in thicknesses ranging from 9.5 mm to 19 mm ($^3/_8$ to $^3/_4$ in.) were cut. Cutting procedure development was carried out to develop tolerant cutting procedures for square edges, and also bevelled edges. Both square and bevelled edges were used for joint preparations in subsequent welding trials.

Gas Plasma Cutting

Cutting trials were carried out by varying the cutting speeds across a wide range while maintaining the cutting power, using 200 A cutting current with the Hypertherm MAX 200 power source. The plasma torch was carried by a mechanized carriage, Figure 14, and linear cuts were made side by side on sections of plate, Figure 15. Successively increasing travel speeds were used, increasing in increments of 125 mm/min (5 in./min). This procedure was conducted for each combination of cutting gas (oxygen, air, and nitrogen) and the five combinations of plate material and thick-

TABLE 4 Composition of plate steels

Plate Grade	Thick (mm)	C	Mn	P	S	Si	Al	Cu	Ni	Cr	V
36	9.5	0.15	0.69	0.013	0.009	0.24	0.042	0.22	0.012	0.022	0.001
36	12.7	0.13	0.73	0.028	0.017	0.25	0.036	0.24	0.009	0.033	0.003
50	19	0.19	1.09	0.021	0.015	0.26	0.037	0.025	0.002	0.024	0.056
50W	12.7	0.12	0.90	0.013	0.011	0.34	0.035	0.24	0.28	0.55	0.027
50W	19	0.12	0.91	0.016	0.014	0.38	0.041	0.26	0.32	0.592	0.037

TABLE 5 Matrix of plasma cutting trials

Material/Thickness	Plasma Cutting Processes	Tests on Square Edges
M270 Grade 36 (A36) 9.5 mm (⅜ in.)	Air Nitrogen Oxygen U/W Nitrogen U/W Oxygen	Profile measurement Metallography Microhardness
M270 Grade 36 (A36) 12.7 mm (½ in.)	Air Nitrogen Oxygen U/W Nitrogen U/W Oxygen	Profile measurement Metallography Microhardness Gas Analysis
M270Grade 50W (A588 50W) 12.7 mm (½ in.)	Air Nitrogen Oxygen U/W Nitrogen U/W Oxygen	Profile measurement Metallography Microhardness Gas analysis
M270Grade 50W (A588 50W) 19 mm (¾ in.)	Air Nitrogen Oxygen U/W Nitrogen U/W Oxygen	Profile measurement Metallography Microhardness
M270 Grade 50 (A572 50) 19 mm (¾ in.)	Air Nitrogen Oxygen U/W Nitrogen U/W Oxygen	Profile measurement Metallography Microhardness Gas analysis

U/W = Underwater cutting with water injection

Beveled edges with a 30 degree angle for single-V and single-beveled joints were also produced. Profile measurement included surface roughness, drag angle, kerf width, cut angle and dross level (Grades 1-5).

ness, making a matrix of 15 combinations. The assigned cut identification numbers are shown in Table 6. Cutting was carried out parallel to the plate rolling direction in each case and with the plate in the as-received condition (i.e., complete with any mill scale). Cutting was stopped about 50 mm (2 in.) from the opposite edge from which the cut was initiated. This allowed all specimens to be retained in the orientation in which they were cut. This technique facilitated specimen identification and direct comparison with other cutting trials. Specimens were subsequently cut from the "sprue" by cold sawing about 25 mm (1 in.) from the end, enabling accurate measurement of kerf width and cut angle. The criteria used to evaluate the cut edges were edge squareness (i.e., angular deviation from a 90-deg edge), edge roughness, kerf width, drag angle, and dross level (where appropriate).

These cutting trials established the range of cutting speeds which produced dross-free edges, the best cutting speed in terms of edge squareness, and the maximum cutting speed to sever the plate for each combination of plasma gas, material type, and thickness (Table 7). Typical cut quality for the best cutting conditions is shown in Figures 16 through 20 for all combinations of material type, thickness, and plasma cutting technique. These figures show the cut edge appearance, including drag angles, and a qualitative comparison of edge quality.

A subjective assessment was made of the dross level on a scale of 0 to 5, with 5 being the highest level. Notes were taken of dross adherence (i.e., if the dross could be removed without tools such as scrapers) where applicable. The dross levels were recorded photographically in each case.

Results showed that the largest tolerance band of dross-free cutting parameters is achieved with oxygen plasma gas, followed by air and nitrogen plasma gases (Table 7). For example, the "dross-free window" of cutting parameters for Grade 36 plate, 9.5 mm ($^3/_8$ in.) thick, is 2030 to 3300 mm/min (80 to 130 in./min) for oxygen plasma compared with 2795 to 3175 mm/min (110 to 125 in./min) for air plasma cutting, and no dross-free cutting conditions for nitrogen plasma cutting.

The maximum cutting speeds achieved using air and oxygen plasma cutting were often close to double those for nitrogen plasma cutting. For example, 4190 mm/min (165 in./min) for air, and 3685 mm/min (145 in./min) for oxygen, compared with 2415 mm/min (95 in./min) for nitrogen plasma cutting on 9.5-mm ($^3/_8$-in.)-thick Grade 36 plate; and 4165 mm/min (160 in./min) for oxygen, and 3050 mm/min (120 in./min) for

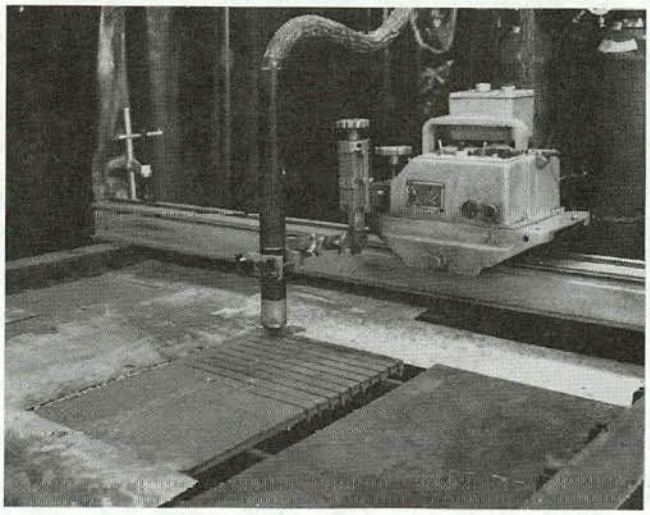

Figure 14. Mechanized plasma cutting system and plate cutting technique used for cutting parameter development.

air, compared with 1905 mm/min (75 in./min) for nitrogen plasma cutting on 12.7-mm ($^1/_2$-in.)-thick Grade 50W plate. Results on all grades and thicknesses of material showed faster maximum cutting speed for air plasma and oxygen plasma compared with nitrogen cutting. Air and oxygen plasma produce higher cutting speeds for an equal electrical cutting power because of the extra thermal effect of the exothermic oxidation of iron.

Naturally, the range of cutting speeds decreased with increasing plate thickness for all plasma gases, and the range of dross-free cutting speeds also decreased. For Grade 50 plate 19 mm ($^3/_4$ in.) thick, the maximum cutting speed was reduced to 1650 mm/min (65 in./min) for air plasma, 1270 mm/min (50 in./min) for oxygen plasma, and 510 mm/min (20 in./min) for nitrogen plasma cutting. The window of dross-free parameters was narrow at only 1015 to 1270 mm/min (40 to 50 in./min) for air plasma, while there were no dross-free conditions for nitrogen and oxygen cutting (Table 7).

Underwater Plasma Arc Cutting

The cutting technique employed was the same as that for the gas plasma cutting carried out at EWI, Figure 15. ESAB/L-TEC, Florence, SC, carried out the underwater oxygen and underwater nitrogen plasma cutting trials. Plasma cutting trials were carried out on all the combinations of parent plate type and thickness to develop parameters for optimum cut-edge quality. A CM-300 cutting machine was used with a Series 2000/70 CNC and a PT15 XL water-injection cutting torch. Underwater oxygen plasma cutting was carried out at 260 A as this is the optimum current for the torch consumables. Some cutting was also carried out at 200 A for direct comparison with the results achieved using dry plasma cutting at EWI, but results were poor as the torch consumables are designed for operation at 260 A. Cutting with underwater nitrogen was carried out at 400 and 200 A. The higher current with nitrogen gives cutting speeds comparable to 260 A with underwater oxygen plasma. Cutting speeds for optimum edge quality were also developed for bevel cutting. These parameters were used to produce a 30-deg weld edge preparation for subsequent welding trials (Table 8). Cutting speed was naturally slower than for cutting of square edges as the effective thickness of the plate was greater. Dross-free cutting conditions were more readily achieved using underwater plasma cutting, and higher cutting power was used, resulting in the higher speeds obtained for underwater bevel cutting compared with gas-plasma cutting. Plate was shipped back to EWI for characterization of the cut edges. Examination of the plate cut at L-Tec was carried out and specimens were prepared for metallographic examination. Narrower HAZ regions were expected as a result of the quenching effect of the water and the higher cutting speeds.

Optimum cutting conditions for both square and bevel cutting conditions were developed through cutting trials at a range of travel speeds with an arc current of 200 A for air, nitrogen, and oxygen plasma gases; 260 A for underwater

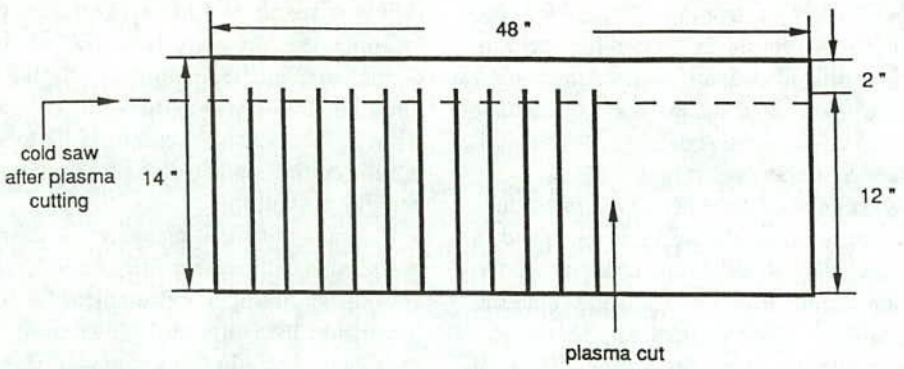

Figure 15. Layout of plasma cutting specimens for cutting parameter development.

TABLE 6 Cut numbering sequence for plasma cutting trials

Cutting trials at: 200 A, Hypertherm MAX 200 with air, nitrogen, and oxygen
260 A, L-Tec with U/W oxygen
400 A, L-Tec with U/W nitrogen

Material Grade	Material Thickness mm (in)	Plasma Gas	Cut Specimen Numbers	Best Cut Specimen Number
36	9.5 (3/8)	Nitrogen	C75-C90	C86
36	9.5 (3/8)	Air	C140-C168	C157
36	9.5 (3/8)	Oxygen	C100-C127	C117
36	9.5 (3/8)	U/W Oxygen	C525-C535	C535
36	9.5 (3/8)	U/W Nitrogen	C460-C480	C475
36	12.7 (1/2)	Nitrogen	C230-C238	C234
36	12.7 (1/2)	Air	C275-C295	C286
36	12.7 (1/2)	Oyxgen	C250-C264	C258
36	12.7 (1/2)	U/W Oxygen	C400-C422	C416
36	12.7 (1/2)	U/W Nitrogen	C425-C449	C444
50W	12.7 (1/2)	Nitrogen	C55-C65	C60
50W	12.7 (1/2)	Air	C1-C20	C10
50W	12.7 (1/2)	Oxygen	C30-C45	C39
50W	12.7 (1/2)	U/W Oxygen	C640-C662	C658
50W	12.7 (1/2)	U/W Nitrogen	C600-C624	C619
50W	19 (3/4)	Nitrogen	C355-C362	C358
50W	19 (3/4)	Air	C315-C323	C319
50W	19 (3/4)	Oxygen	C335-C344	C339
50W	19 (3/4)	U/W Oxygen	C680-C690	C683
50W	19 (3/4)	U/W Nitrogen	C700-C715	C709
50	19 (3/4)	Nitrogen	C220-C224	C221
50	19 (3/4)	Air	C180-C188	C184
50	19 (3/4)	Oxygen	C200-C205	C202
50	19 (3/4)	U/W Oxygen	C550-C562	C557
50	19 (3/4)	U/W Nitrogen	C570-C583	C573

U/W = Underwater cutting with water injection

oxygen plasma; and 400 A for underwater nitrogen plasma cutting. The maximum cutting speeds and dross-free cutting ranges for all 25 combinations of plasma cutting gas, plate material, and plate thickness are shown in Table 7. Typical cut quality for the best cutting conditions is shown in Figures 16 through 20 for all combinations of material type, thickness, and plasma cutting technique. These figures show the cut-edge appearance, including drag angles, and a qualitative comparison of edge quality.

KERF WIDTH AND ANGLE

Kerf width is the width between each side of the cut, usually measured from the top edge of the plate as the cut is generally wider at this point. Kerf width was measured with vernier calipers. The kerf angle was measured on the right-hand side of the cut in each case as clockwise gas swirl rings are employed in the cutting torch. This produces the squarer edge on the right-hand side of the cut; and for shape cutting operations, programming would be used with the required part on the right of the cut.

Specimens were produced to assess kerf width and angle by stopping the cut before completely severing the plate. Kerf measurements, including the top and bottom width (Table 9), were made at the end of the cut to avoid any potential distortion. For example, for 12.7-mm ($^1/_2$-in.)-thick Grade 50W plate, the kerf width varied from 3.8 to 5.2 mm (0.150 to 0.205 in.) at the top and from 3.8 mm (0.150 in.) to zero at the bottom as the cutting speed increased to the maximum for full-penetration cutting. For dross-free cuts on 12.7-mm ($^1/_2$-in.)-thick Grade 50W plate,

TABLE 7 Summary of plasma cutting procedure development trials, cutting speeds for square edges

Cutting trials at: 200 A, Hypertherm MAX 200 with air, nitrogen, and oxygen
260 A, L-Tec with U/W oxygen
400 A, L-Tec with U/W nitrogen

Material Grade	Material Thickness mm (in)	Plasma Gas	Dross-Free Window (in/min)	"Best" Quality (in/min)	Maximum Speed (in/min)
36	9.5 (⅜)	Nitrogen	None	85	95
36	9.5 (⅜)	Air	110-125	115	165
36	9.5 (⅜)	Oxygen	80-130	115	145
36	9.5 (⅜)	U/W Oxygen	100-150	150	ND
36	9.5 (⅜)	U/W Nitrogen	120-150	140	160
36	12.7 (½)	Nitrogen	30-55	50	65
36	12.7 (½)	Air	85-90	85	125
36	12.7 (½)	Oyxgen	60-125	110	140
36	12.7 (½)	U/W Oxygen	80-115	110	135
36	12.7 (½)	U/W Nitrogen	115-135	125	145
50W	12.7 (½)	Nitrogen	30-60	55	75
50W	12.7 (½)	Air	60-80	75	120
50W	12.7 (½)	Oxygen	85-130	125	160
50W	12.7 (½)	U/W Oxygen	70-130	120	155
50W	12.7 (½)	U/W Nitrogen	105-125	125	145
50W	19 (¾)	Nitrogen	10-25	25	35
50W	19 (¾)	Air	None	50	65
50W	19 (¾)	Oxygen	45-55	50	70
50W	19 (¾)	U/W Oxygen	None	65	75
50W	19 (¾)	U/W Nitrogen	70-80	75	85
50	19 (¾)	Nitrogen	None	20	25
50	19 (¾)	Air	40-50	50	65
50	19 (¾)	Oxygen	None	35	50
50	19 (¾)	U/W Oxygen	55-70	65	80
50	19 (¾)	U/W Nitrogen	None	45	70

U/W = Underwater cutting with water injection
ND = Not determined

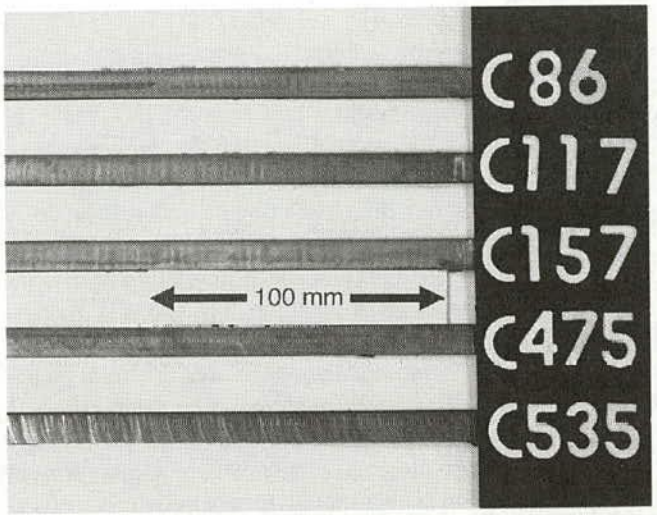

Figure 16. Cut edge apprearance for best cut quality on 9.5-mm (3/8-in.)-thick Grade 36 plate cut by nitrogen, oxygen, air, underwater nitrogen, and underwater oxygen PAC, respectively.

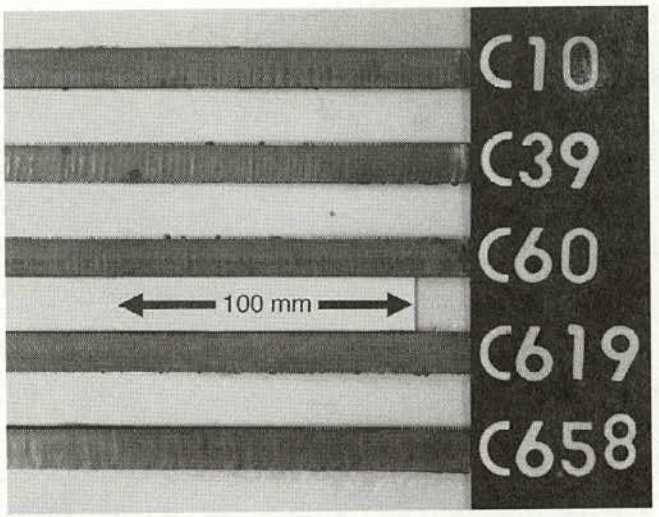

Figure 18. Cut edge appearance for best cut quality on 12.7-mm (1/2-in.)-thick Grade 50W plate cut by air, oxygen, nitrogen, underwater nitrogen, and underwater oxygen PAC, respectively.

the kerf width was 3.8 to 4.4 mm (0.150 to 0.175 in.) at the top and 1.5 to 2.0 mm (0.060 to 0.080 in.) wide at the bottom. For dross-free cuts on 9.5-mm (3/8-in.)-thick Grade 36 plate, the kerf width was 3.9 to 4.4 mm (0.155 to 0.175 in.) at the top and 0.8 to 2.0 mm (0.030 to 0.080 in.) wide at the bottom for oxygen plasma, while 1.3 to 1.5 mm (0.050 to 0.060 in.) for air plasma. No dross-free condition was found for nitrogen plasma cutting of 9.5-mm (3/8-in.)-thick Grade 36 plate. Similar measurements were made for the other combinations of material type, thickness, and plasma gas.

Measurements for drag angle are included to indicate the angle that the surface striations make from a vertical line on the cut face, Table 9. The angle of the striations indicates the optimization of the cutting parameters for the material type and thickness. Too much drag angle indicates that the cutting speed is too high; the result is increased bevel angle on the cut edge.

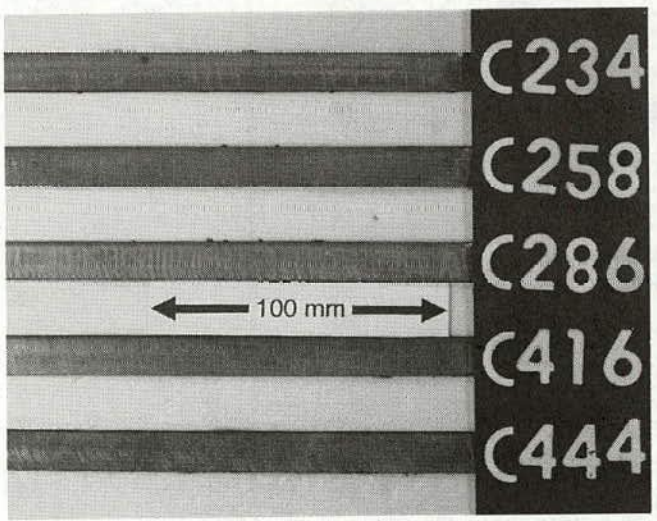

Figure 17. Cut edge appearance for best cut quality on 12.7-mm (1/2-in.)-thick Grade 36 plate cut by nitrogen, oxygen, air, underwater nitrogen, and underwater oxygen PAC, respectively.

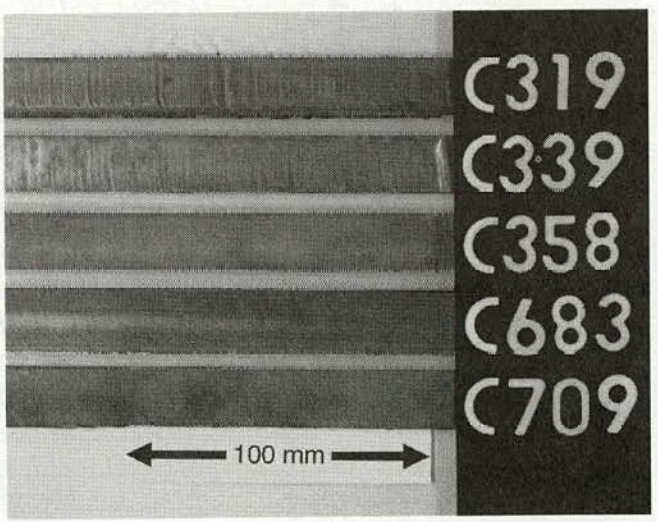

Figure 19. Cut edge appearance for best cut quality on 19-mm (3/4-in.)-thick Grade 50W plate cut by air, nitrogen, oxygen, underwater oxygen, and underwater nitrogen PAC, respectively.

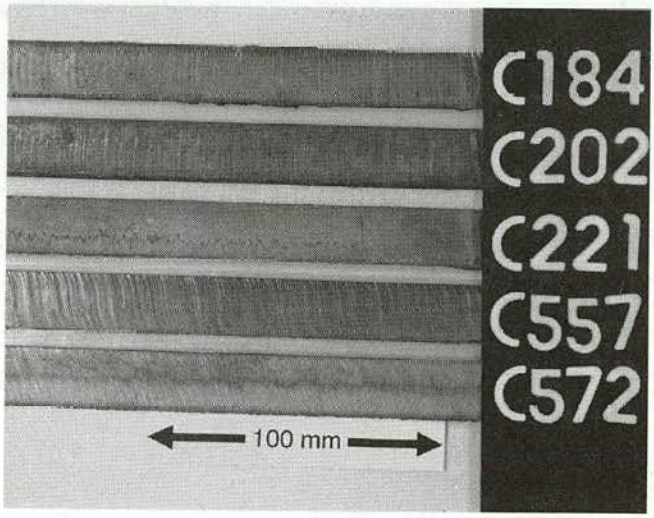

Figure 20. Cut edge appearance for best cut quality on 19-mm (3/4-in.)-thick Grade 50 plate cut by air, oxygen, nitrogen, underwater oxygen, and underwater nitrogen PAC, respectively.

DROSS LEVELS

Dross is the material that is removed from the cut to form the kerf. In a good-quality cut, all material will be completely removed, leaving a cleanly cut edge on the bottom surface of the plate. Dross, which remains on the bottom edge, generally indicates an unoptimized cutting procedure. The dross will vary in quantity and the degree of adherence to the plate, depending on the cutting speed in relation to the cutting power, the condition of the torch consumables, the type of plasma gas, and the composition of the base material. Whether the edge is subsequently to be used as a joint preparation, or left as a free edge, freedom from adherent dross is universally required in fabrication codes. Consequently, any dross present after cutting has to be removed. Dross forms at low speeds and also at high speeds. Low-speed dross tends to form in discreet and readily removable pieces, (i.e., with low adherence to the plate). High-speed dross tends to form a continuous bead and is generally very adherent, requiring grinding to remove it. Between the two conditions there is a dross-free window or range of cutting speeds where no appreciable

TABLE 8 Summary of plasma cutting procedure development trials, bevel cutting for joint-edge preparation

Cutting trials at: 200 A, Hypertherm MAX 200 with air, nitrogen, and oxygen
260 A, L-Tec with U/W oxygen
400 A, L-Tec with U/W nitrogen

Material Grade	Material Thickness mm (in)	Plasma Gas	Cutting Speed for "Best Quality"	
			mm/min	in/min
36	12.7 (½)	Nitrogen	760	30
36	12.7 (½)	Air	635	25
36	12.7 (½)	Oyxgen	635	25
36	12.7 (½)	U/W oxygen	2160	85
36	12.7 (½)	U/W nitrogen	2415	95
50W	12.7 (½)	Nitrogen	760	30
50W	12.7 (½)	Air	635	25
50W	12.7 (½)	Oxygen	635	25
50W	12.7 (½)	U/W oxygen	2160	85
50W	12.7 (½)	U/W nitrogen	2160	85
50W	19 (¾)	Nitrogen	510	20
50W	19 (¾)	Air	635	25
50W	19 (¾)	Oxygen	635	25
50W	19 (¾)	U/W oxygen	1395	55
50W	19 (¾)	U/W nitrogen	1905	75
50	19 (¾)	Nitrogen	380	15
50	19 (¾)	Air	635	25
50	19 (¾)	Oxygen	635	25
50	19 (¾)	U/W oxygen	1395	55
50	19 (¾)	U/W nitrogen	1905	75

U/W = Underwater cutting with water injection

TABLE 9 Summary of plasma cutting procedure development trials, cut quality for square edges

Material Grade	Material Thickness mm (in)	Plasma Gas	Cutting Speed (in/min)	Kerf Angle (deg)	Kerf Width Top		Drag Angle (deg)
					mm	in.	
36	9.5 (⅜)	Nitrogen	85	0	4.1	0.160	0
36	9.5 (⅜)	Air	115	4	3.9	0.153	1
36	9.5 (⅜)	Oxygen	115	7	4.2	0.167	4
36	9.5 (⅜)	U/W Oxygen	150	4	3.7	0.146	14
36	9.5 (⅜)	U/W Nitrogen	140	-2	3.8	0.150	26
36	12.7 (½)	Nitrogen	50	6	4.6	0.180	4
36	12.7 (½)	Air	85	5	4.5	0.177	6
36	12.7 (½)	Oxygen	110	5	5.0	0.195	5
36	12.7 (½)	U/W Oxygen	110	4	4.7	0.185	11
50W	12.7 (½)	U/W Nitrogen	125	-2	4.9	0.192	25
50W	12.7 (½)	Nitrogen	55	3	4.7	186	0
50W	12.7 (½)	Air	75	2	4.3	0.168	5
50W	12.7 (½)	Oxygen	125	4	4.4	0.175	0
50W	12.7 (½)	U/W Oxygen	120	3	4.7	0.185	7
50W	12.7 (½)	U/W Nitrogen	125	-4	4.3	0.168	5
50W	19 (¾)	Nitrogen	25	6	5.1	0.200	5
50W	19 (¾)	Air	50	5	4.1	0.160	7
50W	19 (¾)	Oxygen	50	5	4.7	0.185	6
50W	19 (¾)	U/W Oxygen	65	-2	5.5	0.216	25
50W	19 (¾)	U/W Nitrogen	75	-3	5.7	0.224	25
50	19 (¾)	Nitrogen	20	5	5.2	0.205	3
50	19 (¾)	Air	50	2	4.1	0.160	9
50	19 (¾)	Oxygen	35	4	5.3	0.209	2
50	19 (¾)	U/W Oxygen	65	0	5.5	0.216	13
50	19 (¾)	U/W Nitrogen	45	-8	5.7	0.224	16

U/W = Underwater cutting with water injection

dross is formed on the cut edges. For maximum edge quality and maximum productivity, the cutting speed used should be within the dross-free window, but at the highest practicable speed. Generally speaking, the best overall productivity will be achieved by consistently obtaining dross-free cuts, and using the highest cutting speed consistent with this condition.

Dross was assessed in a qualitative manner during this work. The dross level was given a number from 0 to 5, with zero representing a dross-free cut and 5 representing very heavy dross. The dross level of most optimized cutting conditions is zero. The number is also relative to the thickness of the plate material. The ease of dross removal is also important; some can be removed by hand, without tools, while some requires chipping hammers or grinding to remove it. Comparisons of dross adherence were made in this manner.

The underside of Grade 50W plate, 12.7 mm ($^1/_2$ in.) thick, cut by air plasma shows typical dross conditions for a range of cutting speeds at constant cutting power, Figure 21. At low speed, C1, there is dross in the form of splash-like droplets, while at higher speeds, near C19, dross becomes continuous and very adherent until through-thickness cutting is no longer achieved. In between, there is a range of cutting speeds at which nominally dross-free cutting is achieved on the left-hand side of the cut in the figure (right-hand in terms of the cutting direction).

On thicker plate, the range of dross-free cutting speeds is narrower. The underside of Grade 50 plate, 19 mm ($^3/_4$ in.) thick, cut by air plasma again shows typical dross conditions for a range of cutting speeds at constant cutting power (Figure 22). The cutting conditions yielding dross-free cut edges are shown in Table 7.

EFFECT OF PLATE ROLLING DIRECTION AND SURFACE CONDITION

Plasma cutting trials were carried out to examine the effect of cutting transverse to the plate rolling direction and the effect on dross adherence of abrasive cleaning to remove the

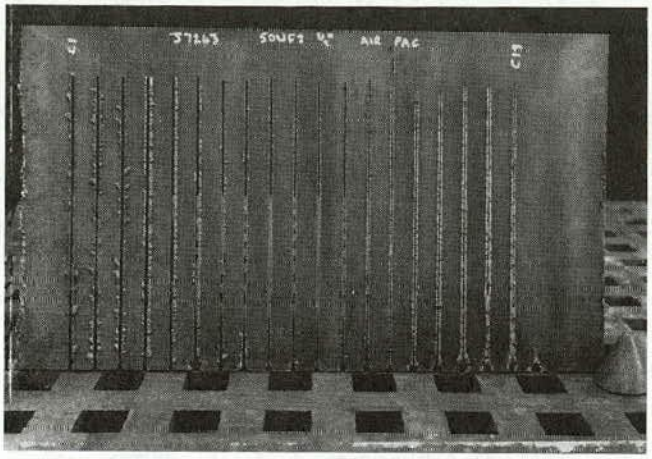

Figure 21. Underside of Grade 50W plate, 12.7 mm (1/2 in.) thick, cut by air plasma, illustrating dross condition.

mill scale from the top and bottom surfaces of the plates. Four specimen plates were prepared from 12.7-mm (1/2-in.)-thick Grade 36 and 19-mm (3/4-in.)-thick Grade 50 plate. Two plates were blast cleaned and two left in the as-received condition. One of each was cut longitudinally and transversely to the plate rolling direction using air plasma cutting. The cutting direction did not affect the cut quality achieved. Results indicated that blast cleaning resulted in more dross on the underside of the cut and this was more adherent, presumably because of metal-to-metal contact. In the uncleaned specimens, any dross adhered to the mill scale, especially on the Grade 50 plate which had a thicker scale.

SURFACE ROUGHNESS OF PLASMA-CUT EDGES

Surface roughness measurements were made on a Talysurf 4 machine which uses a surface-contact probe to scan a portion of the surface, usually about 3 mm (1/8 in.) long. Measurements were made at the midlength and midthickness of the specimens in each case. The Talysurf 4 calculates an average surface roughness, R_A, from the peaks and troughs of the striations on the cut surface.

Surface roughness measurements on specimens of plasma-cut edges cut by oxygen, air, and nitrogen plasma cutting in air, and underwater cutting with oxygen and nitrogen were completed for each of the five base material-type/thickness combinations. Measurements of average surface roughness, R_A, were made on three specimens cut at low, optimum, and maximum cutting speeds. A total of 60 measurements were made, and the results are summarized in Table 10. The maximum roughness of all the specimens was 8.6 μm (338 μin.) which is well within the 25.4 μm (1000 μin.) allowable. Most specimens had a roughness between 1.3 and 3.8 μm (50 and 150 μin.). The conclusion is that plasma cutting of all types readily produces cut edges with acceptable surface roughness to meet Bridge Welding Code requirements.

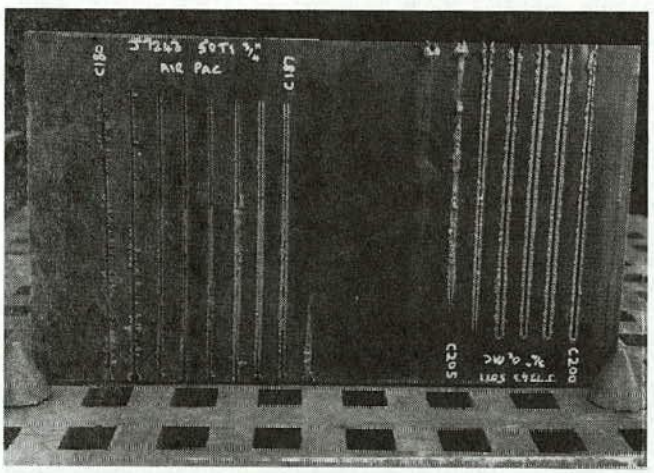

Figure 22. Underside of Grade 50 plate, 19 mm (3/4 in.) thick, cut by air plasma, illustrating dross condition.

METALLOGRAPHIC EXAMINATION OF PLASMA-CUT EDGES

Metallographic specimens were taken near the end of each cut to assure consistency in the position from which specimens were removed and to ensure steady-state conditions. For each combination of cutting gas, material type, and thickness, several specimens of plasma-cut edges (at low, high, and intermediate cutting speeds) were prepared for characterization by profile measurements for surface roughness, metallography, and microhardness measurements. Results showed that the width of the HAZ becomes slightly narrower with increasing cutting speed and that hardness levels up to 500 VHN can be produced at the cut edge, with higher hardness levels for air and nitrogen plasma compared with oxygen plasma cutting.

The typical cut edge appearance and HAZ for Grade 50W plate, 19 mm (3/4 in.) thick, showed that the visible HAZ is usually 0.6 mm (0.024 in.), and is a maximum of 1 mm (0.040 in.). The widest HAZ was produced by nitrogen plasma cutting, which was the slowest cutting speed of the five. Although the visible HAZ is this wide, the hardened portion is narrower.

Initial metallographic characterization of plasma-cut edges was carried out for plate cut by oxygen, nitrogen, and air plasma gases. Micrographs of the cut edges were prepared at magnifications of ×100 and ×400. A distinct, white etching, nitrogen-rich layer was seen on the surface of the cut edge HAZ on edges cut by both air and nitrogen plasma gases. This layer was absent from the edges cut using oxygen plasma gas. For 12.7-mm (1/2-in.)-thick Grade 36 plate, the widest zone, that for air plasma cutting, is only 0.05 mm (0.002 in.) wide.

TABLE 10 Surface roughness measurements for plasma-cut edges

Cutting trials at: 200 A, Hypertherm MAX 200 with air, nitrogen, and oxygen
260 A, L-Tec with U/W oxygen
400 A, L-Tec with U/W nitrogen

Material Grade	Material Thickness mm (in)	Plasma Gas	Cutting Speed mm/min (in/min)	Specimen Number	Surface Roughness Average, Ra microns (microinch)
36	9.5 (⅜)	Nitrogen	2160 (85)	C86	2.7 (106)
36	9.5 (⅜)	Air	2920 (115)	C157	2.3 (92)
36	9.5 (⅜)	Oxygen	2920 (115)	C117	5.55 (219)
36	9.5 (⅜)	U/W Oxygen	3810 (150)	C535	5.5 (216)
36	9.5 (⅜)	U/W Nitrogen	3555 (140)	C475	2.95 (116)
36	12.7 (½)	Nitrogen	1270 (50)	C234	1.85 (73)
36	12.7 (½)	Air	2160 (85)	C286	3.6 (141)
36	12.7 (½)	Oyxgen	2795 (110)	C258	2.6 (102)
36	12.7 (½)	U/W Oxygen	2795 (110)	C416	1.7 (66)
36	12.7 (½)	U/W Nitrogen	3175 (125)	C444	2.75 (108)
50W	12.7 (½)	Nitrogen	1395 (55)	C60	1.25 (50)
50W	12.7 (½)	Air	1905 (75)	C10	2.2 (85)
50W	12.7 (½)	Oxygen	3175 (125)	C39	3.7 (145)
50W	12.7 (½)	U/W Oxygen	3050 (120)	C658	1.6 (62)
50W	12.7 (½)	U/W Nitrogen	3175 (125)	C619	1.75 (69)
50W	19 (¾)	Nitrogen	635 (25)	C358	1.6 (61)
50W	19 (¾)	Air	1270 (50)	C319	5.2 (203)
50W	19 (¾)	Oxygen	1270 (50)	C339	5.2 (203)
50W	19 (¾)	U/W Oxygen	1650 (65)	C683	1.9 (76)
50W	19 (¾)	U/W Nitrogen	1905 (75)	C709	2.1 (83)
50	19 (¾)	Nitrogen	510 (20)	C221	3.1 (122)
50	19 (¾)	Air	1270 (50)	C184	2.65 (105)
50	19 (¾)	Oxygen	890 (35)	C202	7.3 (288)
50	19 (¾)	U/W Oxygen	1650 (65)	C557	4.15 (164)
50	19 (¾)	U/W Nitrogen	1145 (45)	C573	6.3 (249)

U/W = Underwater cutting with water injection
ND = Not determined

The narrow (nitrided) layer was produced at the immediate edge of the cut with plasma gases containing nitrogen when cutting in air (i.e., for air and nitrogen plasma cutting). A martensitic band beyond this changed progressively to partially transformed martensite and ferrite, and finally to a mixed ferrite and pearlite microstructure in the parent material. Metallographic characterization of cut edges produced by underwater oxygen and underwater nitrogen plasma cutting revealed interesting results. It was noticeable from micrographs of the cut edges prepared at a magnification of ×400, that this white etching layer was not visible for underwater nitrogen plasma cutting. This was clear by comparing the edges for Grade 50W plate, 12.7 mm ($^1/_2$ in.) thick, cut using all five plasma cutting techniques.

Microhardness measurements on cross sections of the cut edges showed a consistent trend compared with cuts made in air. The underwater-cut edges had a lower hardness compared with edges cut with the same gases in air, and the depth of hardening was lower in the former case. Maximum edge hardness for underwater cutting with oxygen ranged from 250 to 330 VHN, while for underwater nitrogen the maximum edge hardness ranged from 187 to 341 VHN.

EDGE HARDNESS

Microhardness measurements on cross sections of the cut edges showed a consistent trend which mirrored the presence

or absence of the white etching layer observed in microstructural examination. Gas analysis has shown this layer to have higher nitrogen levels. This would be expected to result in additional hardening through lattice distortion by nitrogen in interstitial solid solution.

The results for materials cut using oxygen, air, and nitrogen plasma gases, and for underwater cutting with oxygen and nitrogen show that the hardest edges were produced using nitrogen and air plasma cutting (Table 11). The distance from the cut edge through the HAZ until hardness less than 350 VHN was achieved is shown in the last column in Table 11. A blank in this column is recorded for edges that were below 350 VHN at a point 0.02 mm (0.001 in.) from the cut edge when measured on a macrosection. Cutting of the Grade 50 plate resulted in the highest surface hardness, partly because this material has the highest carbon equivalent and hardenability, and partly because the cutting speeds were lower (Figure 23).

Underwater cutting resulted in a reduction in edge hardness for all material types and thicknesses. Underwater oxygen-plasma cutting reduced hardness by up to 25 VHN compared with cutting above water. The reduction was modest as the edges cut in air generally also had a low hardness. Typical hardness results for underwater oxygen plasma cutting are shown in Figure 24. Reduction in hardness was more pronounced when comparing underwater nitrogen plasma cutting with cutting with the same gas above water. A typical reduction in the maximum edge hardness of 40 VHN was found. Typical hardness results for underwater nitrogen plasma cutting are shown in Figure 25. Because of the nitrogen effect in increasing hardness, it is expected that the cooling effect of the water would influence the time for diffusion of nitrogen into the cut edge, resulting in lower hardness. This would also be influenced by the higher cutting speed for underwater nitrogen PAC at 400 A.

Edges cut with oxygen had typical maximum hardness values ranging from 250 to 350 VHN, while air plasma ranged from 280 to 540 VHN. Nitrogen-cut edges had maximum values ranging from 330 to 440 VHN. For underwater oxygen, the range was 240 to 330 VHN, and for underwater nitrogen 290 to 400 VHN. In all cases, hardness levels fell below 350 VHN within 0.3 mm (0.012 in.) of the cut edge.

GAS ANALYSIS OF PLASMA-CUT EDGES

The nitrogen and oxygen contents of the cut edge were measured by a Leco gas carrier unit connected to a mass spectrometer to achieve bulk analysis in the areas from the cut edge to about 2 mm (0.080 in.) from the edge. The Leco unit melts the specimen and a helium carrier gas conveys the

TABLE 11 Edge hardness for plasma-cut edges

Material Grade	Material Thickness mm (in)	Plasma Gas	Specimen Number	Hardness HV Load 0.05 kg	
				0.02 mm	<350 HV
36	12.7 (½)	Nitrogen	C234	440	0.12 mm
36	12.7 (½)	Air	C286	540	0.12 mm
36	12.7 (½)	Oyxgen	C258	340	–
36	12.7 (½)	U/W Oxygen	C416	327	–
36	12.7 (½)	U/W Nitrogen	C444	402	0.22 mm
50W	12.7 (½)	Nitrogen	C60	330	–
50W	12.7 (½)	Air	C10	280	–
50W	12.7 (½)	Oxygen	C39	265	–
50W	12.7 (½)	U/W Oxygen	C658	240	–
50W	12.7 (½)	U/W Nitrogen	C619	290	–
50W	19 (¾)	Nitrogen	C358	334	–
50W	19 (¾)	Air	C319	342	–
50W	19 (¾)	Oxygen	C339	256	–
50W	19 (¾)	U/W Oxygen	C683	262	–
50W	19 (¾)	U/W Nitrogen	C709	299	–
50	19 (¾)	Nitrogen	C220	457	0.12 mm
50	19 (¾)	Air	C184	475	0.32 mm
50	19 (¾)	Oxygen	C202	670?	0.32 mm
50	19 (¾)	U/W Oxygen	C557	260	–
50	19 (3/4)	U/W Nitrogen	C573	395	0.22 mm

U/W = Underwater cutting with water injection

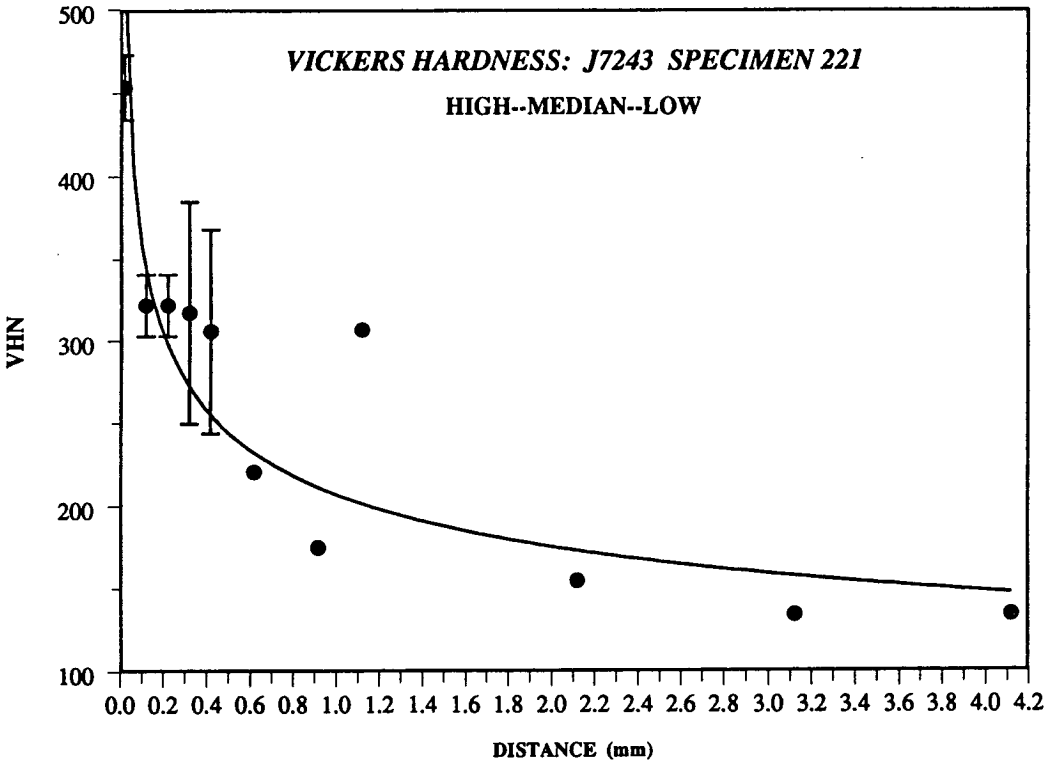

Figure 23. Hardness profile from the cut edge toward the parent plate. Nitrogen PAC on Grade 50 plate, 19 mm (3/4 in.) thick.

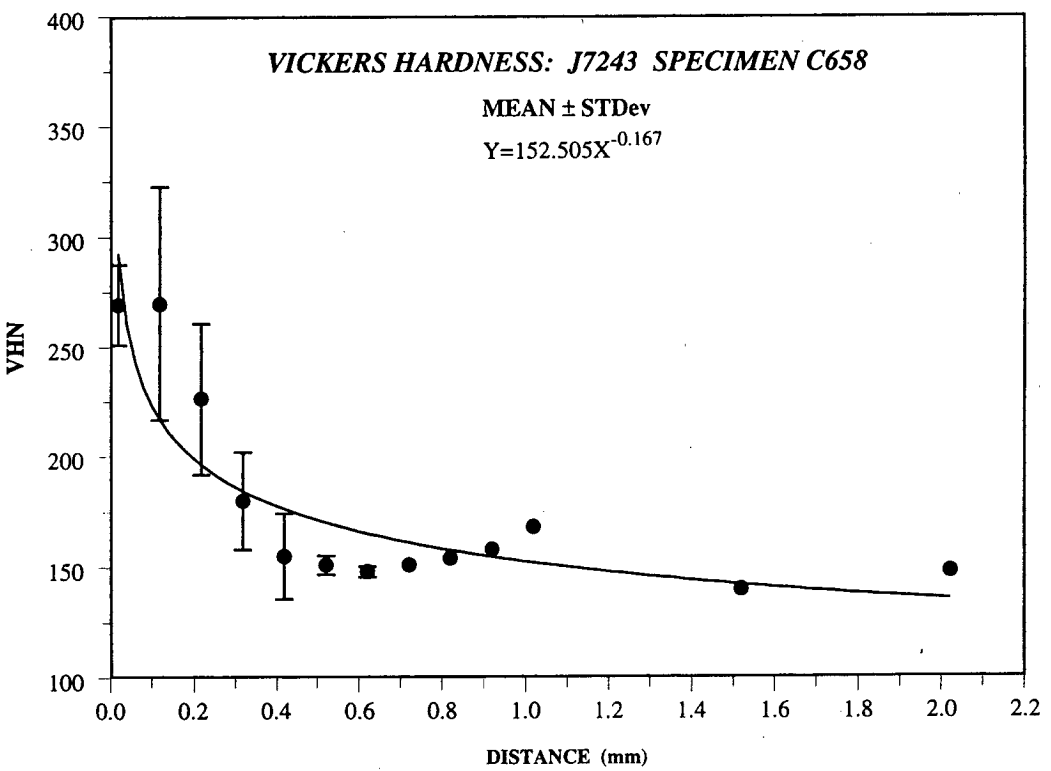

Figure 24. Hardness profile from the cut edge toward the parent plate. Underwater oxygen PAC on Grade 50W plate, 12.7 mm (1/2 in.) thick.

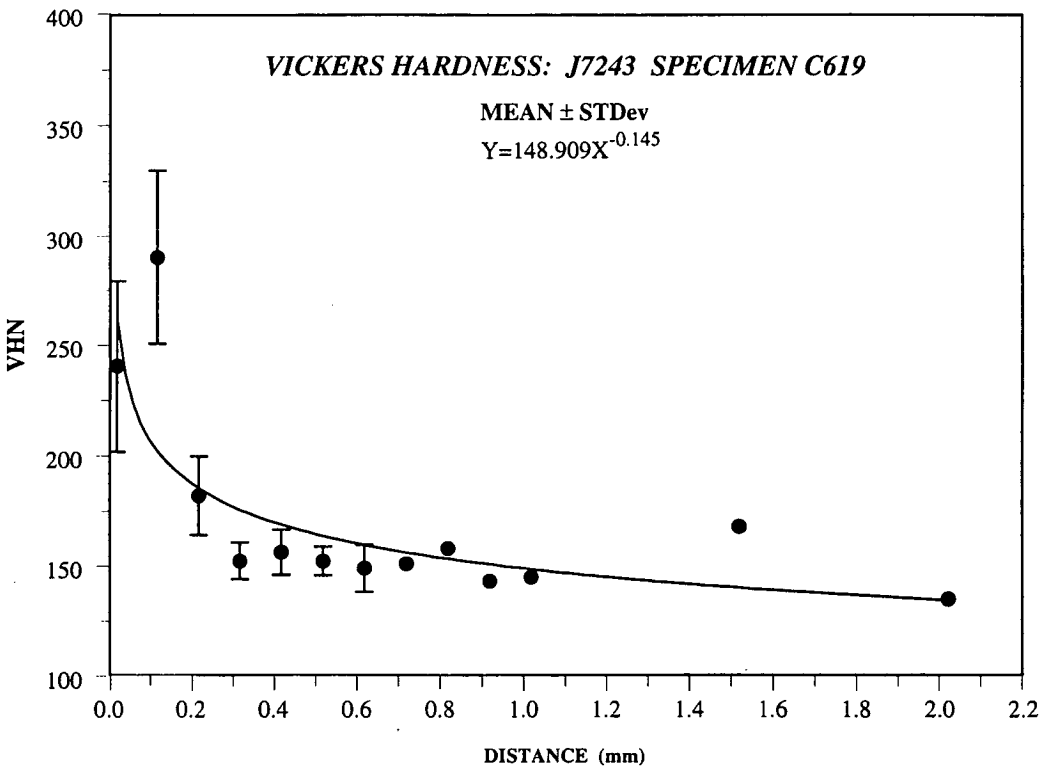

Figure 25. Hardness profile from the cut edge toward the parent plate. Underwater nitrogen PAC on Grade 50W plate, 12.7 mm ($^1/_2$ in.) thick.

gas released from the specimen to the mass spectrometer for analysis. The 2-mm (0.080-in.) portion of the edge, including the as-cut surface and HAZ, represents the maximum amount of material likely to be remelted in a subsequent welding operation by FCAW or SAW.

Specimens of plasma-cut edges cut by oxygen, air, and nitrogen were sent for gas analysis to determine nitrogen and oxygen levels in the cut edges. Results showed that levels of both oxygen and nitrogen (and consequently the total gas content) were lower in plate cut by oxygen plasma compared with both air and nitrogen plasma cutting (Table 12). Typical values for total gas content for oxygen plasma cutting ranged from 90 to 140 ppm, with about a 50/50 proportion of oxygen and nitrogen. Total gas content for air plasma ranged from 190 to 580 ppm (with one result at 730 ppm) with the proportions of oxygen to nitrogen ranging from 50/50 to 25/75. Total gas content for nitrogen plasma ranged from 180 to 360 ppm with the proportions of oxygen to nitrogen ranging from 50/50 to 25/75. These results would predict that porosity problems would be least when welding over oxygen plasma-cut edges, and higher when welding over edges cut by nitrogen and air. Radiographic inspection of welds confirmed this prediction for nitrogen, but only one weld made on edges cut by air plasma was rejected due to porosity.

Specimens of plasma-cut edges cut by underwater oxygen and underwater nitrogen were sent for gas analysis to determine nitrogen and oxygen levels in the cut edges. Results showed that the total gas contents (nitrogen and oxygen) for seven of the ten specimens ranged from 110 to 130 ppm. These results indicated that the total gas content was nominally independent of the cutting gas and parent material for underwater cutting. The total gas contents were in the same range as for oxygen plasma cutting in air, indicating a similar weldability as far as porosity is concerned.

One specimen of Grade 50 plate, 19 mm ($^3/_4$ in.) thick, cut with underwater nitrogen PAC contained 430 ppm total gas content. This specimen was cut at a substantially slower speed than the others, 1145 mm/min (45 in./min) compared to 1650 or 1905 mm/min (65 or 75 in./min), allowing more time for gas diffusion into the cut edge.

WELDING TRIALS

Arc welding was carried out for three series of specimens using flux cored arc welding (FCAW) and submerged arc welding (SAW). This included single-vee butt joints, Figure 26, and fillet joints, Figure 27, Table 13; single-bevel butt joints for Charpy testing, Figure 28, Table 14; and the welded panels for fatigue testing, Table 15. Plate for underwater oxygen and underwater nitrogen plasma cutting of beveled weld edge preparations was cut at EASB/L-Tec.

The welding consumable for the flux cored arc welding (FCAW) trials was Outershield 71 (AWS A5.20-79, E71-T1) wire, 1.6 mm (0.063 in.) diameter. For submerged arc weld-

TABLE 12 Leco Gas Analysis results for oxygen and nitrogen in plasma-cut edges

Cutting trials at: 200 A, Hypertherm MAX 200 with air, nitrogen, and oxygen
260 A, L-Tec with U/W oxygen
400 A, L-Tec with U/W nitrogen

Material Type	Material Thickness mm (in)	Plasma Gas	Specimen Numbers	Oxygen ppm	Nitrogen ppm	Total O_2 & N_2 ppm
36	9.5 (⅜)	Nitrogen	C85	49.8	166.3	216.1
36	9.5 (⅜)	Air	C156	157.5	424.2	581.7
36	9.5 (⅜)	Oxygen	C116	63.5	39.6	103.1
36	9.5 (⅜)	U/W Oxygen	C535	60.2	54.1	114.3
36	9.5 (⅜)	U/W Nitrogen	C475	88.9	42.4	131.3
36	12.7 (½)	Nitrogen	C234	122.0	307.0	429.0
36	12.7 (½)	Air	C286	156.0	181.0	337.0
36	12.7 (½)	Oyxgen	C258	128.0	96.0	224.0
36	12.7 (½)	U/W Oxygen	C416	89.6	71.6	161.2
36	12.7 (½)	U/W Nitrogen	C444	51.0	64.4	115.4
50W	12.7 (½)	Nitrogen	C59	198.0	152.5	350.5
50W	12.7 (½)	Air	C9	123.9	119.9	243.8
50W	12.7 (½)	Oxygen	C38	50.9	69.4	120.3
50W	12.7 (½)	U/W Oxygen	C658	117.2	61.5	178.7
50W	12.7 (½)	U/W Nitrogen	C619	69.2	60.7	129.9
50W	19 (¾)	Nitrogen	C358	79.0	117.0	196.0
50W	19 (¾)	Air	C319	87.0	152.0	239.0
50W	19 (¾)	Oxygen	C339	78.0	63.0	141.0
50W	19 (¾)	U/W Oxygen	C683	54.2	54.4	108.6
50W	19 (¾)	U/W Nitrogen	C709	57.0	53.9	110.9
50	19 (¾)	Nitrogen	C221	107.0	100.0	207.0
50	19 (¾)	Air	C183	46.4	128.7	175.1
50	19 (¾)	Oxygen	C202	57.3	146.4	203.7
50	19 (¾)	U/W Oxygen	C557	61.4	66.7	128.1
50	19 (¾)	U/W Nitrogen	C573	282.2	150.4	432.6

U/W = Underwater cutting with water injection

ing (SAW), the consumables were L-61 wire (AWS A5.17-80), 2.4 mm (0.095 in.) diameter, and 860 flux. These consumables are manufactured by Lincoln Electric, and are widely used in bridge fabrication.

Plasma cutting parameters developed for bevel cutting were used to produce a 30-deg weld edge preparation for subsequent welding trials. The parameters were developed to yield the best edge quality in terms of freedom from dross and to produce smooth edges. Bevel cutting trials were completed for 12.7-mm ($^1/_2$-in.)-thick M270 Grades 36 and 50W using all five plasma cutting techniques. Bevel cutting trials were also completed for 19-mm ($^3/_4$-in.)-thick M270 Grades 50 and 50W using all five plasma cutting techniques. Plate preparation for welding trials also included pieces with square edges for fillet welding and single-bevel joints for Charpy impact test weldments.

Preliminary welding trials were carried out using FCAW to verify selected welding parameters and bead placement strategy. The welding trials were carried out using M270 Grade 50W plate, 12.7 mm ($^1/_2$ in.) thick, and M270 Grade 50, 19 mm ($^3/_4$ in.) thick. Two pieces of plate, bevel cut to a 30-deg weld edge preparation, were butted together yielding a 60-deg included angle single-vee joint preparation. A 3-mm ($^1/_8$-in.) root gap was used over a steel backing bar (Figure 26). The backing bar were cut 9.5 mm ($^3/_8$ in.) thick, from M270 Grade 36 plate to strips 50 mm (2 in.) wide. The joint preparation, root gap, and backing bar were the same for the 12.7-mm ($^1/_2$-in.)- and 19-mm ($^3/_4$-in.)-thick plate. A total of 7 joints were welded to establish a welding procedure for the two plate thicknesses. The joint in the 12.7-mm ($^1/_2$-in.) plate was welded in six passes; 2 placed along the centerline of the joint, and 2 deposited side by side for the fill and capping passes, Figure 29. The joint in the 19-mm ($^3/_4$-in.) plate was

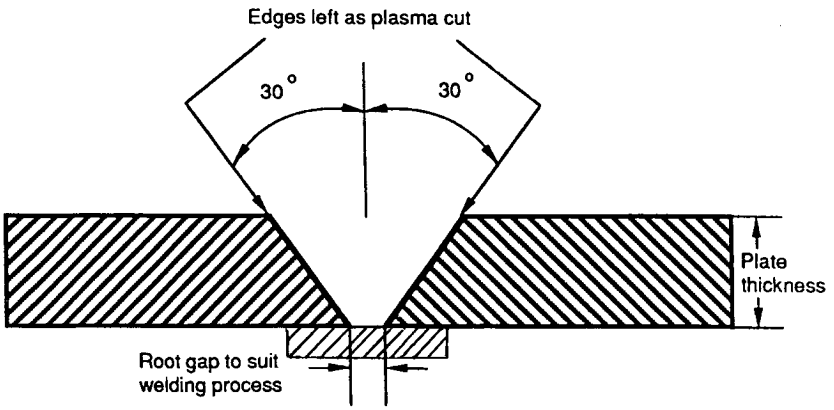

Figure 26. Weld preparation for the single-vee butt joint.

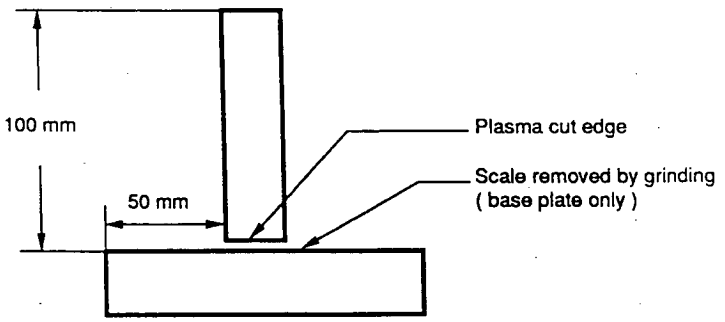

Figure 27. Weld preparation for fillet-welded T-butt joint.

TABLE 13 Matrix of arc welding trials

Material/Thickness	Plasma Cutting Processes	Tests
M270 Grade 36 12.7 mm (½ in.)	Air Nitrogen Oxygen U/W Nitrogen U/W Oxygen	Butt welding at 2 arc energies Fillet welding at 2 arc energies Metallography Hardness
M270 Grade 50W 12.7 mm (½ in.)	Air Nitrogen Oxygen U/W Nitrogen U/W Oxygen	Butt welding at 2 arc energies Fillet welding at 2 arc energies Metallography Hardness
M270 Grade 50W 19 mm (¾ in.)	Air Nitrogen Oxygen U/W Nitrogen U/W Oxygen	Butt welding at 2 arc energies Metallography Hardness
M270 Grade 50 19 mm (¾ in.)	Air Nitrogen Oxygen U/W Nitrogen U/W Oxygen	Butt welding at 2 arc energies Metallography Hardness

U/W = Underwater cutting with water injection

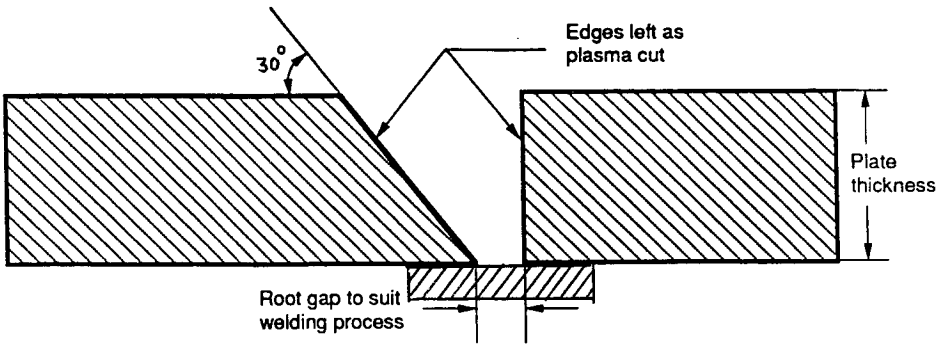

Figure 28. Weld preparation for the single-bevel butt joint.

TABLE 14 Test matrix to assess the toughness of welded plasma-cut edges

Material	Thickness mm (in)	Cutting Process	Welding Process	Surface Roughness (μm)	No. of Charpy Tests					
					-40°F			RT		
					FL	FL+1	FL+2	FL	FL+1	FL+2
M270 Grade 36	12.7 (½)	Air	SAW	<5	3	3	3	3	3	3
		N_2	SAW	<5	3	3	3	3	3	3
		O_2	SAW	<5	3	3	3	3	3	3
		U/W O_2	SAW	<5	3	3	3	3	3	3
		U/W N_2	SAW	<5	3	3	3	3	3	3
		OFC	SAW	<5	3	3	3	3	3	3
		Machined	SAW	<5	3	3	3	3	3	3
M270 Grade 50W	12.7 (½)	Air	SAW	<5	3	3	3	3	3	3
		N_2	SAW	<5	3	3	3	3	3	3
		O_2	SAW	<5	3	3	3	3	3	3
		U/W O_2	SAW	<5	3	3	3	3	3	3
		U/W N_2	SAW	<5	3	3	3	3	3	3
		OFC	SAW	<5	3	3	3	3	3	3
		Machined	SAW	<5	3	3	3	3	3	3
M270 Grade 50	19 (¾)	Air	SAW	<5	3	3	3	3	3	3
		N_2	SAW	<5	3	3	3	3	3	3
		O_2	SAW	<5	3	3	3	3	3	3
		U/W O_2	SAW	<5	3	3	3	3	3	3
		U/W N_2	SAW	<5	3	3	3	3	3	3
		OFC	SAW	<5	3	3	3	3	3	3
		Machined	SAW	<5	3	3	3	3	3	3
Total = 378 tests										

Key:
(1) U/W = Underwater cutting with water injection
(2) FL = Fusion line notch location
FL+1 = Fusion line + 0.04-in. notch location
FL +2 = Fusion line + 0.08-in. notch location
(3) RT = Room temperature

TABLE 15 Test matrix to assess the fatigue behaviour of welded plasma-cut edges

Material	Thickness mm (in)	Cutting Process	Welding Process	Joint Type	Surface Roughness (μm)	No. of S-N Curves
M270 Grade 50W	12.7 (½)	U/W N_2	SAW	Single V	<5	1
		U/W O_2	SAW	Single V	<5	1
		U/W O_2	FCAW	Single V	<5	1
		U/W N_2	SAW	Single V	>15	1
		U/W O_2	SAW	Single V	>15	1
		Machined	SAW	Single V	–	1
		U/W O_2	FCAW	Unloaded fillet	>15	1

U/W = Underwater cutting with water injection
Six specimens were tested for each S-N curve

welded in passes; 2 placed along the centerline of the joint, then layers of 2 or 3 beads deposited side by side, with 3 beads for the capping pass/layer (Figure 30). The welding procedures for these welds are also shown in Figures 29 and 30. These joints were cross-sectioned and found to be without discontinuities. Full metallographic preparation was carried out.

SAW of single-bevel and single-vee butt joints was carried out for both 12.7- and 19-mm ($^1/_2$- and $^3/_4$-in.)-thick plate. A total of 11 development welds for FCAW and SAW were produced and inspected by radiography before the joints (detailed in Table 13) were welded.

Following completion of the development welding trials, weldments detailed in Tables 13 and 14 were fabricated. Forty groove-welded butt joints were completed, 20 by SAW and 20 by FCAW. A 13-mm ($^1/_2$-in.) root gap and split pass welding technique was used for SAW over a steel backing bar (Figure 26). The backing bar was cut from M270 Grade 36 plate, 9.5 mm ($^3/_8$ in.) thick, into strips 50 mm (2 in.) wide. The joint preparation, root gap, and backing bar were the

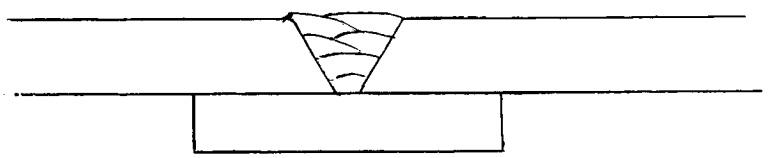

Welding Process:	FCAW
Consumable Type:	E71T-1, Lincoln Outershield E71T-1
Wire Diameter:	1.6 mm (1/16-in.)
Shielding Gas:	Argon-20CO_2 at 35 cfh
Welding Current:	300 A
Arc Voltage:	28 V
Wire feed speed:	5.97 m/min (235 in/min)
Travel Speed:	305 mm/min (12 in/min)
Heat Input:	1.65 kJ/mm (42 kJ/in.)
Polarity	DCEP
Stickout:	19 mm (¾ in.)
Preheat:	10°C (50°F)
Interpass:	21°C (70°F) min., 205°C (400°F) max.
Backing Bar:	9.5-mm (⅜-in.) thick, 50-mm (2-in.) wide, M270 Grade 36

Figure 29. Welding procedure for 12.7-mm ($^1/_2$-in.) single-vee butt joint welded by FCAW.

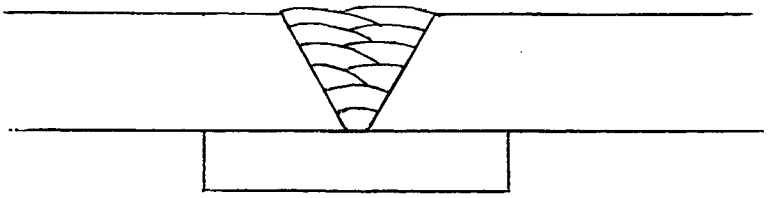

Welding Process:	FCAW
Consumable Type:	E71T-1, Lincoln Outershield E71T-1
Wire Diameter:	1.6 mm (1/16-in.)
Shielding Gas:	Argon-20CO_2 at 35 cfh
Welding Current:	300 A
Arc Voltage:	28 V
Wire feed speed:	5.97 m/min (235 in/min)
Travel Speed:	305 mm/min (12 in/min)
Heat Input:	1.65 kJ/mm (42 kJ/in.)
Polarity	DCEP
Stickout:	19 mm (¾ in.)
Preheat:	10°C (50°F)
Interpass:	21°C (70°F) min., 205°C (400°F) max.
Backing Bar:	9.5-mm (⅜-in.) thick, 50-mm (2-in.) wide M270 Grade 36

Figure 30. Welding procedure for 19-mm ($^3/_4$-in.) single-vee butt joint welded by FCAW.

same for the 12.7-mm ($^1/_2$-in.)- and 19-mm ($^3/_4$-in.)-thick plate. Single-vee welds were typically completed in 10 passes for 12.7-mm ($^1/_2$-in.) plate, and 18 passes for 19-mm ($^3/_4$-in.) plate. Single-bevel welds were typically completed in 8 passes for 12.7-mm ($^1/_2$-in.) plate, and 18 passes for 19-mm ($^3/_4$-in.) plate. The welding procedures employed for SAW are detailed in Figures 31 and 32 for the single-vee and single-bevel joints, respectively.

For the single-bevel joints welded by SAW, 21 welds with edges prepared by dry nitrogen, oxygen, air plasma, underwater oxygen, underwater nitrogen plasma cutting, oxyfuel cutting, and machining were completed (Table 14). All these welds were subjected to NDE, inspected visually and by radiography (Table 16).

Of the 40 welds produced by SAW, 38 joints passed visual and radiographic inspection (Tables 16 and 17). One of the SAW weldments that failed was welded on edges plasma cut with nitrogen and was a single-vee joint with slag defects (weld W39). The other failed joint was a vee groove joint welded on edges prepared using air plasma cutting, and was rejected for porosity.

Of the 20 welds produced by FCAW, 12 passed visual and radiographic inspection. Of the eight that failed, seven of these, cut with all five plasma cutting processes, showed slag inclusions (Table 16). Two welds, both made on edges cut with nitrogen plasma, had rejectable levels of porosity. Porosity resulted from welding directly to the as-cut edge when cut with nitrogen. Rejectable porosity was not encountered when welding on edges prepared by the other four plasma cutting techniques.

Examination of macrosections of these joints revealed that the majority of slag inclusions were at the edges of the penetration profile in the base of the root pass. The slag was trapped between the weld and the backing bar. In these instances the slag was never wider than 1 mm (0.040 in.) or deeper than 0.5 mm (0.020 in.). This would readily be ground out when removing the backing bar and thus is not considered particularly significant. There would have been no loss of effective thickness with the excess weld metal (reinforcement) in the joint region. The backing bar was left on for radiography as, depending on loading conditions in the bridge structure, the backing bar is left on as long as loading is not transverse to the weld.

An example of a weld with rejectable defects, associated with slag and sidewall fusion defects, or porosity, is weld W14, Figure 33. Of the 11 welds produced from nitrogen plasma-cut edges, three (27 percent) had rejectable porosity.

A total of 20 fillet weld soundness specimens were made, 10 each with SAW and FCAW. Three pass fillet welds were made to achieve a fillet leg length of 12.7 mm ($^1/_2$ in.) minimum in each case. Fillet weld soundness testing, by metallographic sectioning and examination according to section 15.5 of the Bridge Welding Code, showed all welds to be acceptable (Table 18). Macrosections of welds W88 and W79 show the typical weld cross sections for air plasma cut and welded

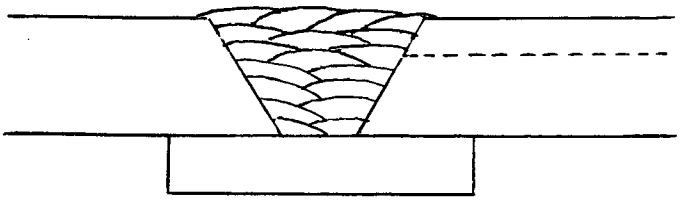

Welding Process:	SAW
Consumable Type:	EM12K wire Lincoln L61 with 860 flux
Wire Diameter:	2.4 mm (3/32 in.)
Shielding Gas:	N/A
Welding Current:	400 A
Arc Voltage:	29 V
Wire feed speed:	1.98 m/min (78 in/min)
Travel Speed:	305 mm/min (12 in/min)
Heat Input:	2.5 kJ/mm (64 kJ/in)
Polarity	DCEP
Stickout:	25 mm (1 in.)
Preheat:	10°C (50°F)
Interpass:	21°C (70°F) min., 205°C (400°F) max.
Backing Bar:	9.5-mm (⅜-in.) thick, 50-mm (2-in.) wide, M270 Grade 36

Figure 31. Welding procedure for 12.7- and 19-mm ($^1/_2$- and $^3/_4$-in.) single-vee butt joint welded by SAW.

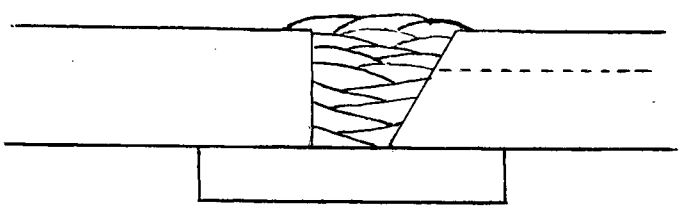

Welding Process:	SAW
Consumable Type:	EM12K wire Lincoln L61 with 860 flux
Wire Diameter:	2.4 mm (3/32 in.)
Shielding Gas:	N/A
Welding Current:	400 A
Arc Voltage:	32 V
Wire feed speed:	1.98 m/min (78 in/min)
Travel Speed:	305 mm/min (12 in/min)
Heat Input:	2.5 kJ/mm (64 kJ/in)
Polarity	DCEP
Stickout:	25 mm (1 in.)
Preheat:	10°C (50°F)
Interpass:	21°C (70°F) min., 205°C (400°F) max.
Backing Bar:	9.5-mm (⅜-in.) thick, 50-mm (2-in.) wide, M270 Grade 36

Figure 32. Welding procedure for 12.7- and 19-mm ($^1/_2$- and $^3/_4$-in.) single-bevel butt joint welded by SAW.

TABLE 16 Summary of V-groove welded butt joint specimens (*continued on next page*)

Material Grade	Material Thickness mm (in)	Cutting Technique	Welding Process	Weld No.	Radiography Pass/Fail	Defect
36	12.7 (½)	Nitrogen	SAW	W39	Fail	Slag
36	12.7 (½)	Air	SAW	W38	Pass	–
36	12.7 (½)	Oxygen	SAW	W37	Pass	–
36	12.7 (½)	U/W Oxygen	SAW	W62	Pass	–
36	12.7 (½)	U/W Nitrogen	SAW	W61	Pass	–
36	12.7 (½)	Nitrogen	FCAW	W29	Pass	–
36	12.7 (½)	Air	FCAW	W28	Pass	–
36	12.7 (½)	Oyxgen	FCAW	W30	Pass	–
36	12.7 (½)	U/W Oxygen	FCAW	W53	Fail	Slag
36	12.7 (½)	U/W Nitrogen	FCAW	W52	Pass	–
50W	12.7 (½)	Nitrogen	SAW	W34	Pass	–
50W	12.7 (½)	Air	SAW	W26	Pass	–
50W	12.7 (½)	Oxygen	SAW	W33	Pass	–
50W	12.7 (½)	U/W Oxygen	SAW	W75	Pass	–
50W	12.7 (½)	U/W Nitrogen	SAW	W74	Pass	–
50W	12.7 (½)	Nitrogen	FCAW	W31	Pass	–
50W	12.7 (½)	Air	FCAW	W15	Pass	Slag
50W	12.7 (½)	Oxygen	FCAW	W32	Pass	–
50W	12.7 (½)	U/W Oxygen	FCAW	W54	Fail	Slag
50W	12.7 (½)	U/W Nitrogen	FCAW	W55	Fail	Slag
50W	19 (¾)	Nitrogen	SAW	W63	Pass	–
50W	19 (¾)	Air	SAW	W27	Pass	–
50W	19 (¾)	Oxygen	SAW	W64	Pass	–
50W	19 (¾)	U/W Oxygen	SAW	W66	Pass	–
50W	19 (¾)	U/W Nitrogen	SAW	W65	Pass	–
50W	19 (¾)	Nitrogen	FCAW	W36	Fail	Porosity
50W	19 (¾)	Air	FCAW	W42	Pass	–
50W	19 (¾)	Oxygen	FCAW	W25	Pass	–
50W	19 (¾)	U/W Oxygen	FCAW	W49	Pass	–
50W	19 (¾)	U/W Nitrogen	FCAW	W50	Pass	–

plate, welded with SAW and FCAW, respectively (Figures 34 and 35). Macrosections of welds W96 and W84 show the typical weld cross sections for underwater oxygen plasma-cut and welded plate, welded with SAW and FCAW, respectively, Figures 36 and 37.

SAW and FCAW of panels were carried out, and fatigue specimens were machined. Grade 50W plate, 12.7 mm ($^1/_2$ in.) thick, was welded to produce the panels described in Table 15. A fixture was fabricated to minimize distortion in the relatively large plate sections. The fixture and welding equipment for SAW are shown in Figure 38, and the FCAW system in Figure 39. Seven welded panels 1220 mm by 610 mm (48 in. by 24 in.) were fabricated, five with SAW and two with FCAW, of which one had fillet welded attachments, rather than a butt joint.

HARDNESS LEVELS—WELDMENTS

Hardness measurements of weldment cross sections were carried out for 23 welds. The hardness traverses included the base metal, HAZ (three measurements), and fusion zone. The results showed that the hardness ranges were predominantly 160 to 230 VHN across the range of base materials, plasma cutting techniques, and welding processes.

TABLE 16 (*continued*)

Material Grade	Material Thickness mm (in)	Cutting Technique	Welding Process	Weld No.	Radiography Pass/Fail	Defect
50	19 (¾)	Nitrogen	SAW	W68	Pass	–
50	19 (¾)	Air	SAW	W67	Pass	–
50	19 (¾)	Oxygen	SAW	W69	Pass	–
50	19 (¾)	U/W Oxygen	SAW	W76	Pass	–
50	19 (¾)	U/W Nitrogen	SAW	W70	Pass	–
50	19 (¾)	Nitrogen	FCAW	W40	Fail	Slag/Porosity
50	19 (¾)	Air	FCAW	W14	Fail	Slag
50	19 (¾)	Oyxgen	FCAW	W41	Fail	Slag
50	19 (¾)	U/W Oxygen	FCAW	W87	Pass	–
50	19 (¾)	U/W Nitrogen	FCAW	W51	Pass	–

U/W = Underwater cutting with water injection

The highest values were typically in the HAZ near the fusion boundary. In three cases, hardness in the part of the HAZ nearest the fusion zone reached a maximum of 250 to 254 VHN. One of each of these specimens was cut by air, oxygen, and nitrogen. One specimen, from weld W15, had HAZ hardness measurements of 260, 268, and 309 VHN. This was Grade 50W material cut using air plasma, and was the highest value recorded. All four of these specimens were Grade 50 or 50W material welded by FCAW. Base metal hardness values ranged from 160 to 230 VHN from the Grade 36 to the Grade 50W material. Most of the values recorded were in the range of 160 to 200 VHN, with a typical increase in hardness of only 50 VHN in the HAZ. These results showed that the hardness of welds produced on plasma-cut edges is well within acceptable limits.

PAINTABILITY TESTING

Nineteen rectangular pieces of Grade 50W plate, 12.7 mm ($^1/_2$ in.) thick, were cut with square edges on four sides, each piece measuring 305 mm (12 in.) long by 152 mm (6 in.) wide. All four sides were thermally cut using the cutting procedures developed earlier. Twelve specimens were cut for the three plasma gases (air, oxygen, and nitrogen) three with underwater plasma cutting; and four by oxyfuel cutting to benchmark the performance of the painted plasma-cut specimens. From the pairs of plate specimens, the edges of one from each pair were manually ground to conform to the requirements of the D1.5 Bridge Welding Code, section 3.2, subsection 3.2.9. The other half were not edge/corner rounded. This plate was blast cleaned and primed at a structural steel fabricator. Half the specimens were painted using an inorganic zinc primer (Carboline 11HS), and the other half with a zinc rich epoxy primer (Ameron 68HS). Initially, two common 3-coat paint systems were selected, but in view of the paint testing requirements, the plate was only primed.

Following discussions with a number of industry specialists, Corrosion Control Consultants and Labs (CCCL) were selected to carry out paint performance testing. ASTM B117 Salt Fog testing and ASTM D3359 Cross-Cut Adhesion tests were selected for the primed plate described above.

Testing was initially carried out for ASTM D3359 Cross-Cut Adhesion on the primed plate described above. Results of D3359 tests showed good adhesion for the Ameron 68HS epoxy zinc rich primer on all edges. Paint quality for the Carboline 11HS was poor both in terms of adhesion and coverage. The paint coating was stripped off and reapplied by CCCL before testing to D3359. The test assesses the adherence of the paint coating on a classification scale from 0B to 5B, with 5B being the highest. A lattice of cuts is made through the coating and an adhesive tape peel test conducted to measure coating adherence. The classifications are as follows:

- 5B The edges of the cuts are completely smooth; none of the squares of the lattice is detached.
- 4B Small flakes of the coating are detached at intersections; less than 5 percent of the area is affected.
- 3B Small flakes of the coating are detached along edges and at intersections of the cuts. The area affected is 5 to 15 percent of the lattice.
- 2B The coating has flaked along the edges and on parts of the squares. The area affected is 15 to 35 percent of the lattice.

TABLE 17 Summary of single-bevel groove welded butt joint specimens

Material Grade	Thickness mm (in)	Cutting Technique	Welding Process	Weld No.	Radiography Pass/Fail	Defect
36	12.7 (½)	Nitrogen	SAW	W19	Pass	–
36	12.7 (½)	Air	SAW	W12	Pass	–
36	12.7 (½)	Oxygen	SAW	W20	Pass	–
36	12.7 (½)	U/W Oxygen	SAW	W57	Pass	–
36	12.7 (½)	U/W Nitrogen	SAW	W58	Pass	–
36	12.7 (½)	Machined	SAW	W45	Pass	–
36	12.7 (½)	Oxyfuel Gas	SAW	W46	Pass	–
50W	12.7 (½)	Nitrogen	SAW	W16	Pass	–
50W	12.7 (½)	Air	SAW	W18	Pass	–
50W	12.7 (½)	Oxygen	SAW	W17	Pass	–
50W	12.7 (½)	U/W Oxygen	SAW	W59	Pass	–
50W	12.7 (½)	U/W Nitrogen	SAW	W60	Pass	–
50W	12.7 (½)	Machined	SAW	W48	Pass	–
50W	12.7 (½)	Oxyfuel Gas	SAW	W47	Pass	–
50	19 (¾)	Nitrogen	SAW	W24	Fail	Slag/ Porosity
50	19 (¾)	Air	SAW	W13	Fail	Porosity
50	19 (¾)	Oxygen	SAW	W23	Pass	–
50	19 (¾)	U/W Oxygen	SAW	W76	Pass	–
50	19 (¾)	U/W Nitrogen	SAW	W56	Pass	–
50	19 (¾)	Machined	SAW	W43	Pass	–
50	19 (¾)	Oxyfuel Gas	SAW	W44	Pass	–

U/W = Underwater cutting with water injection

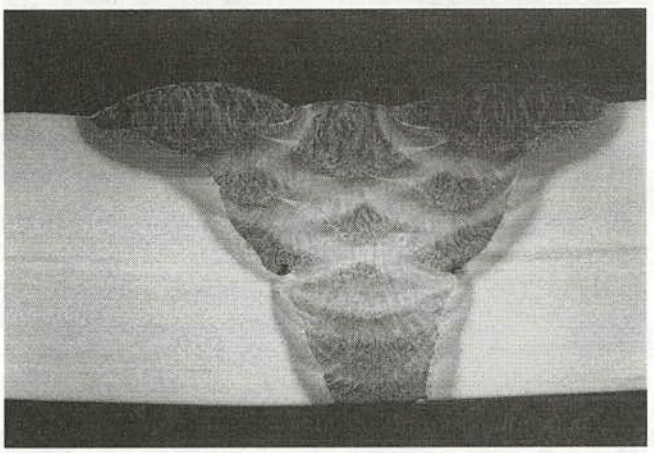

Figure 33. Multipass single-vee FCAW joint, W14, in 19-mm ($^3/_4$-in.)-thick Grade 50 plate cut by air PAC. Original mag. × 2.5; as shown × 1.75.

1B The coating has flaked along the edges of cuts in large ribbons and whole squares have detached. The area affected is 35 to 65 percent of the lattice.

0B Flaking and detachment worse than Grade 1B.

All specimens passed the ASTM D3359 Cross-Cut Adhesion test with assessments of 4B for all but one, which was ranked 3B.

A total of 2,000 hours of ASTM B117 Salt Fog testing was performed, followed by repeat test for paint adherence to the cut edge, and assessment of the corrosion performance of the rounded/unrounded edges. No sign of corrosion was seen on any of the specimens after a 2,000-hr exposure. Cross-cut adhesion testing to ASTM D3359 was carried out to compare the results with those obtained prior to corrosion testing. Only four of the 19 specimens showed any changes, three with unrounded edges, of which two were plasma cut and one was oxyfuel cut. The fourth specimen was cut with nitrogen and edge rounded. Three of

TABLE 18 Summary of fillet-welded T-butt joint specimens

Material Grade	Thickness		Cutting Technique	Welding Process	Weld No.	Visual/ Metallography Pass/Fail	Defect
	mm	in.					
36	12.7	½	Nitrogen	SAW	W92	Pass	–
36	12.7	½	Air	SAW	W88	Pass	–
36	12.7	½	Oxygen	SAW	W93	Pass	–
36	12.7	½	U/W Oxygen	SAW	W95	Pass	–
36	12.7	½	U/W Nitrogen	SAW	W94	Pass	–
36	12.7	½	Nitrogen	FCAW	W81	Pass	–
36	12.7	½	Air	FCAW	W79	Pass (2 mm pore at root)	–
36	12.7	½	Oxygen	FCAW	W77	Pass	–
36	12.7	½	U/W Oxygen	FCAW	W83	Pass	–
36	12.7	½	U/W Nitrogen	FCAW	W85	Pass	–
50W	12.7	½	Nitrogen	SAW	W90	Pass	–
50W	12.7	½	Air	SAW	W91	Pass	–
50W	12.7	½	Oxygen	SAW	W89	Pass	–
50W	12.7	½	U/W Oxygen	SAW	W96	Pass	–
50W	12.7	½	U/W Nitrogen	SAW	W97	Pass	–
50W	12.7	½	Nitrogen	FCAW	W82	Pass	–
50W	12.7	½	Air	FCAW	W80	Pass	–
50W	12.7	½	Oxygen	FCAW	W78	Pass	–
50W	12.7	½	U/W Oxygen	FCAW	W84	Pass	–
50W	12.7	½	U/W Nitrogen	FCAW	W86	Pass	–

U/W = Underwater cutting with water injection

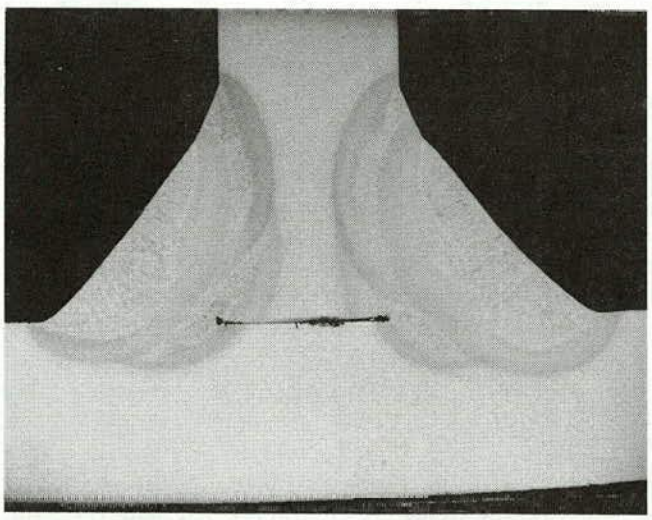

Figure 34. Macrosection of fillet weld soundness test for weld W88, air plasma-cut edge on Grade 36 plate, 12.7 mm ($^1/_2$ in.) thick, welded by SAW. Original mag. × 2.5; as shown × 1.75.

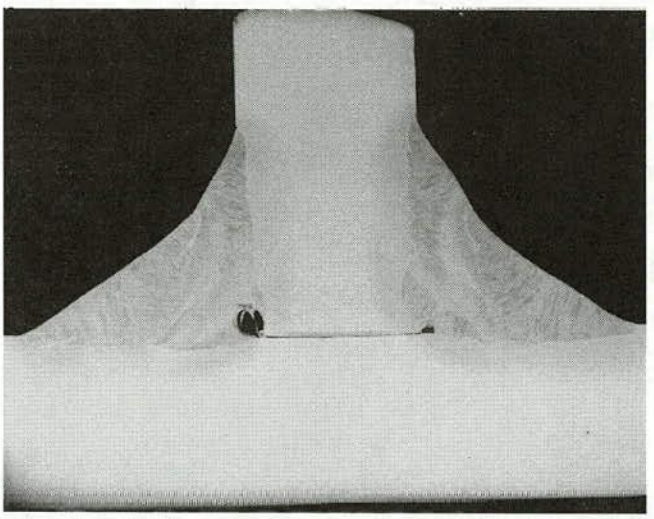

Figure 35. Macrosection of fillet weld soundness test for weld W79, air plasma-cut edge on Grade 36 plate, 12.7 mm ($^1/_2$ in.) thick, welded by FCAW. Original mag. × 2.5; as shown × 1.75.

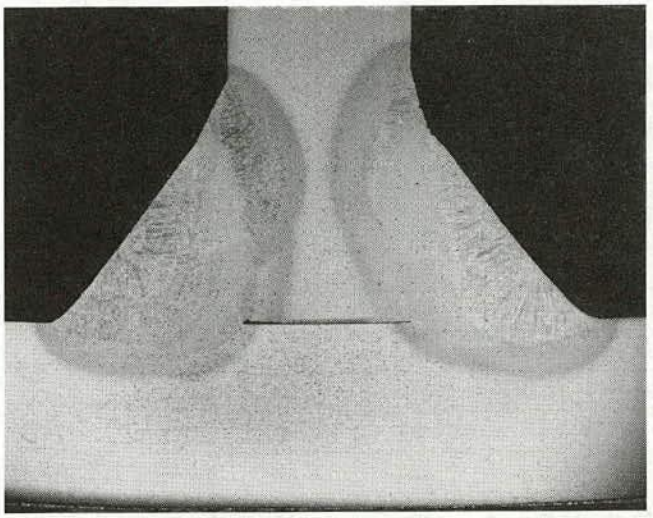

Figure 36. Macrosection of fillet weld soundness test for weld W96, underwater oxygen plasma-cut edge on Grade 50W plate, 12.7 mm ($^1/_2$ in.) thick, welded by SAW. Original mag. × 2.5; as shown × 1.75.

these four changed from a 4B to a 3B classification after corrosion testing. One of the underwater oxygen-cut edges that was not rounded changed from a 4B to a 2B classification. However, the other specimen showed no change, retaining a 4B classification. The complete results are shown in Table 19.

Overall results indicated no significant reduction in performance in terms of paint adherence and no adverse results in the corrosion test. CCCL concluded that the type of cutting did not affect the results, and that adherence and corrosion did not differ whether the steel was edge/corner ground or not.

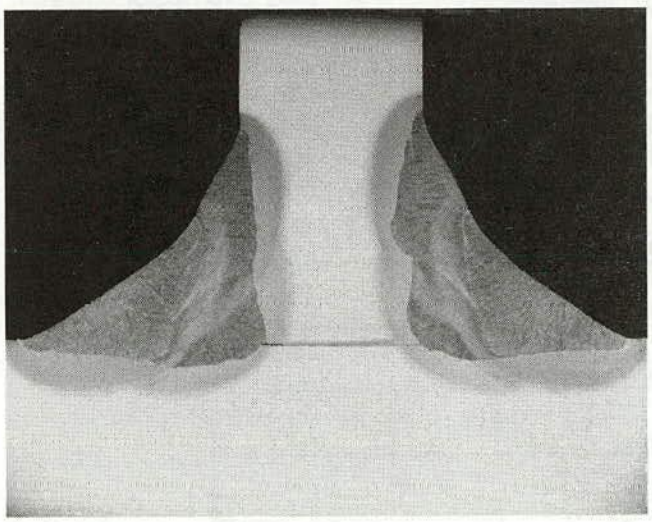

Figure 37. Macrosection of fillet weld soundness test for weld W84, underwater oxygen plasma-cut edge on Grade 50W plate, 12.7 mm ($^1/_2$ in.) thick, welded by FCAW. Original mag. × 2.5; as shown × 1.75.

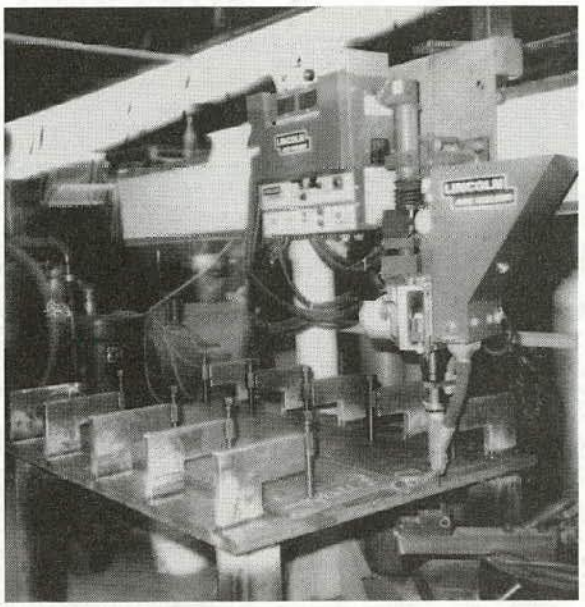

Figure 38. SAW system showing the fixture for welding of panels for fatigue testpieces.

BEND TESTING

Specimens were plasma cut and machined to form face bend specimens on the as-cut surfaces for each combination of dry gases (air, oxygen, and nitrogen), underwater plasma-cut specimens, and oxyfuel-cut edges listed in Table 20. The specimens, were tested in 3-point bending with the plasma-cut face in tension. This was carried out on the as-cut surfaces for each combination of material type, material thickness, and plasma gas listed in Table 20. All the specimens produced by plasma in air passed the ASTM requirements,

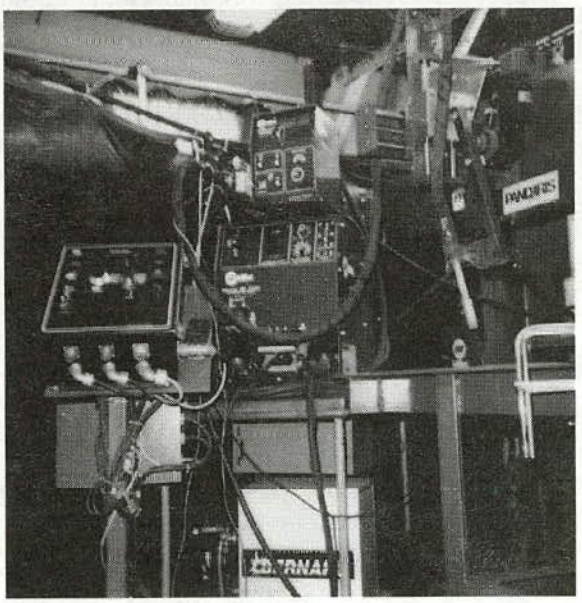

Figure 39. Welding equipment used for FCAW.

TABLE 19 ASTM D3359 cross-cut adhesion test results

Panel No.	Plasma Gas	Primer	Avg. DFT	Adh. No. 1	Adh. No. 2
1R	Air	Ameron 68HS	2.8	4B	4B
2	Air	Ameron 68HS	2.8	4B	3B
3R	Air	Carboline 11HS	2.8	4B	4B
4	Air	Carboline 11HS	3.1	4B	4B
5R	Oxygen	Ameron 68HS	2.6	4B	4B
6	Oxygen	Ameron 68HS	3.2	4B	4B
7R	Oxygen	Carboline 11HS	3.3	4B	4B
8	Oxygen	Carboline 11HS	2.8	4B	4B
9R	Nitrogen	Ameron 68HS	3.1	4B	4B
10	Nitrogen	Ameron 68HS	3.0	4B	4B
11R	Nitrogen	Carboline 11HS	2.9	4B	3B
12	Nitrogen	Carboline 11HS	3.3	3B	3B
13R	U/W Oxygen	Carboline HS	2.9	4B	4B
14	U/W Oxygen	Carboline HS	2.9	4B	4B
15	Did not receive this panel				
16	U/W Oxygen	Ameron 68HS	2.7	4B	2B
17R	Oxyfuel Gas	Ameron 68HS	3.3	4B	4B
18	Oxyfuel Gas	Ameron 68HS	3.3	4B	3B
19R	Oxyfuel Gas	Carboline 11HS	2.7	4B	4B
20	Oxyfuel Gas	Carboline 11HS	2.5	4B	4B

U/W = Underwater cutting with water injection
DFT = Dry film thickness

TABLE 20 Test matrix for face bend tests on as-cut surfaces

Material	Thickness mm (in)	Cutting Process	Surface Roughness (μm)	No. of Face Bend Tests
M270 Grade 36	12.7 (½)	Air, O_2, N_2, U/W O_2, U/W N_2	5	10
		Air, O_2, N_2, U/W O_2, U/W N_2	15	10
M270 Grade 50W	12.7 (½)	Air, O_2, N_2, U/W O_2, U/W N_2	5	10
	12.7 (½)	Air, O_2, N_2, U/W O_2, U/W N_2	15	10
	19 (¾)	Air, O_2, N_2, U/W O_2, U/W N_2	15	5
M270 Grade 50	19 (¾)	Air, O_2, N_2, U/W O_2, U/W N_2	5	10
		Air, O_2, N_2, U/W O_2, U/W N_2	15	10

Number of replicate tests: 2/cutting condition
U/W = Underwater cutting with water injection

for all four combinations of material type and thickness (Tables 21 to 24).

The results for underwater cutting were not as conclusive. For underwater oxygen plasma cutting on Grades 36 and 50W (both 12.7 mm and 19 mm), all but one of the 12 specimens passed the bend test. However, for the Grade 50 plate, all four specimens failed. For underwater nitrogen plasma cutting, 11 of 16 specimens failed, the worst results being for the Grades 36 and 50 material where all four specimens failed in each case. This prompted a metallographic investigation of the edges produced by underwater nitrogen plasma cutting.

Wilson (*62*) conducted a detailed investigation of the actual cut edges in the SEM. He found, at high magnifications, that a network of grain boundary fissures was present on all the cut edges, independent of plate chemistry, temperature, or cutting speed. These fissures were also present in normalized plates, as-rolled plates, and plasma cuts, as well as in oxyfuel cuts. The depths of the fissures extended into the martensitic portion of the HAZ just below the thermal cut edge. Wilson (*62*) reported that these fissures were a direct result of the cutting process and may actually result from thermal etching; these intergranular features are present on all of the thermal cut edges and initiated the cracking in the bend test. In this investigation, a sample of the underwater nitrogen plasma cut in Grade 50 steel was sectioned through the thickness of the plate to examine the cut edge in the SEM for the grain boundary fissures. Figure 40 shows a fissure

TABLE 21 Bend test results

Job No.: J7272	Date: Feb. 17,1995
Material: M270 Gr. 36, 12.7 mm (½ in.)	Specification: ASTM E190

Specimen ID	Roughness	Process	Remarks
F1A-1	5	Air	OK
F1A-2	5	Air	OK
F1A-3	15	Air	OK
F1A-4	15	Air	OK
F1B-1	5	Nitrogen	OK
F1B-2	5	Nitrogen	OK
F1B-3	15	Nitrogen	OK
F1b-4	15	Nitrogen	OK
F1C-1	5	U/W Nitrogen	Crks @ Bottom Edge
F1C-2	5	U/W Nitrogen	Crks @ Bottom Edge
F1C-3	15	U/W Nitrogen	Fractured
F1C-4	15	U/W Nitrogen	Crks @ Bottom Edge
F1D-1	5	Oxygen	OK
F1D-2	5	Oxygen	OK
F1D-3	15	Oxygen	OK
F1D-4	15	Oxygen	OK
F1E-1	5	U/W Oxygen	Crks @ Top Edge
F1E-2	5	U/W Oxygen	OK
F1E-3	15	U/W Oxygen	OK
F1E-4	15	U/W Oxygen	OK
F1F-1	15	Oxyfuel Gas	OK
F1F-2	15	Oxyfuel Gas	OK

U/W = Underwater cutting with water injection

TABLE 22 Bend test results obtained from the different cutting techniques for the 12.7-mm (0.5-in.) Grade 50W steel

Job No.: J7272	Date: Feb. 17,1995
Material: M270 Gr. 50W, 12.7 mm (½ in.)	Specification: ASTM E190

Specimen ID	Roughness	Process	Remarks
F2A-1	5	Air	OK
F2A-2	5	Air	OK
F2A-3	15	Air	OK
F2A-4	15	Air	OK
F2B-1	5	Nitrogen	OK
F2B-2	5	Nitrogen	OK
F2B-3	15	Nitrogen	OK
F2B-4	15	Nitrogen	OK
F2C-1	5	U/W Nitrogen	OK
F2C-2	5	U/W Nitrogen	OK
F2C-3	15	U/W Nitrogen	Crks @ Bottom Edge
F2C-4	15	U/W Nitrogen	Crks @ Bottom Edge
F2D-1	5	Oxygen	OK
F2D-2	5	Oxygen	OK
F2D-3	15	Oxygen	OK
F2D-4	15	Oxygen	OK
F2E-1	5	U/W Oxygen	OK
F2E-2	5	U/W Oxygen	OK
F2E-3	15	U/W Oxygen	OK
F2E-4	15	U/W Oxygen	OK
F2F-1	15	Oxyfuel Gas	OK
F2F-2	15	Oxyfuel Gas	OK

U/W = Underwater cutting with water injection

extending from the cut edge into the HAZ of the cut edge similar to those reported by Wilson.

In this investigation, the results of the face bend and as-cut fatigue specimens may have been influenced by these fissures. No effect of the fissures should be observed in the welded fatigue specimens because the fissures should be consumed by the welding process. The effects of these fissures on the mechanical properties were not determined from this limited investigation. However, they may act as initial cracks in the fatigue specimens and could result in degradation of the fatigue performance. Fatigue specimens were not produced for Grade 50 plate so the specific effect is presently unknown for this material, although underwater nitrogen cutting produced lower fatigue life on Grade 50W plate, 12.7 mm ($^1/_2$ in.) thick, compared with other cutting techniques (see Section 2.32.2). On Grade 36 plate, the poor bend test results for underwater nitrogen cutting were not reflected in the fatigue test results.

RESIDUAL STRESS MEASUREMENTS ON PLASMA-CUT EDGES

Grades 36 and 50W plate, 12.7 mm ($^1/_2$ in.) thick, were cut for residual stress measurements using all five plasma cutting techniques. Two measurements per sample were made according to Table 25. (Detailed results are presented in Appendix D.)

The objective was to evaluate and compare the near-surface residual stress distribution produced as a result of the thermal gradients encountered during the plasma cutting process on each steel and with each gas. This was accomplished with a series of blind-hole measurements made on the cut surfaces.

TABLE 23 Bend test results obtained from the different cutting techniques for the 19-mm (0.75-in.) Grade 50W steel

Job No.: J7272	Date: Feb. 17,1995
Material: M270 Gr. 50W, 19 mm (¾ in.)	Specification: ASTM E190

Specimen ID	Roughness	Process	Remarks
F3A-1	5	Air	OK
F3A-2	5	Air	OK
F3A-3	15	Air	OK
F3A-4	15	Air	OK
F3B-1	5	Nitrogen	OK
F3B-2	5	Nitrogen	OK
F3B-3	15	Nitrogen	OK
F3B-4	15	Nitrogen	OK
F3C-1	5	U/W Nitrogen	OK
F3C-2	5	U/W Nitrogen	OK
F3C-3	15	U/W Nitrogen	OK
F3C-4	15	U/W Nitrogen	Crks @ Bottom Edge
F3D-1	5	Oxygen	OK
F3D-2	5	Oxygen	OK
F3D-3	15	Oxygen	OK
F3D-4	15	Oxygen	OK
F3E-1	5	U/W Oxygen	OK
F3E-2	5	U/W Oxygen	OK
F3E-3	15	U/W Oxygen	OK
F3E-4	15	U/W Oxygen	OK
F3F-1	15	Oxyfuel Gas	OK
F3F-2	15	Oxyfuel Gas	OK

U/W = Underwater cutting with water injection

The measurements were made on plasma-cut edges on Grade 36 and Grade 50 steels. The nominal yield and tensile strength of the Grade 36 plate is 314 MPa (45,600 psi) and 470 MPa (68,150 psi), respectively as reported on the mill certification records. Likewise, the yield and tensile strength of the Grade 50 plate are 396 MPa (57,467 psi) and 525 MPa (76,167 psi), respectively. One residual stress test sample was provided for each material and cutting process. In addition, one oxy-acetylene flame-cut sample from the Grade 50 plate was provided as a benchmark.

The blind-hole drilling process requires that a small hole be produced in the component or material of interest, the hole centered in the middle of a special 3-gauge strain rosette (shown in Figure D-1). Both the diameter and the depth of the hole used were 1 mm (0.040 in.). The introduction of a hole in a stressed component produces a local change or relaxation in the stress field, which is measured by the three strain-sensing elements placed around the hole. A schematic of the hole cross section appears in Figure 41. Using standard constitutive equations, this change in strain can be used to estimate the original undisturbed residual stress field.

In the blind-hole process, the hole is produced by erosion using a fine aluminum oxide powder directed against the surface of the sample, under 0.55 MPa (80 psi) air pressure. A special drilling head is used to properly align the hole over the target in the center of the strain gage rosette and controls the geometry of the hole. Because the hole is produced by erosion, no additional stresses are imparted to the surface, which would be a possibility if the hole were created using a mechanical drill bit. Once the hole has achieved a depth equal to its diameter, the drilling process is stopped and the strain measured by each of the three strain elements is recorded. These data, along with the modulus of elasticity

TABLE 24 Bend test results obtained from the different cutting techniques for the 19-mm (0.75-in.) Grade 50 steel

Job No.: J7272	Date: Feb. 17,1995
Material: M270 Gr. 50W, 19 mm (¾ in.)	Specification: ASTM E190

Specimen ID	Roughness	Process	Remarks
F4A-1	5	Air	OK
F4A-2	5	Air	OK
F4A-3	15	Air	OK
F4A-4	15	Air	OK
F4B-1	5	Nitrogen	OK
F4B-2	5	Nitrogen	OK
F4B-3	15	Nitrogen	OK
F4B-4	15	Nitrogen	Fractured
F4C-1	5	U/W Nitrogen	Fractured
F4C-2	5	U/W Nitrogen	Fractured
F4C-3	15	U/W Nitrogen	Crks @ Both Edges
F4C-4	15	U/W Nitrogen	OK
F4D-1	5	Oxygen	OK
F4D-2	5	Oxygen	OK
F4D-3	15	Oxygen	OK
F4D-4	15	Oxygen	Fractured
F4E-1	5	U/W Oxygen	Crks @ Center & Bottom Edges
F4E-2	5	U/W Oxygen	Fractured
F4E-3	15	U/W Oxygen	Fractured
F4E-4	15	U/W Oxygen	OK
F4F-1	15	Oxyfuel Gas	OK
F4F-2	15	Oxyfuel Gas	OK

and Poissons ratio for the material, are sufficient to calculate the original residual stress condition of the sample. The maximum and minimum principal stresses are determined and are then usually resolved onto reference axes applicable to the structure.

Each plate sample was rectangular in shape, having a width of typically 89 mm (3.5 in.) with a length of about 343 mm (13.5 in.). Two blind-hole rosette gages were laid on one cut edge of each sample. These gages were generally placed about 25 mm (1 in.) apart near the mid-length of the specimen and were positioned so that the hole would be located on the midthickness plane of the plate. The type of gage used was an EA-06-031RE-120 supplied by Measurements Group Inc. in Raleigh, NC. This type of gage requires a hole having a diameter and depth equal to 1 mm (0.040 in.). The length of the strain elements was 0.79 mm (0.031 in.). The sampling volume of the gage is 7.74×10^{-7} mm^3 (0.013 in^3).

Strain readings at various intermediate hole depths were recorded for most holes. These incremental readings were done somewhat randomly as there is no direct method to measure the depth of the hole during drilling. The time required to produce a hole to the nominal depth of 1 mm (0.040 in.) is directly dependent on the hardness of the material being drilled. In the case of the plasma-cut edges, a thin, hardened layer is produced that can require several minutes to drill through using the aluminum oxide powder. Occasionally, the drilling operation is halted and the hole depth measured to determine if additional drilling is required at each hole site. It is at these intermediate depths that the incremental strains were recorded and analyzed to ascertain to some degree the variation in residual stress as a function of hole depth.

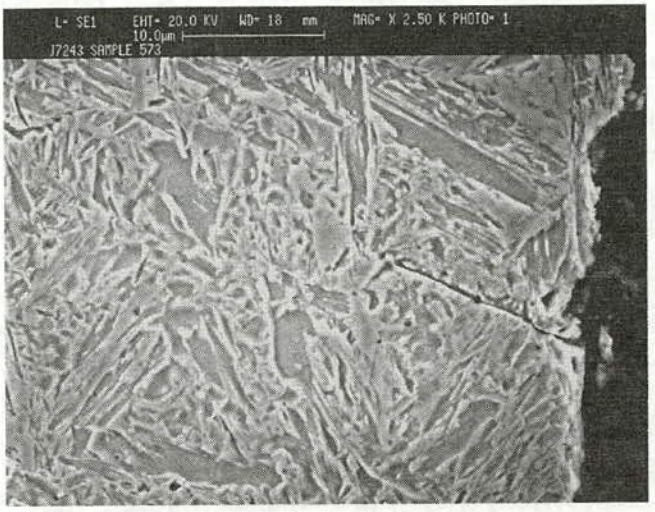

Figure 40. Microfissure on an underwater nitrogen plasma-cut edge. Original mag. ×2,500; as shown ×1,850.

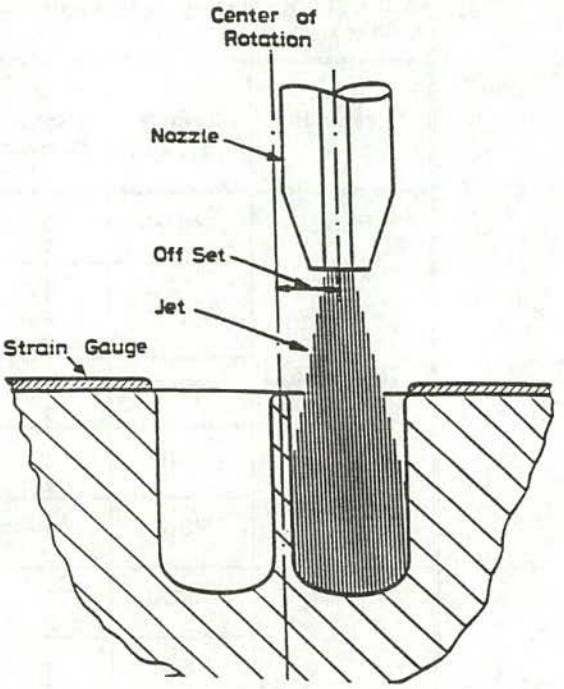

Figure 41. Cross section of drilled hole.

Full Hole Depth Results

Table 26 summarizes the results for the full depth analyses. These values represent the average state of residual stress to a depth of 1 mm (0.040 in.). Following completion of each hole, the maximum and minimum principal stresses were calculated. These principal stresses were resolved onto directions parallel to the cutting direction, called the longitudinal direction, and parallel to the plate thickness, called the through-thickness direction. It is assumed in Table 26 that the residual stress field is uniform with depth. This, of course, is not representative of the true physical condition. However, it is a standard assumed condition when carrying out blind-hole drilling. The incremental depth results presented in Section 2.31.2 do not include this assumption.

Table 26 clearly indicates that the through-thickness stresses are generally small regardless of the type of cutting process and grade of material. These stresses fluctuate around zero with no identifiable trend observed regarding either the grade of steel or the cutting process. Therefore, the level of through-thickness residual stress seems to be independent of the material yield strength and cutting process. This may be related to the low degree of restraint that would exist in this plane during the cutting process. As the cut surface begins to cool, the material at the edge of the cut will

TABLE 25 Test matrix for residual stress measurements of as-cut surfaces

Material	Plasma Cutting Process	Residual Stress Sample Identification
M270 Gr 36	Air	RS1A
	Nitrogen	RS1B
	Oxygen	RS1D
	Nitrogen Underwater	RS1C
	Oxygen Underwater	RS1E
M270 Gr 50	Air	RS2A
	Nitrogen	RS2B
	Oxygen	RS2D
	Nitrogen Underwater	RS2C
	Oxygen Underwater	RS2E
	Oxyfuel Gas	RS2F

TABLE 26 Residual stress results determined by blind-hole drilling, nominal hole depth: 1 mm (0.040 in.)

Material	Sample	Gage Number	Cutting Process	Through-thickness Stress N/mm² (psi)	Longitudinal Stress N/mm² (psi)
A709 Gr 36	RS1A	1	Air	8.6 (1245)	134.6 (19524)
		2		24.4 (3533)	107.5 (15589)
	RS1B	1	Nitrogen	-13.2 (-1915)	-91.8 (-13313)
		2		10.0 (1449)	-16.6 (-2408)
		3		-28.6 (-4152)	-28.7 (-4155)
	RS1C	1	U/W Nitrogen	-26.6 (-3863)	99.0 (14357)
		2		-16.5 (-2389)	80.2 (11630)
	RS1D	1	Oxygen	4.7 (676)	70.5 (10220)
		2		-7.7 (-1116)	96.8 (14034)
	RS1E	1	U/W Oxygen	-7.5 (-1091)	86.5 (12541)
		2		8.6 (1248)	115.9 (16810)
A709 Gr 50	RS2A	1	Air	57.8 (8379)	210.0 (30447)
		2		42.8 (6200)	187.8 (27236)
	RS2B	1	Nitrogen	-41.6 (-6037)	183.2 (26568)
		2		-3.9 (-571)*	211.4 (30650)*
	RS2C	1	U/W Nitrogen	-24.2 (-3505)	141.9 (20570)
		2		-9.5 (-1374)	120.7 (17504)
	RS2D	1	Oxygen	18.8 (2731)	229.4 (33270)
		2		28.0 (4055)	214.9 (31161)
	RS2E	1	U/W Oxygen	-46.4 (-6724)	176.8 (25634)
		2		-4.8 (-703)	100.7 (14596)
	RS2F	1	Oxyfuel Gas	22.5 (3258)	68.1 (9872)
		2		-26.4 (-3828)	63.3 (9177)

U/W = Underwater cutting with water injection

* Hole was drilled only to one-half the intended depth due to equipment failure. Therefore, this result is an average stress over a depth of 0.5 mm (0.020 in.).

N.B. Within limits of reliable accuracy and repeatability, these values should be rounded to the nearest 100 psi.

contract freely in the through-thickness direction as little constraint exists from the adjoining material which has just been removed by the cutting process. Consequently, upon cooling to ambient temperature, the cut surface is left in a state of minimal stress.

The longitudinal stresses (parallel to the cut edge) listed in Table 26 are typically tensile for all cutting processes and each grade of material. The only exception to this is sample RS1B which is discussed separately below. This trend is due to the greater constraint applied to the cut edge along the length of the plate. As the cut edge cools to ambient temperature, it is prevented from contracting freely by the surrounding cooler plate material along the plane of the cut.

The actual production of residual stress is somewhat complex as the stress distribution is composed of the thermal stresses and mechanical stresses set up by the local deformation on the cut surface created by the high velocity plasma gas. The thermal stresses may be most important in the longitudinal direction (parallel to the cut edge) while the mechanical action of the plasma gas may be most important in defining the residual stresses in the plate thickness direction.

It is evident in Table 26 that the longitudinal stresses are always tensile with the exception of sample RS1B which was cut with nitrogen gas. There appears to be no clear explanation why this sample produced compressive longitudinal stresses.

Often, when discussing residual stress values, the absolute value of residual stress is not as significant as is the value of residual stress expressed as a percentage of the material's yield strength. Table 27 lists the full depth residual stress values as a percentage of the plate yield strength. Here it is assumed that the yield strength properties along the length of the plate and in the through-thickness direction (i.e., short transverse direction) are identical. Furthermore, it is assumed that the compressive and tensile yield strengths are equal in absolute magnitude. It is obvious that there is considerable scatter in the results. Comparing results for the two different grades of steel, there does not appear to be any meaningful trend related to the cutting process. However, the longitudinal stresses are somewhat higher for the higher strength material. In general, the level of residual stress would be expected to be dependent on the amount of thermal energy required to complete the cut. Higher thermal inputs would generally produce higher levels of residual stress.

In this study, the magnitude of residual stress produced by plasma cutting was found to be approximately one-third to one-half of yield along the cut edge and near zero in the plate thickness direction. Note that the residual stresses along the cut edge are consistently tensile in magnitude with the exception of plate sample RS1B. The magnitude of these stresses is less than would be expected for welds that had not been thermally stress relieved. Therefore, for structures that are intended to have as-welded fabrications, the residual stresses produced by plasma cutting should not be of concern.

TABLE 27 Full depth residual stress results expressed as a percentage of material yield strength[1]

Material	Sample	Gage Number	Cutting Process	Through-Thickness Stress Ratio[2]	Longitudinal Stress Ratio[3]
M270 Gr 36	RS1A	1 2	Air	2.7 7.7	42.8 34.2
	RS1B	1 2	Nitrogen	-4.2 3.2	-29.2 -5.3
	RS1C	1 2	U/W Nitrogen	-8.5 -5.2	31.5 25.5
	RS1D	1 2	Oxygen	1.5 -2.4	22.4 30.8
	RS1E	1 2	U/W Oxygen	-2.4 2.7	27.5 36.9
	Mean for all Processes			2.8	28.6
M270 Gr 50	RS2A	1 2	Air	14.6 10.8	53.0 47.4
	RS2B	1 2	Nitrogen	-10.5 -1.0	46.2 53.3
	RS2C	1 2	U/W Nitrogen	-6.1 -2.4	35.8 30.5
	RS2D	1 2	Oxygen	4.8 7.1	57.9 54.2
	RS2E	1 2	U/W Oxygen	-11.7 -1.2	44.6 25.4
	RS2F	1 2	Oxyfuel Gas	5.7 -6.7	17.2 16.0
	Mean for all Processes			5.9	40.1

U/W = Underwater cutting with water injection

[1] Assumes that the material yield strength in compression has the same absolute magnitude as in tension.
[2] Through-thickness residual stress divided by the material yield strength, expressed in %.
[3] Longitudinal residual stress divided by the material yield strength, expressed in %.

Intermediate Depth Results

During drilling of most of the blind-holes, strain values were recorded at one or more intermediate hole depths. Six of the 23 gages did not have any intermediate results recorded. These gages were identified as RS2B-1, RS2B-2, RS2C-2, RS1D-1, RS1D-2, and RS2D-2. In general, the intermediate hole depths ranged from about 0.25 mm (0.010 in.) to the final hole depth of about 1 mm (0.040 in.). Typically, two or three intermediate residual stress values were recorded for each hole. The longitudinal intermediate residual stress values are presented in Appendix D, Figures D-3 through D-8, with the through-thickness values presented in Figures D-9 through D-14.

Considering the longitudinal values in Figures D-3 through D-8, all of the residual stresses are tensile with the exception of the nitrogen plasma-cut panel in which the longitudinal stresses fluctuate around zero. Notice that Figures D-3 through D-8 are plotted on the same scale to facilitate comparison between the two grades of steel and the cutting processes. For the higher strength Grade 50 plate, the plasma with air and underwater oxygen cutting processes result in higher levels of longitudinal residual stress. This is consistent with the full hole depth results presented in Tables 26 and 27, which suggests that regardless of cutting process, the higher strength material generally produces higher levels of residual stress.

The intermediate longitudinal residual stress results clearly show, with the exception of the nitrogen cut panel, that at depths of about 0.25 mm (0.010 in.) from the cut edge and beyond, the longitudinal stresses are tensile in nature. It is impossible in this study to determine the magnitude and sign of the stresses at locations closer to the cut edge. Furthermore, due to the limited number of intermediate hole depths possible with this measurement technique, detailed distributions are difficult to define. For this reason, a linear distribution has been imposed on Figures D-3 through D-8. These idealized distributions imply that the stress field is relatively uniform over the regions between 0.5 mm and 1 mm (0.020 and 0.040 in.) in depth. However, as the magnitude of these stresses approaches 50 percent of the material's yield strength, particularly for the higher-strength steel, these stresses could have implications for the structural performance of plasma-cut edges. This is discussed further in Chapter 3.

Figures D-9 through D-14 illustrate consistent residual stress distributions for each cutting process for the plate thickness direction. In general, these stresses tended to fluctuate around zero and did not reveal any meaningful trends for either plate material or cutting process. As with the longitudinal stress diagrams, Figures D-9 through D-14 are plotted on the same scale for comparison purposes. Again, due to limited data, the trends have been idealized as linear relationships that suggest a rather uniform stress distribution exists in most samples as distance from the cut edge increases. Regardless, these results suggest that the residual stresses in the plate thickness direction are insignificant in terms of the structural integrity of plasma-cut edges.

FATIGUE TESTING OF AS-CUT PLASMA-CUT EDGES

A CNC program was developed to cut the test pieces for fatigue specimens using robotic plasma cutting. A five-axis articulated arm robot was employed to cut specimens at EWI, Figure 42. A CNC cutting machine was employed at ESAB/L-Tec to cut the specimens for underwater oxygen and underwater nitrogen plasma cutting.

Plasma cutting of fatigue test specimens using the optimized parameters, developed in the earlier linear cutting trials, was carried out for all grades and thicknesses of plate described in Table 28, using air, nitrogen, and oxygen plasma cutting in air, and underwater plasma cutting with oxygen and nitrogen. Specimen configurations for fatigue testing of plate and weldments are shown in Figure 43. Sets of ten specimens were cut in each case, from M270 Grades 36 and 50W plate, 12.7 mm ($^1/_2$ in.) thick. Because of the large volume of results, these are presented in Appendix E.

The objective of the fatigue tests was to compare the fatigue performance of all the cutting processes for two strengths of 12.7-mm (0.5-in.) steels (Grade 36 and Grade 50W), and to compare these with the standard AASHTO design curve. The intent was to show that the fatigue performance is at least equal to or better than the standard design curve for plain members. Within each grade of steel, one S-N curve was also generated for a machined edge and one for an oxyfuel as-cut edge. These were used as a basis for comparison.

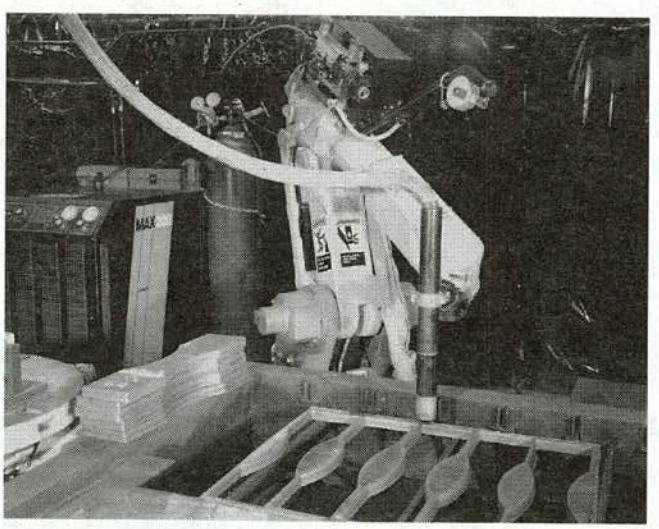

Figure 42. Robotic plasma arc cutting system employing a 5-axis robot and mechanized plasma cutting torch to produce fatigue testpieces.

TABLE 28 Proposed matrix to assess the fatigue behavior of as-cut edges

Material	Thickness (in)	Cutting Process	Surface Roughness (μm)	No. of S-N Curves
A709 Grade 36	½	Air	<5	1
		Nitrogen	<5	1
		Oxygen	<5	1
		U/W Nitrogen	<5	1
		U/W Oxygen	<5	1
		Machined	<5	1
		Oxyfuel Gas	<5	1
A709 Grade 50W	½	Air	<5	1
		Oxygen	<5	1
		Nitrogen	<5	1
		U/W Oxygen	<5	1
		U/W Nitrogen	<5	1
		Machined	<5	1
		Oxyfuel Gas	<5	1
A709 Grade 50W	¾	Oxygen	<5	1
		U/W Oxygen	<5	1
A709 Grade 50W	¾	Oxygen	>15	1
		U/W Oxygen	>15	1

U/W = Underwater cutting with water injection
Ten specimens tested for each S-N curve

The effect of specimen thickness and surface roughness was investigated using 19-mm (0.75-in.)-thick Grade 50W steel. These last series of tests were limited to plasma cutting using oxygen and underwater oxygen. The effect of surface roughness was investigated by testing a series of oxygen plasma specimens with a rougher surface cut at higher speed. The two levels of surface roughness tested in this program reflect the two extremes of smooth and rough conditions. No surface roughness measurements were conducted on the actual test specimens, although they were made on linear specimens at the same speeds.

Fatigue testing was conducted to develop S-N curves for the different techniques in order to assess the effects of the cutting process, grade of material, surface roughness, and material thickness. The testing was conducted using a uniaxial sinusoidal cyclic tensile loading with a stress ratio, R, of 0.1. All the testing was carried out at room temperature to failure or until 5.0×10^6 cycles was reached. The specimens were tested in the as-cut condition. If present, any excess dross was removed from the bottom side of the plate, but no edge rounding was done.

Fatigue Results for the 12.7-mm (0.5-in.) Grade 36 Plate

The fatigue test results for the Grade 36 material are shown in Figures E-1 through E-7, Appendix E, and summarized in Figure 44. The edge quality of the cut surfaces were representative of the cut edge quality from the optimized parameters. In most cases, the fatigue cracking initiated at the bottom side of the plasma-cut edge and propagated through the thickness of the plate. However, there were also examples of cracking initiating at the top side of the plasma-cut edge. A couple of the specimens failed outside of the test area or in the grip section as reported in the results in Appendix E.

In Figures E-1 through E-7, the results are shown in comparison with the corresponding AASHTO design curve for a plain member, Category A. All the cutting technique fatigue results were above the AASHTO Category A design curve in the 10^6 cycle fatigue range with a few results from the air, underwater nitrogen, and underwater oxygen plasma-cut and the oxyfuel-cut fatigue specimens falling below the

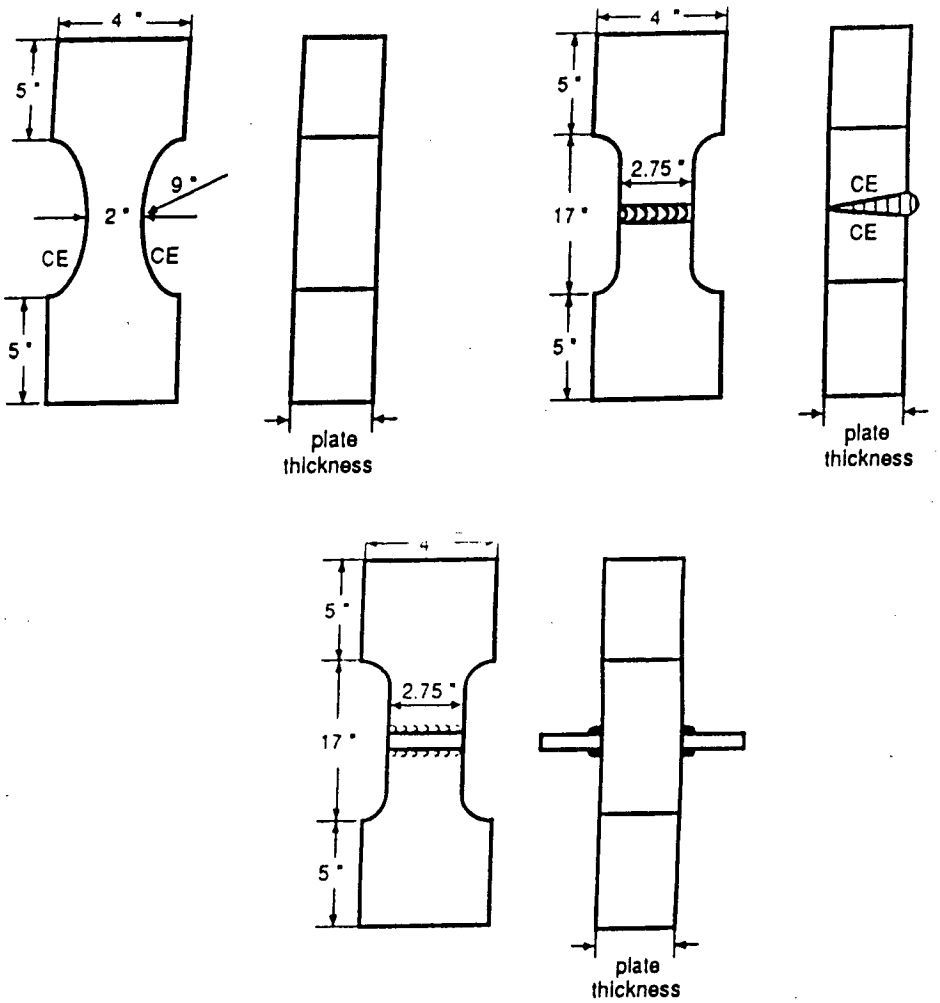

Figure 43. Specimen configurations for fatigue testing.

design curve in the 10^5 cycle range although only at high applied and back welds.

Fatigue Results for the 12.7-mm (0.5-in.) Grade 50W Plate

The fatigue test results for the 12.7-mm (0.5-in.)-thick Grade 50W material are shown in Figures E-8 through E-14, Appendix E, and summarized in Figure 45. The edge quality of the air, nitrogen, and oxygen plasma surfaces, and the oxyfuel surfaces were representative of the cut edge quality from the optimized parameters. The edge quality of the underwater nitrogen and underwater oxygen were not consistent between the set of specimens and were not representative of the best cut edge quality. No surface roughness measurements were taken on the actual fatigue specimens.

In most cases, the fatigue cracking initiated at the bottom side of the plasma-cut edge and propagated through the thickness of the plate. However, there were also examples of cracking initiating at the top side of the plasma-cut edge. Several of the specimens failed in the grip section or outside of the test area. One of the underwater nitrogen specimens failed at a large notch outside of the test area.

In Figures E-8 through E-14, the results are shown in comparison with the corresponding AASHTO design curve for a plain member, Category A. All the cutting technique fatigue results were above the AASHTO Category A design curve except for a few underwater nitrogen plasma-cut specimens falling below the design curve in the 10^5 cycle range, at high applied stresses.

Fatigue Results for the 19-mm ($^3/_4$-in.) Grade 50W Plate

The fatigue test results for the 190-mm (0.75-in.)-thick Grade 50W material are shown in Figures E-15 through E-18, Appendix E, and summarized in Figure 46. Two sets of the oxygen plasma specimens were tested with two surface roughnesses. One set was fabricated using the best cut

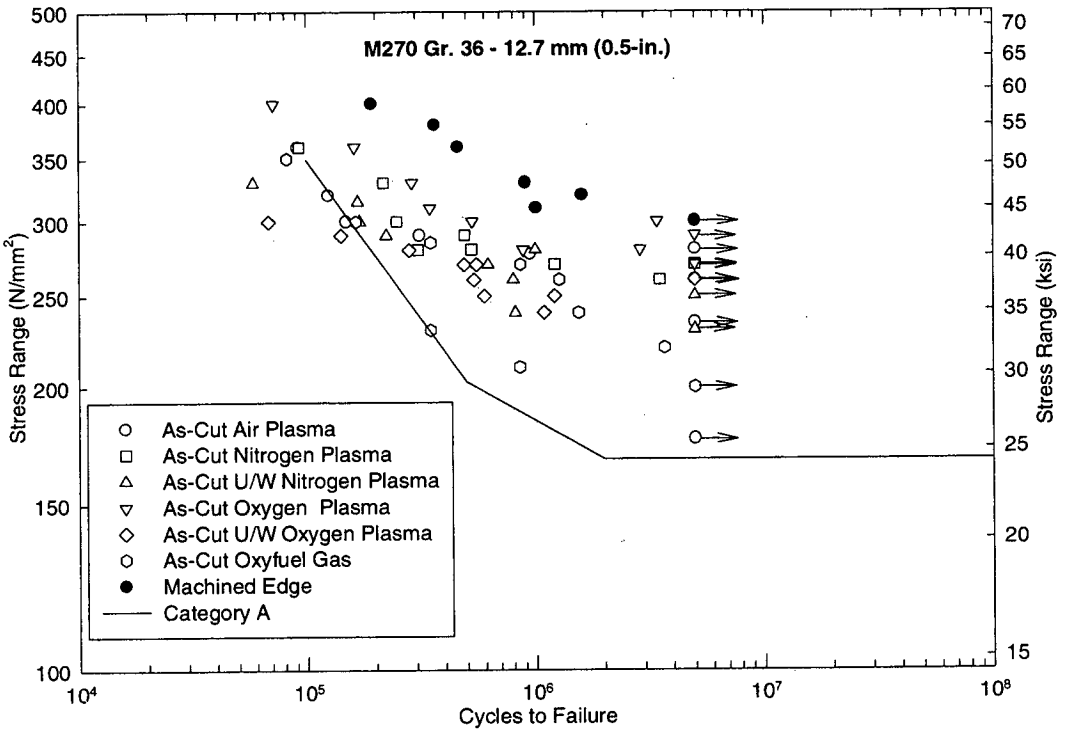

Figure 44. Summary of the fatigue results for as-cut edges on Grade 36 plate, 12.7 mm ($^1/_2$ in.) thick.

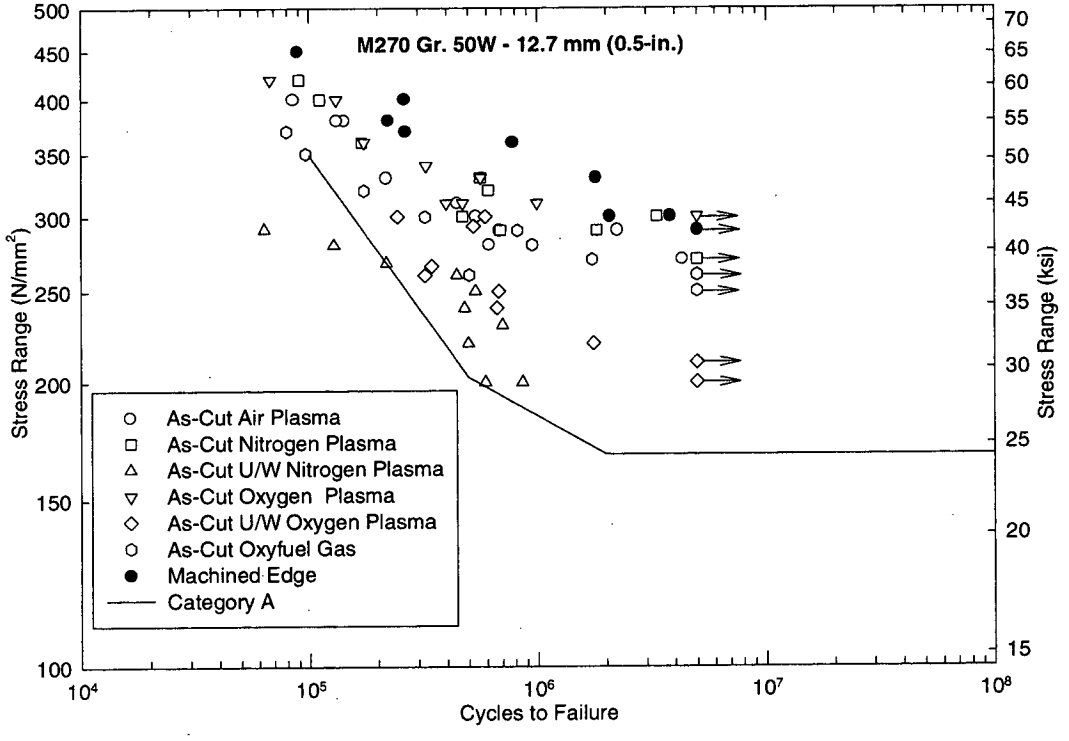

Figure 45. Summary of the fatigue results for as-cut edges on Grade 50W plate, 12.7 mm ($^1/_2$ in.) thick.

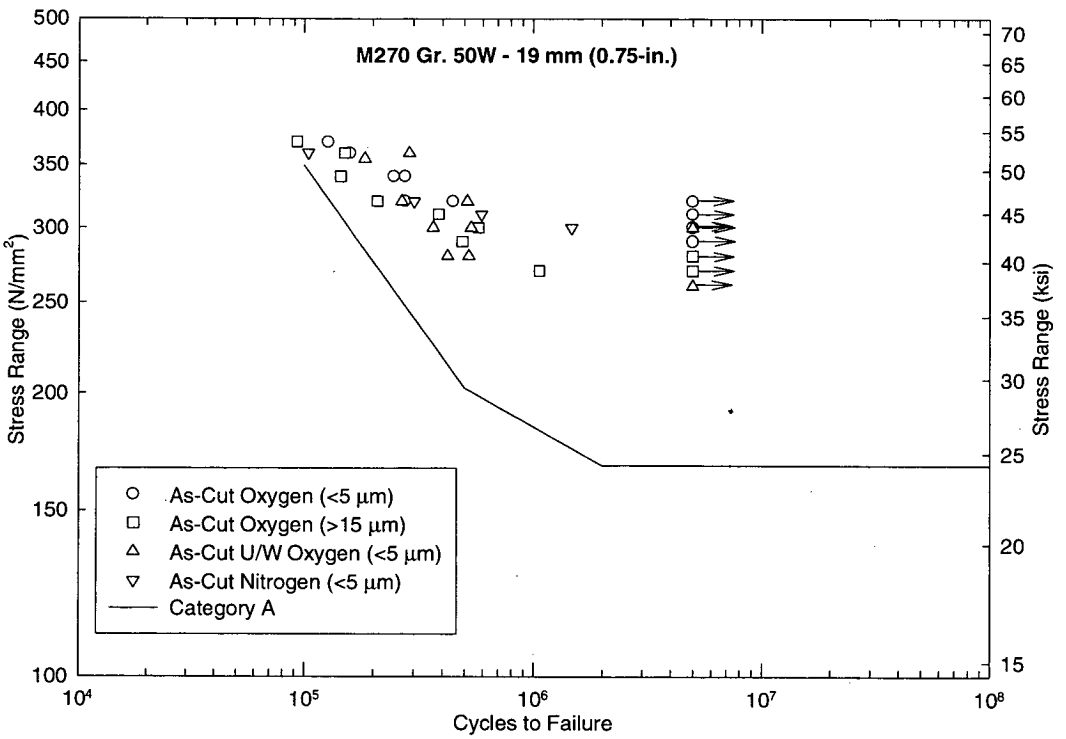

Figure 46. Summary of the fatigue results for as-cut edges on Grade 50W plate, 19 mm (3/4 in.) thick.

edge parameters and the second set of cutting parameters was selected to produce a rougher surface. This was done to investigate the effects of the edge quality. One set of underwater oxygen specimens with the best cut edge quality was tested. The edge quality of the best cut edges was representative of the edge quality produced from the optimized parameters. No surface roughness measurements were taken on the actual fatigue specimens.

In most cases, the fatigue cracking originated at the bottom side of the plasma-cut edge and propagated through the thickness of the plate; however, there were examples of cracking originating at the top edge of the plasma cut. All the failures occurred in the test area.

In Figures E-15 through E-18, the results are shown in comparison with the corresponding AASHTO design curve for a plain member, Category A. All the cutting technique fatigue results were above the AASHTO Category A design curve.

Effects of the Cutting Techniques on the As-Cut Fatigue Results

By comparing the fatigue test data for the different cutting techniques with the AASHTO design curves, their adequacy can be analyzed. The fatigue results for a particular joint detail type should be distributed above the lower bound provided by the design curve. These curves represent the 95 percent lower confidence level, therefore most of the fatigue results should lie above the design curve, but some test results may lie below the design curve.

The fatigue results for the different cutting techniques were near or above the AASHTO Category A design curve. Only three test results were below the expected scatter for the plain member design curve with surface quality that was representative of the best cut quality. These fatigue results were from the underwater nitrogen and underwater oxygen cutting techniques in the 10^5 cycle range. No explanation was determined for these results, except that the low values were due to the normal scatter of the fatigue results.

Large scatter was observed in the fatigue data for the underwater plasma cutting. One cause of this scatter was due to the surface quality of the cut edge. The surface quality varied from one location on the specimen to the next, due to the curvature of the fatigue specimens. The surface quality also varied between specimens for the same cutting technique.

The underwater plasma cutting processes appear to degrade the fatigue performance for the 12.7-mm (0.5-in.)-thick Grade 36 and 50W steels. The underwater oxygen plasma-cut 19-mm (0.75-in.)-thick Grade 50W steel did not show the same dramatic degradation that was seen in the 12.7-mm (0.5-in.)-thick results. Inspection of the test specimens show that the surface roughnesses are not consistent between the series of fatigue specimens and that the 12.7 mm (0.5 in.) is poorer quality than the representative surface of

the best cut surface roughness. So this degradation of the fatigue performance between the two grades is due to the inconsistencies of the surface quality of the specimens and not the material grade.

Effects of the Surface Roughness of the Specimens

Two series of specimens were tested for the 19-mm (0.75-in.)-thick oxygen plasma-cut edge with different surface roughnesses. An increase of the fatigue performance was observed with the increase in the surface quality. This is due to the stress concentration at the bottom of the serrations of the cut surfaces. The deeper and sharper the notch is, the closer the notch resembles a crack and thus the higher the stress concentration.

Large serrations or notches can occur at the beginning of a cut or when a cut is being lost. These notches have a strong influence on the fatigue performance because they act as stress raisers. This effect of a notch was observed when a premature failure occurred at a notch outside of the test area. The surface roughness of the as-cut fatigue specimens appears to have greater influence on the fatigue performance than any other factor.

Effects of the Material Grades

The results from the machined edges indicate that there is no difference between the grades of steel. The results obtained from the air, nitrogen, and oxygen plasma-cut edges and the oxyfuel-cut edges for Grade 50W steel generally lie above those for the Grade 36 steel, while the results obtained from the underwater nitrogen and oxygen plasma-cut edges for Grade 50W steel generally lie below those for the Grade 36 steel. The results from the air, nitrogen, and oxygen plasma-cut edges and the oxyfuel-cut edges would suggest that the high-strength steels may gain extra benefit from plasma cutting effects. Based on the results from this investigation, no explanation of the increased fatigue performance for the high grade of material was reached.

The degradation of the underwater nitrogen and underwater oxygen plasma fatigue performance is because of the differences in the surface roughness between the two grades for their respective cutting processes. As discussed earlier, this degradation of the surface roughness is due to the lack of consistency of the surface quality between the specimen in a series and not the cutting process or material grade.

Effects of the Plate Thickness

No effect of plate thickness was noticed in the nitrogen and oxygen plasma-cut fatigue specimens. The surface roughness, between the corresponding cutting techniques on the 12.7-mm (0.5-in.) and the 19-mm (0.75-in.) plates, was consistent. An improvement of the fatigue performance was noticed with the increase in plate thickness for the underwater oxygen plasma-cut edges. The cause of this increase is believed to be due to the improved surface quality of the 19-mm (0.75-in.) fatigue specimens. Based on the limited data and the knowledge that the surface roughness varied between the plate thickness for the underwater oxygen plasma-cut edges, no effects of plate thickness were observed on the fatigue performance.

FATIGUE TESTING OF WELDED PLASMA-CUT EDGES

Test panels were welded using the same procedures developed for the welding trials. The test matrix for the panels is shown in Table 15. All seven of the welded panels for fatigue testing were radiographed and subsequently machined to produce the dogbone specimens. Two types of joints were tested:

1) A single-vee where the grooves have been prepared by plasma cutting, and
2) A nonload-carrying fillet-welded joint (see Figure 43).

In the last case, the welds will not be made against a plasma-cut surface, because fillet welds are the most common joint detail in bridges. The objective of the fatigue testing of the welded plasma-cut edges was to investigate the effects the plasma-cut edge has on the fatigue performance of the welded panels.

Very limited fatigue testing of the welded joints was proposed, primarily because it is believed that if the fusion line and the HAZ of the welded plasma-cut surface is sound, then the fatigue life of the joint will be controlled by the weld geometry.

In view of the above arguments, the objective of the test matrix in Table 15 was to show that the S-N curves are at least equal to or better than the standard design curves for each joint type and comparable to the machined bevels. Only two cutting processes were selected in order to minimize the extent of testing, and the underwater cutting processes were selected purely for convenience in terms of noise and fume control. Since the fatigue life of welded joints is not generally affected by tensile strength, hardness, or microstructure, only one grade of steel was tested.

Two surface roughnesses of the plasma-cut edge were included in the test matrix. Panels were plasma-cut using the cutting parameters associated with smooth and rough surfaces. The panels were then welded using SAW and FCAW procedures and then radiographed to ensure that the test specimens were free of any defect.

Fatigue testing was conducted to develop S-N curves for the different welded plasma-cut panels to assess the effects of the cutting process, cut surface roughness, and welding process. The testing was conducted using a uniaxial sinusoidal cyclic tensile loading with a stress ratio, R, of 0.1. All the testing was carried out at room temperature to fail-

ure or until 5.0×10^6 cycles were reached. The plasma-cut panels were welded in the as-cut condition. The panels were radiographed to ensure that there were no defects in the test area. It is well known that geometry effects of the weld will dominate the fatigue performance of the test specimens over the effects of the plasma-cut edge. For this reason, the weld caps and the backing bars were removed from the fatigue specimens to eliminate any geometry effects on the specimen.

V-Groove Butt-Welded Joint

The fatigue test results for the SAW 12.7-mm (0.5-in.)-thick Grade 50W specimens are shown in Figures E-19 through E-23, in Appendix E, and summarized in Figure 47, for the different cutting processes. In most cases, the fatigue cracking initiated in the weld propagated through the thickness of the plate in the weld metal. However, there were also a few examples of failures occurring in the radius of the specimen. One specimen failed in the grip section.

The fatigue test results for the FCAW 12.7-mm (0.5-in.)-thick Grade 50W specimens are shown in Figure E-24, Appendix E. The fatigue cracking initiated in the weld propagated through the thickness of the plate in the weld metal except for one specimen that failed in the plate material.

In Figures E-19 through E-24, the results are shown in comparison with the corresponding AASHTO design curve for a full penetration groove-welded connection with the welds ground flush, Category B, and with the design curve for the plain member, Category A. In these cases the fatigue results were better than the design curve for both Category C and for Category A. Also, no difference was noticed between the series of welded panels cut with the different plasma cutting processes with different surface roughnesses or with the welded panels with the machined edges. This suggests that the portion of the plasma-cut surface is absorbed in the weld or that the quality of the plasma-cut edge is as good as or better than the welded material. No effects of the plasma cutting process or the surface roughness were seen on the fatigue performance of the butt-welded specimens.

Fillet-Welded Attachment

The fatigue test results for the FCAW fillet-welded attachment, using the underwater oxygen panels of 12.7-mm (0.5-in.)-thick Grade 50W for the attachments, are shown in Figure E-25, in Appendix E, and compared with the groove weld results in Figure 47. The fatigue cracking initiated at the weld toes and propagated through the thickness of the plate.

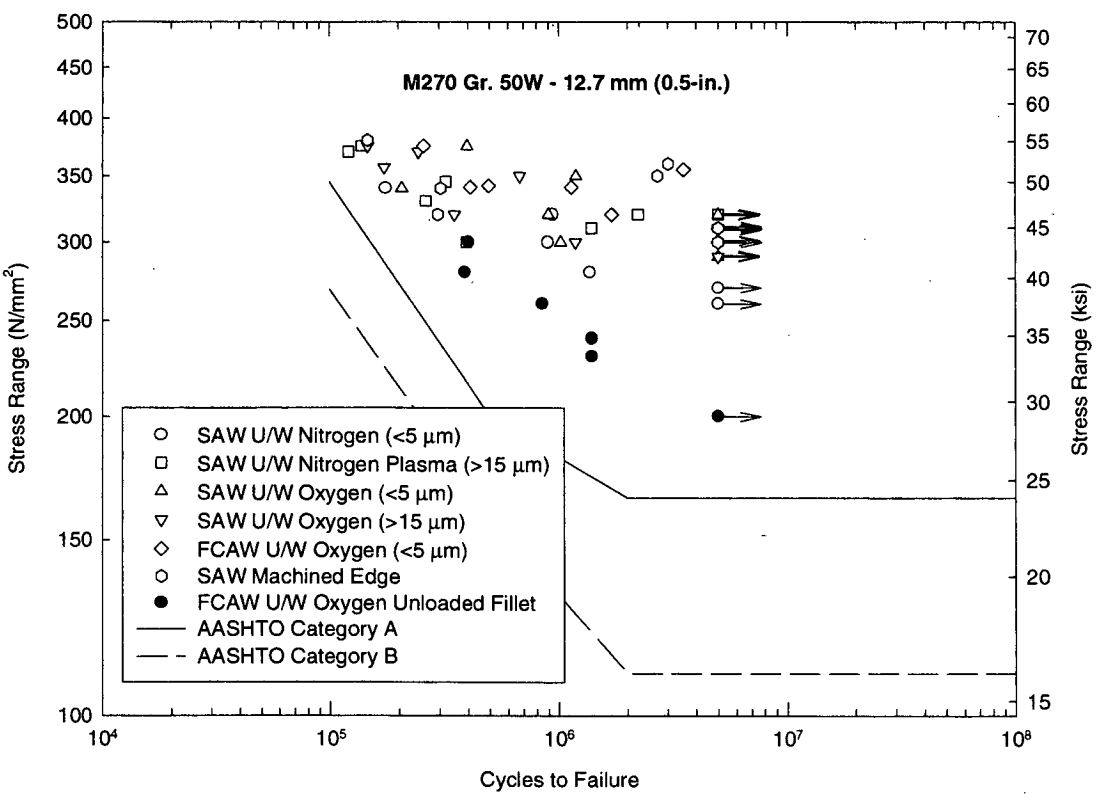

Figure 47. Summary of the fatigue results for welded PAC edges.

In Figure E-25, the results are shown in comparison with the corresponding AASHTO design curve for a fillet-welded attachment, Category C, and with the design curve for the plain member, Category A. In this case, the fatigue results were better than the design curve for both Category C and for Category A. As expected, the plasma-cut edge of the attachment panels has no effect of the performance of the weld joint.

CHARPY TESTING

Machining and testing of Charpy specimens was carried out for 21 welds, a total of 378 specimens. Test pieces were prepared according to the specifications of ASTM E23; the test plan is shown in Table 14.

Results for the Grade 36 material showed values averaging from 46 to 106 ft-lb at room temperature. At −40°F, averages ranged from 18 to 34 ft-lb at the fusion boundary and from 17 to 102 ft-lb at 1 mm into the HAZ. Base material Charpy values were 115 ft-lb at room temperature, and 8 ft-lb at −40°F, for Grade 36 material.

The toughness of welds made on underwater oxygen and underwater plasma-cut edges of Grade 36 plate was lower than for other plasma cutting techniques. Although the toughness of the welds made on these edges was better than for the base material at −40°C (−40°F), it was considerably lower at room temperature (Table 29).

Results for the Grade 50 material showed values averaging from 58 to 154 ft-lb at room temperature. At −40°C (−40°F), averages ranged from 18 to 50 ft-lb at the fusion boundary and from 38 to 73 ft-lb at 1 mm (0.040 in.) into the HAZ. Base material Charpy values were 42 ft-lb at room temperature, and 8 ft-lb at −40°C (−40°F), for Grade 50 material.

TABLE 29 Summary of Charpy test results

Weld No.	Material Grade	Cutting Process	Average Absorbed Energy (ft-lbs)					
			-40°C (-40°F)			RT		
			FL	FL+1	FL+2	FL	FL+1	FL+2
W12	36	Air	64	75	9	118	152	137
W19	36	Nitrogen	44	54	98	106	106	129
W20	36	Oxygen	34	102	19	68	140	96
W58	36	U/W Nitrogen	23	17	12	53	50	37
W57	36	U/W Oxygen	23	19	8	46	44	26
W46	36	Oxyfuel Gas	34	102	28	101	145	136
W45	36	Machined	19	76	12	72	127	63
W13	50	Air	50	69	13	99	154	123
W24	50	Nitrogen	25	65	24	93	72	80
W23	50	Oxygen	35	73	25	87	113	99
W56	50	U/W Nitrogen	18	38	7	84	93	64
W76	50	U/W Oxygen	23	73	66	84	94	123
W44	50	Oxyfuel Gas	27	49	10	73	98	58
W43	50	Machined	23	68	6	79	111	27
W18	50W	Air	22	55	19	85	133	125
W16	50W	Nitrogen	27	47	29	96	105	133
W17	50W	Oxygen	33	41	59	95	143	152
W60	50W	U/W Nitrogen	27	88	23	77	135	139
W59	50W	U/W Oxygen	22	22	47	75	96	123
W47	50W	Oxyfuel Gas	32	50	22	96	114	62
W48	50W	Machined	33	83	22	82	109	76
M3	36	Base Metal		8			115	
M2	50	Base Metal		8			42	
M1	50W	Base Metal		23			68	

Charpy results for the Grade 50W material showed values averaging from 62 to 143 ft-lb at room temperature. At −40°C (−40°F), averages ranged from 22 to 33 ft-lb at the fusion boundary and from 22 to 88 ft-lb at 1 mm (0.040 in.) into the HAZ. Base material Charpy values were 68 ft-lb at room temperature, and 23 ft-lb at −40°C (−40°F), for Grade 50W material.

For welds made on cut edges in both the Grade 50 and 50W plate material, the toughness met or exceeded that of the base material in almost every case. Exceptions were generally only a few foot-pounds lower than the base metal results.

TENSILE TESTING

All tensile testing was carried out with cross-weld specimens machined to produce parallel surfaces on the specimen. Specimens were prepared and tested according to ASTM E8 specifications. Cross-weld tensile test pieces and metallographic specimens were machined and tested from a total of 34 welds. Results showed that all welds passed, failing at yield and tensile strengths in excess of the parent material specifications. Test results are summarized in Table 30.

Of 18 specimens welded by FCAW, 17 failed in parent material, with typical yield strengths of 379 N/mm^2 (55 ksi), and ultimate tensile strengths of 517 N/mm^2 (75 ksi) for welds in Grade 50W plate, 12.7 and 19 mm ($^1/_2$ and $^3/_4$ in.) thick. Typical yield strengths of 310 N/mm^2 (45 ksi) and ultimate tensile strengths of 483 N/mm^2 (70 ksi) were recorded for welds in Grade 36 plate, 12.7 mm ($^1/_2$ in.) thick. The one specimen which failed in the weld metal had a yield strength of 402 N/mm^2 (58.3 ksi) and an ultimate tensile strength of 575 N/mm^2 (83.4 ksi), made on 19-mm ($^3/_4$ in.)-thick Grade 50 plate cut by underwater oxygen plasma. These values are in excess of the required minimums, so this specimen passed the testing criteria.

TABLE 30 Summary of cross-weld tensile test results *(continued on next page)*

Specimen No.	Material Grade	Thickness (in)	Cutting Process	Welding Process	Mechanical Property		
					YS (ksi)	UTS (ksi)	%Elgn
W38	36	½	Air	SAW	46.1	71.0	28.2
W37	36	½	Oxygen	SAW	47.9	70.6	36.8
W39	36	½	Nitrogen	SAW	47.6	70.6	27.8
W62	36	½	U/W Oxygen	SAW	47.6	71.8	25.5
W61	36	½	U/W Nitrogen	SAW	48.1	70.9	22.8
W28	36	½	Air	FCAW	47.0	71.2	25.1
W30	36	½	Oxygen	FCAW	47.9	72.8	23.0
W29	36	½	Nitrogen	FCAW	42.6	70.8	24.8
W53	36	½	U/W Oxygen	FCAW	45.6	71.0	24.1
W52	36	½	U/W Nitrogen	FCAW	45.8	69.7	23.3
–	36	½	Base Metal	–	47.1	70.7	21.0
–	36	½	Specification	–	36.0	58.0	–
W26	50W	½	Air	SAW	55.1	72.6	23.9
W33	50W	½	Oxygen	SAW	55.3	71.0	26.7
W34	50W	½	Nitrogen	SAW	56.4	72.8	25.6
W72	50W	½	U/W Oxygen	SAW	56.8	74.3	25.1
W74	50W	½	U/W Nitrogen	SAW	57.9	76.6	22.5
W15	50W	½	Air	FCAW	55.7	79.1	26.8
W32	50W	½	Oxygen	FCAW	51.8	75.3	29.6
W31	50W	½	Nitrogen	FCAW	53.2	76.8	25.0
W54	50W	½	U/W Oxygen	FCAW	54.1	77.2	26.1
W55	50W	½	U/W Nitrogen	FCAW	54.3	77.9	24.2
–	50W	½	Base Metal	–	54.5	73.4	26.0
–	50W	Up to 4	Specification	–	50.0	70.0	–
W67	50	¾	Air	SAW	55.3	79.0	28.2
W69	50	¾	Oxygen	SAW	57.3	72.3	24.2
W68	50	¾	Nitrogen	SAW	58.6	75.5	31.1

TABLE 30 *(continued)*

Specimen No.	Material Grade	Thickness (in)	Cutting Process	Welding Process	Mechanical Property		
					YS (ksi)	UTS (ksi)	%Elgn
W100	50	¾	U/W Oxygen	SAW	57.8	72.3	28.1
W70	50	¾	U/W Nitrogen	SAW	57.6	73.1	22.8
W14	50	¾	Air	FCAW	62.9	85.9	20.5
W41	50	¾	Oxygen	FCAW	56.6	85.5	31.2
W40	50	¾	Nitrogen	FCAW	56.9	85.1	30.0
W87	50	¾	U/W Oxygen	FCAW	58.3	83.4	33.0
W51	50	¾	U/W Nitrogen	FCAW	57.2	84.8	27.3
--	50	¾	Base Metal	--	64.8	86.4	21.0
--	50	Up to 4	Specification	--	50.0	65.0	--
W42	50W	¾	Air	FCAW	53.9	77.7	29.9
W25	50W	¾	Oxygen	FCAW	56.3	78.5	24.1
W36	50W	¾	Nitrogen	FCAW	54.9	77.0	33.3
W49	50W	¾	U/W Oxygen	FCAW	53.6	75.9	31.1
W50	50W	¾	U/W Nitrogen	FCAW	57.2	80.2	27.3
--	50W	¾	Base Metal	--	58.8	77.6	27.0
--	50W	Up to 4	Specification	--	50.0	70.0	--

U/W = Underwater cutting with water injection

Of 16 specimens welded by SAW, 12 failed in the weld metal, although not because of any weld discontinuities. Nine of the 12 were joints produced in 19-mm ($^3/_4$-in.)-thick Grade 50 and Grade 50W plate, welded with a Lincoln L61 consumable. This consumable is stated to be qualified to AWS A5.17 and AWS A5.23 and, although undermatching the actual strength of the plate supplied, still produces welds with strength exceeding specification requirements for the Grade 50 and 50W material as well as the Grade 36 plate. Two weld metal failure locations were recorded for welds in Grade 50W plate, 12.7 mm ($^1/_2$ in.) thick; the yield strengths were 392 and 399 N/mm^2 (56.8 and 57.9 ksi), while the ultimate tensile strengths were 512 and 528 N/mm^2 (74.3 and 76.6 ksi), respectively. The twelfth weld was produced on 12.7-mm ($^1/_2$-in.)-thick Grade 36 plate, and had yield and tensile strength essentially identical to the values quoted in the mill certificates for the plate supplied: 330 N/mm^2 (47.9 ksi) yield, and 487 N/mm^2 (70.6 ksi) ultimate tensile strength.

CHAPTER 3

INTERPRETATION, APPRAISAL, AND APPLICATION

USER'S GUIDE FOR PLASMA ARC CUTTING

The User's Guide is presented in the form of an appendix to facilitate its separate circulation as a discussion document. The purpose of the User's Guide is to provide guidelines for design engineers, fabricators, and inspectors, including specific recommendations for the use of plasma arc cutting.

Modifications and additions to the draft guide have been made based on the results of the experimental program (Task 6 of the project). The data produced in Task 6 were reviewed, and the recommended guidelines were updated if necessary. Modifications were made to the recommendations on the treatment of edges that will not subsequently be welded. An additional section dealing with the weldability of plasma-cut edges was added. Recommendations for single-pass fillet welds and/or low-heat input welds, such as gusset-to-flange welds made against plasma-cut edges, were added. Additional information on achieving good cut quality and recommended cutting speeds was provided. A copy of the guidelines was sent to Ohio DOT, several fabricators, and a consultant in the bridge industry.

After passing through all the relevant review stages, it is expected that the guidelines will be incorporated in the ANSI/AASHTO/AWS D1.5 Bridge Welding Code as part of Section 3, Workmanship, within Subsection 3.2 "Preparation of Base Metal." Alternatively, since the guidelines contain both descriptive and operational information, it may be considered appropriate to add them to the Code as an appendix.

The provisions covering the preparation of base metal by oxyfuel cutting in Section 3 of the Bridge Welding Code will also be employed for plasma arc cutting. The information in the User's Guide applies specifically to plasma-cut edges. However, if a hardness limit of R_c35 is introduced for plasma-cut edges welded with low-heat input processes, it should also apply to oxyfuel-cut edges. No results produced in the laboratory testing portion of the program indicated the need for stricter provisions for plasma-cut edges than for oxyfuel-cut edges.

INTERPRETATION, APPRAISAL, AND APPLICATION

Many plasma cutting techniques are available and each will have a different effect on the quality and characteristics of a cut edge, including the edge hardness and the cutting speed attainable for a particular cutting power. The use of oxygen as a plasma cutting gas, for example, results in increased thermal energy from the reaction of oxygen with iron in steel as well as from the higher heat content of the gas. This means that lower cutting power levels are required to cut the same thickness with nitrogen plasma gas. The weldability of plasma-cut edges is often questioned from the viewpoint of the need to dress the cut edges before welding. However, an equally or more important question is whether the free edges should be dressed or left in the as-cut condition, because research findings indicate a reduction in fatigue life for dressed plasma-cut edges due to removal of the surface, which has a beneficial compressive residual stress.

The findings of the survey showed a varied response in the interpretation of the state DOTs on two points: 1) is plasma arc cutting to be allowed, and 2) is grinding of the resultant cut edge needed? The lack of any mention of plasma cutting in the Bridge Welding Code led a number of states to prohibit use of the process, while others did not interpret the lack of mention as a prohibition. Most states that allowed the use of plasma arc cutting applied the same quality criteria as are applied to oxyfuel edges in the Code. However, many states that allowed plasma cutting on this basis actually had no fabricators using it. Grinding requirements varied from no grinding to grinding of all edges, with the requirements of the Code regarding surface roughness applied by others.

Research in Task 6 supported findings from the literature stating that grinding the edge of a plasma cut actually reduces, rather than enhances, the fatigue life of the edge. Therefore, grinding of the edge could be considered unnecessary, if not detrimental, except for removal of defects as described in the Code and for edge rounding for painting. If edge grinding were not required, productivity levels could rise in some states. The Bridge Welding Code does not contain any specifications on hardness limits for plasma-cut edges (free edges vs. edges incorporated in welds). However, the Construction and Material Specifications of some States include hardness limits for thermal cut edges of HR_c30. This causes considerable logistical problems in determining edge hardness and can routinely involve grinding all plasma-cut edges since the thin martensite layer on the surface can often have a hardness in the range HR_c40 to HR_c60. As fatigue testing of free edges shows that fatigue life is higher for as-cut edge produced by plasma arc cutting

compared with oxyfuel cutting, an edge hardness limit should not be incorporated into the Bridge Welding Code. Similarly, as mechanical testing of welds on as-cut edges shows no reduction in mechanical properties compared with machined or oxyfuel-cut edges, there would be no need to grind edges that are to be welded. Only in the case of welded edges prepared by nitrogen plasma was the outcome somewhat different.

The weldability of a plasma-cut edge depends on the cutting technique and plasma cutting gas, the type and thickness of the base material, the microstructure, hardness and depth of the HAZ, the joint preparation, the welding process, the heat input, the surface condition, and any pick-up of porosity-forming gases in the cut edge. The structural performance of free edges is largely dependent on the surface roughness of the edge and the presence or absence of any edge notches or imperfections such as microcracks.

Use of plasma cutting can greatly improve productivity compared with oxyfuel cutting, primarily by increasing the cutting speed without loss of edge quality. For large plasma cutting systems, abundant electrical power is required and the cutting equipment itself is considerably more expensive than oxyfuel cutting torches. Plasma arc cutting torch consumables (including the electrode and nozzle) have to be replaced periodically; a nozzle typically lasts twice as long as a zirconium insert electrode for cutting with air or oxygen. Electrode life is related to the number of starts of the cutting cycle; electrodes typically last 200 to 400 starts depending on the plasma gas and cutting power. Despite the higher cost for equipment, power, and torch consumables, the plasma cutting process is more economical and effective than oxyfuel cutting for cutting structural steels in thicknesses up to 19 mm or 25 mm, depending on material throughput.

Safety aspects of plasma cutting are different from those of oxyfuel cutting. The primary safety considerations for oxyfuel cutting are safe use and storage of fuel gases, hot metal particles, and fume emissions. Plasma cutting introduces additional considerations, which are ultraviolet arc radiation, high noise levels, electric shock avoidance, and increased levels of oxides of nitrogen in the fume, particularly when using air or nitrogen plasma gases. Use of underwater cutting or water injection cutting with a water shroud will reduce noise, particulate fume, and arc glare (with a suitable dye in the water). Both types of cutting involve use of a water table that captures particulate fume constituents. Since these are automated cutting techniques, many of the operator safety concerns are considerably reduced by the relatively remote operation of the cutting process.

The cutting speed advantage of plasma cutting is only achieved when using mechanized and particularly automated cutting. Greatest advantage and convenience is achieved when using the process in conjunction with a shape cutting machine fitted with CNC or DNC controllers. The DNC system maximizes the productivity of cutting operations because it allows direct input of cutting data from computer-aided design (CAD) systems; the use of these is on the increase, even at fairly small companies. While oxyfuel cutting can also be operated by this type of system, the most significant improvements can be achieved by replacing an older oxyfuel cutting system, either with optical tracing or tape-driven CNC, with a DNC plasma cutting system. Particular attention needs to be paid to material flow both to and from the plasma cutting operation to maximize the amount of time spent cutting rather than loading and unloading plate and cut parts. This is most readily achieved by having a cutting area which is at least twice the area of the standard plates which are cut.

The use of plasma arc cutting for bridge steels can be recommended as a means of increasing the productivity of thermal cutting operations. The results of the laboratory trials in this project have shown that the plasma arc cutting process can be used to increase the cutting speeds compared with oxyfuel cutting, and to produce both square edges and bevelled edges for joint preparations. The smoothness of the edges routinely meets the requirements of the ANSI/AASHTO/AWS Bridge Welding Code.

To ensure the minimum amount of dross, the correct cutting procedures must be adhered to by selecting the correct cutting speed for the material type, thickness, and electrical power of the cutting system. The cutting gas that maximizes the likelihood of dross-free cuts is oxygen, followed by air, and nitrogen. Oxygen plasma cutting produces the widest range of dross-free cutting conditions, and when any dross is formed on the plate, it is highly oxidized and easily removed (having a similar consistency to the dross produced by oxyfuel cutting). Cutting under water with oxygen narrows the window of dross-free cutting conditions, but the dross is easily removed when formed. Air plasma cutting produces dross-free cutting ranges similar to oxygen plasma, but when dross is produced, it is substantially metallic, and usually has to be ground off because it is tightly adherent. Nitrogen plasma cutting produces much narrower tolerance windows for dross-free cutting, both when cutting is performed in air or under water. In addition, the dross produced is mostly resolidified metal, and has to be ground off in a manner similar to that for air plasma cutting. It is quite common to employ at least one full-time operator to remove dross from cut edges produced by nitrogen plasma cutting. This operation can be eliminated and labor costs saved by changing to oxygen plasma gas.

Plasma cutting with air and nitrogen produces nitriding of the cut edges, which can result in porosity in weldments. Nitrogen plasma cutting can produce rejectable porosity in weldments subject to radiographic inspection, as was found in this work. Oxygen plasma cutting does not result in nitriding of the edge. Consequently, the overall recommendation is to use oxygen plasma cutting to obtain the maximum consistency of dross-free cutting conditions and maximum weldability of the edge.

When welding over plasma-cut edges, there is no need to dress the cut face (edge removal for the sake of edge hardness), but any dross present on the bottom surface of the plate

adjacent to the cut edge must be removed whether or not the edge is to be welded. The weldability of plasma-cut edges using the FCAW and SAW processes is good, although some porosity can be expected when welding over as-cut edges prepared by nitrogen plasma cutting. If radiographic quality standards are to be consistently met when plasma cutting with nitrogen, removal of 0.5 mm (0.020 in.) from the edge by grinding (i.e, removal of visible evidence of the cut striations) prior to welding is recommended. The cross-weld hardness profiles of welds on plasma-cut edges (without any edge dressing) consistently showed results below HR_c21 (240 VHN), and often no more than 200 VHN.

Significance of Residual Stresses on Plasma-Cut Edges

The level of residual stress produced on plasma-cut edges in structural steels may have the potential to influence structural performance under certain conditions. This is particularly true for stresses acting parallel to the cut edge. These longitudinal residual stresses were found to approach 50 percent of the material's room-temperature yield strength in tension. The through-thickness residual stresses acting parallel to the plate thickness were found to be insignificant in this study and, thus, are not considered to be an important factor in controlling structural performance of plasma-cut steels. Since actual surface residual stress measurements could not be made in this study, the general level of residual stress acting at depths between 0.25 mm (0.010 in.) and 1 mm (0.040 in.) are also considered to exist on the cut surface.

Residual stresses can influence a number of failure modes including fatigue, fracture, buckling, and various forms of stress corrosion cracking. Compressive residual stresses can reduce buckling strength but can improve fatigue and fracture performance while assisting in inhibiting stress corrosion cracking. Likewise, tensile residual stresses can reduce fatigue performance and toughness properties and promote stress corrosion cracking.

In this program, fatigue and fracture toughness properties of plasma-cut edges were evaluated. Since the through-thickness residual stresses were minimal, it is the longitudinal residual stresses that will be considered. These stresses were found to be tensile in nature and had magnitudes as large as one-half of the material yield strength.

In general, high tensile residual stresses do not play a significant role in fatigue when the loading is restricted to the tensile regime, as was done in this program. This is because fatigue behavior is primarily controlled by the net stress range. Since residual stress is constant at any location within a structure, the application of a cyclic load will not change the net stress range. However, tensile residual stresses can reduce the fatigue performance of structures that are partially or entirely loaded in compression. This is attributed to the superposition of the applied and residual stresses. If the residual stresses are large enough, the superposition of the applied compressive stress with the tensile residual stress can result in an effective stress which is either in pure tension or a pulsating stress fluctuating between tension and compression. This can lead to fatigue failure when the applied loading is fully compressive.

The fatigue results produced as part of this program show no clear trend with respect to the residual stress distributions discussed in this section. Since the applied loading during the fatigue tests was parallel to the cut edge, the residual stresses acting in this same direction are of interest. Clearly, if the residual stresses were compressive along the cut edge, one might expect to see some improvement in the fatigue behavior, possibly even approaching the behavior observed in specimens with machined edges. Compressive residual stresses would tend to reduce the stress concentration effect of local ripples and undulations along the cut edge. However, since the residual stresses are tensile in this plane and the applied loading is also tensile, only the effect of the surface roughness will be dominant in influencing fatigue behavior. Hence, the fatigue behavior will be dominated by local geometry effects.

The level of residual stress on plasma-cut edges as measured in this program could potentially reduce the fatigue performance of plasma-cut plate sections loaded either partially or entirely under cyclic compressive loads. The local geometry of the cut edge along with the local residual stress distribution and the applied loading would combine to control fatigue performance. To effectively determine the significance of these residual stresses under compressive fatigue, some additional experimental work should be carried out. However, if a bridge structure can be shown to be structurally sound with the presence of as-welded fabrications (from a fatigue, fracture, or stress-corrosion perspective), then the tensile residual stresses produced by plasma cutting should be tolerable. The residual stress state produced by welding would be expected to be more severe than the level of residual stress measured in this program on plasma-cut edges. This is largely related to differences in constraint between a weld and a cut edge. Therefore, for structures intended to be used in the as-welded state, the residual stresses produced by plasma cutting should not be of concern.

Mechanical properties of as-cut edges produced by plasma cutting are good. Bend tests for as-cut edges showed acceptable results compared to oxyfuel-cut edges. Fatigue testing of as-cut edges produced results which were consistently as good or better than edges produced by oxyfuel cutting. It is important to note that these results were obtained when comparing as-cut edges (i.e., those which had not been corner/edge ground) to the baseline of AASHTO in Category A oxyfuel-cut edges that had been edge ground according to the requirements of the ANSI/AASHTO/AWS Bridge Welding Code. This is a very important result when considered in conjunction with the performance of unrounded edges in the "paintability" testing portion of the work. Cross cut adhesion and 2,000-hr salt fog testing to ASTM specifications showed

no difference in performance between rounded or unrounded plasma-cut or oxyfuel-cut edges for primed plate. The inference of these results is that edge/corner rounding is not necessary for plasma-cut edges, either for fatigue performance or paint adherence.

One exception in the better fatigue life of plasma-cut edges to edge rounded oxyfuel-cut edges was the rougher edges produced by underwater oxygen plasma cutting of 12.7-mm ($^1/_2$-in.) Grade 50W plate. However, the good results obtained with smoother edges of the same material in 19-mm ($^3/_4$-in.)-thick plate showed that the lower results in 12.7-mm ($^1/_2$-in.) plate were the result of the rougher edge, rather than the edges' being plasma cut. This serves to illustrate the importance of good control of the cutting operation, which is true irrespective of the cutting process used, be it oxyfuel or plasma cutting.

The mechanical properties of welded edges met or exceeded the specification requirements. Cross-weld tensile testing showed results which were consistently acceptable for all combinations of plasma cutting processes and welding processes. Charpy impact toughness testing of weldments showed that even in the HAZ, the region of the weld was typically the lowest in toughness compared to the weld metal, and that toughness met or exceeded that of the parent metal for all combinations of parent material, plasma cutting process, and welding process.

CHAPTER 4

CONCLUSIONS AND SUGGESTED RESEARCH

CONCLUSIONS

This work was conducted to determine the effectiveness of plasma arc cutting for bridge fabrication. The study involved development of plasma cutting procedures, characterization of the cut edges (cut gravity, metallography, hardness, and residual stresses), welding trials on as-cut edges, determination of the tensile and impact properties of welded plasma-cut edges, and fatigue properties of welded and as-cut edges.

The range of plasma arc cutting techniques available means that each will have a different effect on the quality and characteristics of a cut edge for the same cutting power and cutting speed. The weldability of plasma-cut edges is often questioned from the viewpoint of the need to dress the cut edges before welding. Research findings indicate that acceptable welds can generally be made by welding directly onto as-cut plasma-cut edges with most plasma gases, but nitrogen plasma cutting (in air rather than under water) can often result in porosity levels above acceptable limits. An equally or more important question is whether free edges should be dressed by grinding or left in the as-cut condition. Research findings indicate good fatigue life for plasma-cut edges in the as-cut condition, without edge corner grinding.

The weldability of the plasma-cut edge will be influenced by the cutting technique and plasma cutting gas, the microstructure and width of the HAZ, the joint preparation, the welding process, the heat input, the surface condition and any pick-up of porosity forming gases in the cut edge. The structural performance of free edges is largely dependent on the surface roughness of the edge and the presence or absence of any edge notches. It is considered unlikely that the residual stresses produced along a plasma-cut edge will have a significant degrading influence on the structural integrity of plasma-cut plates. In general, the levels of tensile residual stress were less than 50 percent of the yield strength. Furthermore, the through-thickness stresses (short transverse direction) were insignificant. The longitudinal stresses were not found to be severe enough to warrant removal of the cut edge by grinding. Clearly, nonstress relieved welds will be more detrimental. Moreover, even with thermal stress relief, weld residual stresses are typically assumed to remain at one-third of yield magnitude parallel to the weld. This level of residual stress is similar to that measured along plasma-cut edges in this study. Residual stresses in the as-cut edges are not sufficiently high to be of concern in structures that also contain as-welded joints, which includes all bridges.

The overall conclusion to this study is that plasma cutting should be applied for bridge fabrication as an effective thermal cutting tool to increase overall productivity compared with oxyfuel cutting. Individual conclusions resulting from this study are as follows:

1. The dross-free range of cutting speeds is much wider for cutting with oxygen and air than with nitrogen plasma cutting.
2. Cutting under water reduces the range of dross-free cutting speeds compared with cutting in air.
3. Oxygen plasma cutting produces a heavily oxidized, easily removable dross (similar to that for oxyfuel cutting).
4. Nitrogen and, to a substantial extent, air plasma cutting rely almost completely on melting, so any dross is mostly resolidified metal. If adherent, it has to be removed by grinding.
5. Cutting under water can be carried out at the same speed using 260 A for oxygen plasma as 400 A with nitrogen plasma.
6. Cutting with nitrogen and air plasma causes nitriding of the plasma-cut edge. This causes edge hardening, and can result in rejectable porosity when cutting with nitrogen in air (rather than under water). Oxygen plasma cutting does not cause nitriding, and thus the weldability of the edge is better.
7. FCAW and SAW can be successfully carried out on a routine basis to radiographic quality standards on as-cut edges of all plasma cutting variants, except nitrogen cutting in air. Edge grinding to remove 0.5 mm (0.020 in.) from the cut edge is recommended in the latter case.
8. The cross-weld tensile properties of weldments produced by FCAW and SAW processes on as-cut plasma-cut edges met or exceeded those of the parent material specifications.
9. The Charpy impact toughness of weldments produced by FCAW and SAW on as-cut plasma-cut edges met or exceeded the properties of the base material for all plasma cutting techniques.

10. The fatigue properties of unrounded, as-cut plasma-cut edges exceeded those of AASHTO Category A oxyfuel -cut specimens that had been edge rounded. Occasional lower results for underwater plasma cutting of Grade 36 and 50W plate, 12.7 mm (½ in.) thick, resulted at high stresses (above the usual range for design purposes).
11. Testing of plasma-cut and primed plate using ASTM salt fog and cross-cut adhesion testing showed no significant difference in performance between edges rounded to Bridge Welding Code specifications and unrounded edges.

SUGGESTED RESEARCH

This research has indicated the need for additional work related to partial melting of a plasma-cut edge. This situation occurs when fillet-welding gussets onto flange edges that have been plasma cut, where only a portion of the TCE is remelted. Welding trials and fatigue testing are required to ascertain the effect of the cut edge HAZ when low-heat input welding processes such as shielded metal arc welding are used for field welding. Past field experience in fabrication of steel framed buildings and shipbuilding has shown that weld HAZ cracking can occur as a result of welding onto cut edges in the manner described above, when the edges are cut by oxyfuel and plasma cutting. A hardness limit, with edge grinding requirements, may be required in this case.

Fatigue testing would employ a lapped-joint, fillet-welded specimen where the fillet welds had a leg length of approximately only half the plate thickness.

Further work is also required to investigate the fatigue performance of as-cut edges of Grade 50 material, particularly when cut by underwater nitrogen PAC. This would be supported by metallographic investigation of potential fissures in the cut edge.

USER'S GUIDE FOR PLASMA ARC CUTTING

APPENDIX A

USER'S GUIDE FOR PLASMA ARC CUTTING

1.0 INTRODUCTION

The User's Guide provides guidelines for design engineers, fabricators, and inspectors, including specific recommendations for the use of plasma arc cutting.

Modifications and additions to the draft guide have been made based on the results of the experimental program in NCHRP Project 10-40. The data produced in Task 6 were reviewed, and the recommended guidelines were updated where necessary. Modifications were made to the recommendations on the treatment of edges that will not subsequently be welded. An additional section dealing with the weldability of plasma-cut edges was added. Recommendations for single-pass fillet welds and/or low-heat input welds, such as gusset to flange welds made against plasma-cut edges, were added. Additional information on achieving good cut quality, and recommended cutting speeds was provided. A copy of the guidelines was sent to Ohio DOT, several fabricators, and a bridge consultant.

After passing through all the relevant review stages, it is expected that the guidelines will be incorporated in the ANSI/AASHTO/AWS D1.5 Bridge Welding Code as part of Section 3, Workmanship, within Subsection 3.2 "Preparation of Base Metal." Alternatively, since the guidelines contain both descriptive and operational information, it may be considered appropriate to add them to the Code as an appendix.

The provisions covering the preparation of base metal by oxyfuel cutting in Section 3 of the Bridge Welding Code will also be employed for plasma arc cutting. The information in the following paragraphs applies specifically to plasma-cut edges. However, if a hardness limit of HR_c35 is introduced for plasma-cut edges, it should also apply to oxyfuel-cut edges because oxyfuel-cut edges are typical. No results produced in the laboratory testing portion of the program indicated that stricter provisions are required for plasma-cut edges than for oxyfuel-cut edges.

2.0 PLASMA ARC CUTTING PROCESS—TERMS AND DEFINITIONS

The plasma arc cutting process severs metal by means of a highly concentrated arc jet that has sufficient energy and force not only to melt the metal, but also to eject the molten metal. Because melting rather than oxidation is the predominant cutting mode, plasma arc cutting can be used to cut any metal.

It is important to bear in mind that plasma arc cutting is a fundamentally different process from oxyfuel cutting, relying primarily on the heat generated by an electric arc to melt and sever the parent material. Consequently, additional safety hazards exist from the electrical nature of the process, arc radiation (ultraviolet), and noise levels. The operator should understand these hazards and take appropriate precautions. Appropriate safety information is referenced in AWS C5.2-83 "Recommended Practices For Plasma Arc Cutting."

The plasma arc cutting process can be used with a variety of cutting gases, both with and without water injection. In addition, depending on the equipment design, the cutting process can take place in air or under water. The wide variety of systems available makes it difficult to give definitive cutting speeds for particular thicknesses that apply to all process variants. For example, the oxygen plasma cutting process can cut plate faster than air plasma or nitrogen water injection due to the exothermic oxidation

reaction of oxygen with iron in steel, in addition to the thermal energy of the plasma. Some guidelines for cutting speeds of various plasma cutting systems compared to oxy-acetylene cutting are given in Table A-1. The values for 9.5-, 12.7- and 19-mm ($^3/_8$-, $^1/_2$- and $^3/_4$-in.) plate are those found to produce the best cut quality in terms of freedom from dross and good edge squareness during Project 10-40. The basic types of plasma cutting equipment are gas plasma (Figure A-1), air/oxygen plasma (Figure A-2), and water injection plasma (Figure A-3). Noise and pollution control can be achieved by using a water shroud (Figure A-4), or by cutting with the plate surface submerged 50 mm to 75 mm (2 to 3 in.) below the surface of a water table. Cutting systems using inert gases use tungsten electrodes, while those using air or oxygen use

TABLE A-1 Typical cutting speeds for various plasma arc cutting (PAC) systems compared with oxyfuel cutting

Material Thickness		Cutting Process	Cutting Current (A)	Cutting Speed	
(mm)	(in)			mm/min	in/min
6	¼	Oxyfuel Gas	N/A	68	27
6	¼	Air	200	3050	120
6	¼	Oxygen	200	4060	160
6	¼	U/W Nitrogen	350	3810	150
10	⅜	Oxyfuel Gas	N/A	610	24
10	⅜	Nitrogen	200	2160	85
10	⅜	Air	200	2920	115
10	⅜	Oxygen	200	2920	115
10	⅜	U/W Oxygen	260	3810	150
10	⅜	U/W Nitrogen	400	3555	140
13	½	Oxyfuel Gas	N/A	560	22
13	½	Nitrogen	200	1780	70
13	½	Air	200	2030	80
13	½	Oxygen	200	1905	75
13	½	U/W Oxygen	260	2920	115
13	½	U/W Nitrogen	400	3175	125
19	¾	Oxyfuel Gas	N/A	480	19
19	¾	Nitrogen	200	510	20
19	¾	Air	200	1270	50
19	¾	Oxygen	200	1270	50
19	¾	U/W Oxygen	260	1650	65
19	¾	U/W Nitrogen	400	1650	65
25	1	Oxyfuel Gas	N/A	405	16
25	1	Air	200	635	25
25	1	Oxygen	200	380	35
25	1	U/W Nitrogen	400	760	30

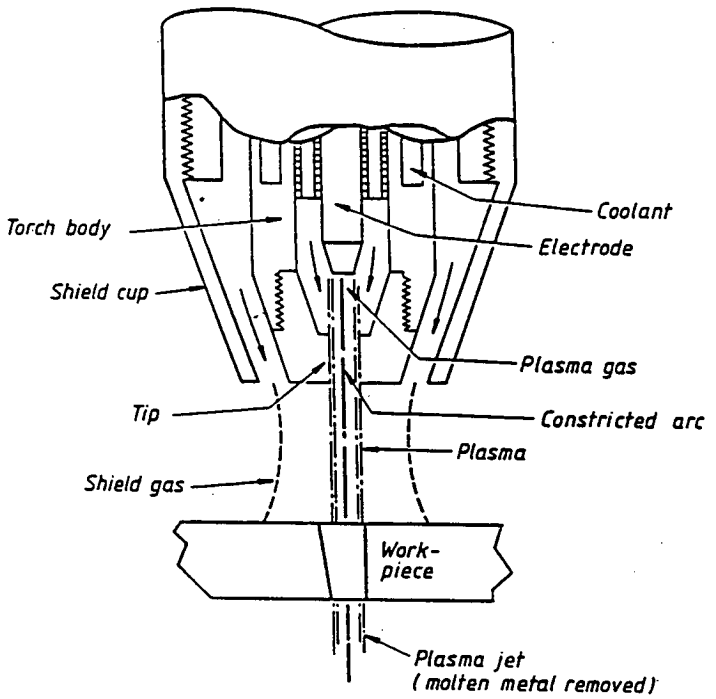

Figure A-1. Schematic of a gas plasma cutting torch in operation.

water-cooled copper insert electrodes with hafnium inserts (Figure A-2). Terms and definitions associated with plasma cutting are included in Appendix A-1 of this User's Guide.

A description of the components and operating procedures for plasma arc cutting can be found in AWS C5.2-83 "Recommended Practices For Plasma Arc Cutting." A good understanding of the process fundamentals is required by the equipment operator to enable good-quality cutting to be achieved consistently. In particular, the need to periodically replace worn torch consumables, particularly the electrode, is of paramount importance. The rec-

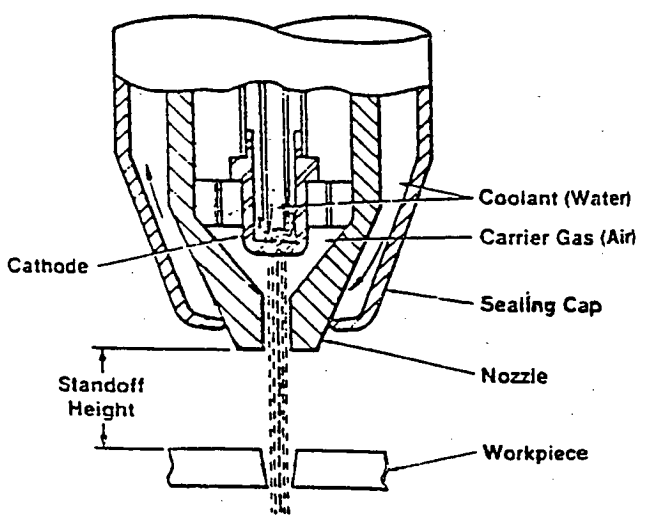

Figure A-2. Schematic of an air plasma cutting torch in operation.

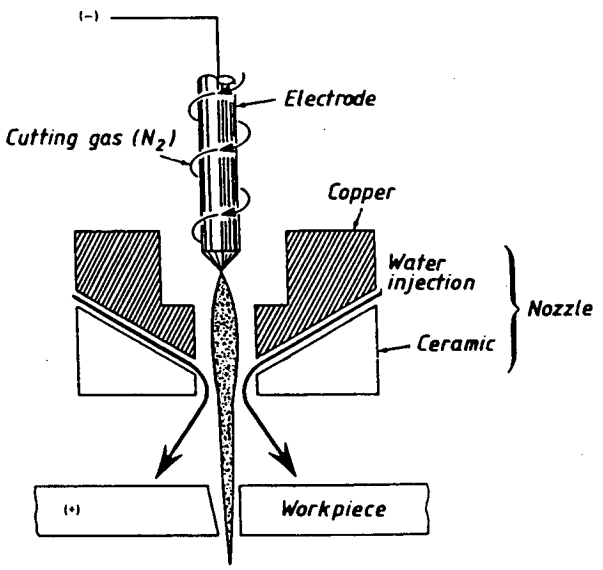

Figure A-3. Usage of water in plasma arc cutting—water injection plasma arc cutting.

ommendations of the torch equipment manufacturer should be followed regarding torch maintenance and consumable replacement intervals.

The plasma arc cutting process uses a very highly concentrated heat source, thus minimizing the heat input to the workpiece. Therefore, cutting speeds are generally much faster than for oxyfuel cutting and plate distortion is much lower. Depending on the cutting power (arc current and voltage) and plate thickness, cutting speeds can be two to six times faster for plasma cutting compared with oxyfuel cutting (Table A-1) for plate thicknesses between 6 mm and 25 mm ($^1/_4$ to 1 in.). Because the heat energy is more concentrated, the thermal energy consumed in cutting is typically only one-third to one-half that of oxyfuel cutting.

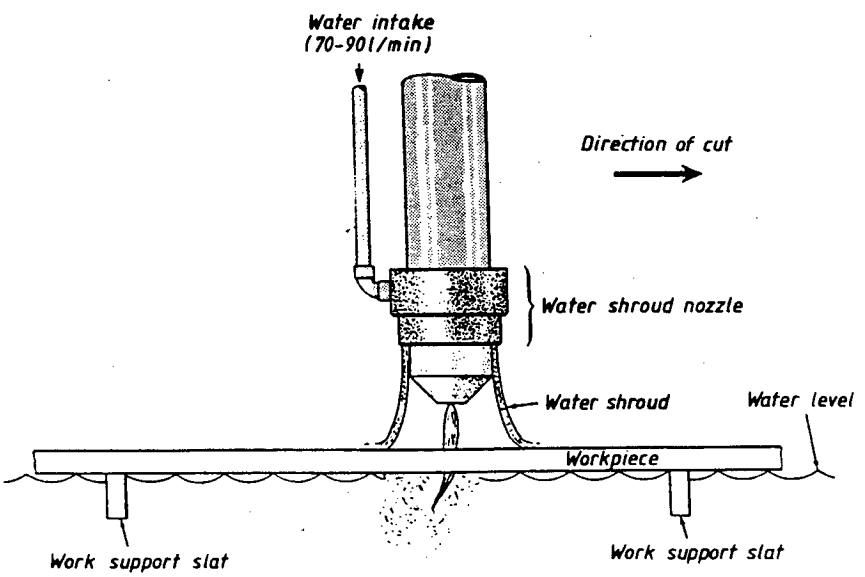

Figure A-4. Usage of water in plasma arc cutting—pollution control using a water shroud.

The higher cutting speed and more localized heat input lower the overall heat input into the plate, increasing the dimensional accuracy of the profiled plates and improving joint fitup for subsequent welding operations.

3.0 CUT EDGE SQUARENESS

To achieve the desired squareness of the edges, it is important to position the cutting torch in a precisely vertical manner and to ensure that torch cables have sufficient length to reach all parts of the cutting area to be used. Most plasma cutting equipment uses a clockwise swirl of the plasma gas aided by a swirl ring inside the torch body. The clockwise swirl results in a square edge on the right-hand side of the cut and a slight bevel on the left-hand side. Thus, it is important to design/program the cutting path so that the edge of the piece part is on the right-hand side when viewed in the cutting direction. Internal cut-outs, such as for manways, should thus be made with the torch travelling in a counterclockwise motion (Figure A-5).

Oxyfuel cutting usually will produce a true 90-deg square edge, while plasma cutting can be expected to give 90 ± 2 deg on the production part side of the cut. This small change in cut edge squareness very rarely gives cause for concern for accurate part fitup and is more than compensated for by the lower distortion of the plasma cutting process compared with oxyfuel cutting.

The kerf width is greater for plasma cutting than for oxyfuel cutting and increases with plate thickness. The width of the plasma-cut will typically be 50 to 100 percent wider than an oxyfuel cut. Therefore, a kerf offset or allowance of one-half of the kerf width must be used when programming a desired shape to achieve the desired final dimensions of the part. For plate thicknesses of 3 to 25 mm ($^1/_8$ to 1 in.), a kerf allowance of 2.4 mm ($^3/_{32}$ in.) is recommended as a guide.

4.0 SURFACE FINISH

Plasma-cut edges shall have a surface roughness acceptable to the requirements of American National Standards Institute, ANSI B46.1, Surface Texture. For materials up to 100 mm (4 in.) thick, a maximum surface roughness value of 25 μm (1,000 μin.) is permitted. The AWS C4.1-G, Oxygen Cutting Surface Roughness Gauge, may be used

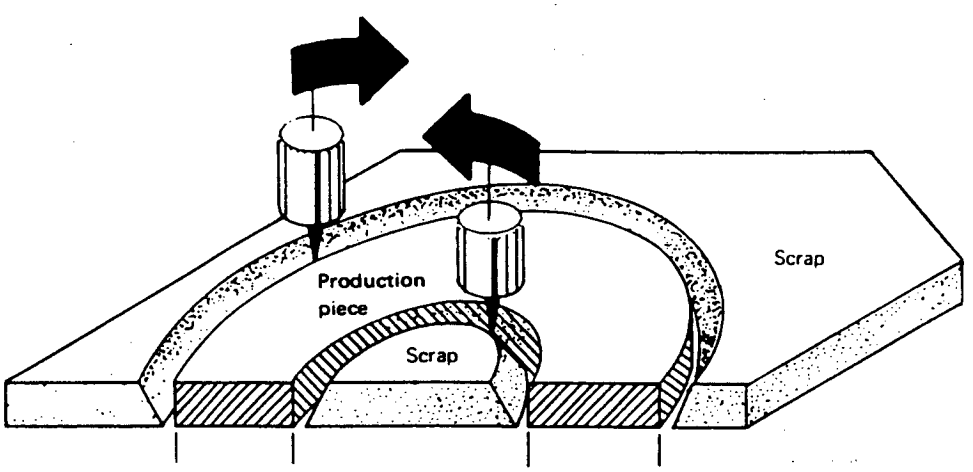

Figure A-5. Direction of cut for external and internal cuts using clockwise plasma gas swirl.

as a guide for evaluating surface roughness of these edges; Sample No. 3 is applicable for material thicknesses up to 100 mm (4 in.). As these gauges are not marked in microinches, a machined roughness guide would also serve the purpose. Surface replicas for plasma cutting should be developed but, at present, are not available.

Presently paragraph 3.2.9 of the Bridge Welding Code requires all corners of cut edges of main stress-carrying members, except bearing stiffeners and girder webs, to have a 1.6-mm ($^1/_{16}$-in.) radius or an equivalent flat surface at a suitable angle. The Code also requires that all corners of cut edges to be painted should be similarly rounded to hold paint. Corrosion testing of rounded and unrounded plasma and oxyfuel-cut edges in Project 10-40 showed negligible differences in the corrosion or paint adherence between rounded and unrounded edges. Therefore, rounding of edges to hold paint is not considered necessary. Fatigue testing in Project 10-40 has shown that plasma-cut edges produced by air, nitrogen and oxygen plasma cutting both in air and under water have superior fatigue performance compared to the AASHTO Category A design cover for oxyfuel-cut edges. Therefore, grinding the cut edge is not necessary and edge or corner rounding of plasma-cut edges is of less benefit. Based on the fatigue results for as-cut edges, the provision of edge/corner grinding can be eliminated from the requirements for main stress-carrying members.

5.0 MAXIMUM CUT QUALITY AND DROSS-FREE CUTTING

Any dross that adheres to the bottom edge of the cut shall be removed by mechanical scraping or grinding. However, adherent dross is indicative of improper cutting procedure. This may be corrected by replacement of worn consumables or adjustment of the cutting current, arc voltage, or travel speed. The arc voltage is directly proportional to the arc length and is controlled by torch standoff from the workpiece. The plasma cutting process, like most processes, works best when operating within a certain tolerance band of controlling parameters. The tolerance for dross-free cutting will depend primarily on the material thickness and the cutting power employed. The process has a dross-free cutting "window," above and below which the dross will be formed at a particular cutting power. Low-speed dross is generally continuous and easier to remove than the high-speed variety. The tolerance of the cutting window also depends on the plasma cutting gas, oxygen and air plasma having a wider tolerance than nitrogen plasma gases.

It is always advisable to use the parameter setting recommended by the equipment manufacturer. This applies to gas pressure, flow rate, torch electrode and nozzle combinations for the cutting current used, torch to work distance, etc. The travel speed (in combination with the cutting current and arc voltage, which determine arc power) is one of the primary determining factors for cut quality. The manufacturer's recommendations can be used in combination with Table A-1 to determine optimum cutting speeds. The values for 9.5-, 12.7-, and 19-mm ($^3/_8$-, $^1/_2$-, and $^3/_4$-in.)-thick plate in Table A-1 are those found to produce the best cut quality in terms of freedom from dross and good edge squareness during Project 10-40.

6.0 METALLURGICAL FACTORS AND EDGE HARDNESS

The higher heat density of plasma cutting produces narrower heat-affected zones (HAZ) than those produced by oxyfuel cutting (Figure A-6). This significant factor is often overlooked when comparing the processes. The thickness of the plasma-cut HAZ is typically 0.5 to 1 mm (0.020 to 0.040 in.) for ferritic steels, including AASHTO M270 Grades 36, 50, and 50W (AISI A36, ASTM A572, and A588) up to about 19 mm ($^3/_4$ in.) thick. For 25-mm (1-in.)-thick plate, the HAZ is typically 1 mm (0.040 in.) when the plate is cut under water and 1.5 mm (0.060 in.) when cut in air.

The metallurgical properties of the plasma-cut edge will depend on the prior chemical composition of the plate material and the thermal history resulting from the cutting oper-

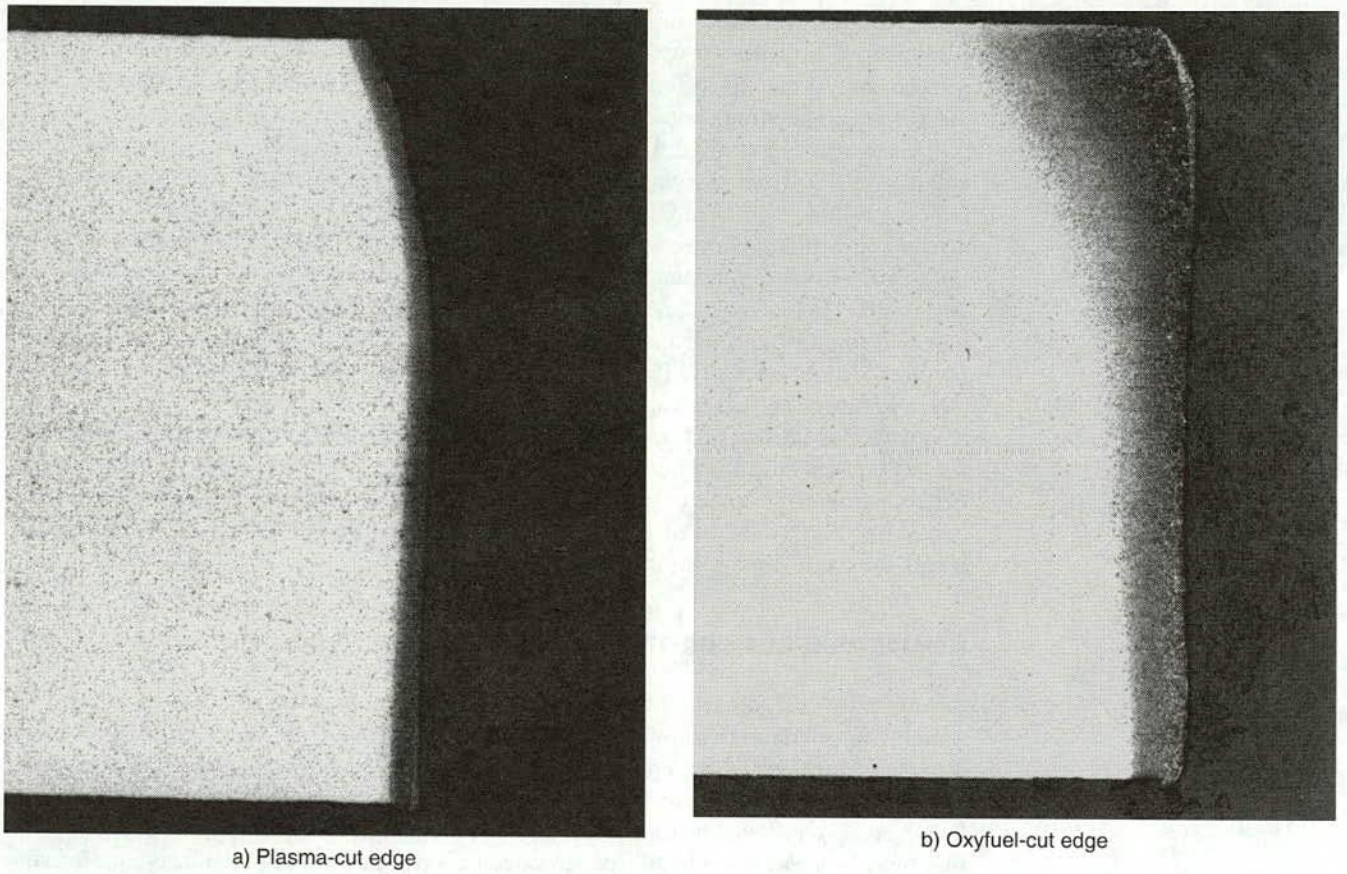

a) Plasma-cut edge

b) Oxyfuel-cut edge

Figure A-6. Macrographs of the heat-affected zones for plasma- cut ND oxyfuel gas-cut ASTM A572 structural steel 13 mm ($^1/_2$ in.) thick. Mag. ×8.

ation. The lower heat input, typical of plasma arc cutting and the fact that preheat is not required, will produce a shorter thermal cycle with more rapid cooling rates. The high cooling rate increases the tendency for formation of martensite. Martensite is a micro-constituent of steel characterized by high hardness and reduced toughness compared with ferrite/pearlite mixtures and bainite. However, because a small negative volume change takes place when martensite is formed, the plate surface will typically have a beneficial compressive stress. Nitrogen in the plasma gas has a tendency to form nitrides in the steel which increase the edge hardness and reduce toughness. However, there is no effective increase in carbon content at the surface caused by the oxidation loss of iron such as that occurring in oxyfuel cutting. The iron loss at the surface of an oxyfuel-cut edge results in considerable hardening of the edge, often as high or higher than that typical for a plasma-cut edge. Both the nitriding and martensite formation in plasma cutting and the effective increase in carbon content in oxyfuel cutting can result in hardness levels of HR_c40 to 60 (400 to 700 Hv) at the immediate surface of the cut edge, but hardness drops rapidly within 0.25 to 0.5 mm (0.010 to 0.020 in.) from the edge.

Plasma cutting under water will result in a narrower HAZ, typically 0.5 mm (0.020 in.) in 12.7-mm ($^1/_2$-in.)-thick plate, and a faster drop in hardness with distance from the cut edge, due to the general cooling effect of the water on the bulk plate, but does not have a large effect on the hardness of the edge. The high temperature of the plasma is slightly outweighed by the cooling effect of the water on the cut face, producing a decrease in hardness of about HR_c3 (30 VHN) compared with cutting in air or above a water table.

Edge hardness drops rapidly with distance from the immediate face of the cut in plasma cutting, more rapidly in fact than for oxyfuel cutting. For structural steel, hardness typi-

cally drops below HR_c23 (250 Hv) within 0.5 mm (0.020 in.) of the cut face. While maximum edge hardness specifications might be useful to an extent, a number of other factors will be involved in determining the performance of the edge if it is to be subsequently welded. These will include the heat input of the welding process and the loading conditions in the region of the original cut edge. The British Bridge Welding Code BS 5700 indicates that a maximum hardness of HR_c35 (343 VHN) is acceptable for edges that will not subsequently be welded. Fatigue results in Project 10-40 indicate improved performance of as-cut edges for all PAC processes, even those with edges harder than HR_c35. This would indicate that general grinding of the edge simply to reduce hardness is not beneficial. This applies to edges that will not subsequently be welded. Because any cut edge that is fully welded will be consumed in the welding process, assuming full fusion is achieved in the joint to achieve an acceptable weld, no hardness limits shall apply to an edge that will subsequently be fully welded. However, for nitrogen plasma cutting in air on material 19-mm ($^3/_4$-in.)-thick or above, 0.5 mm (0.020 in.) should be ground from the surface of the cut edge toward porosity in the weld.

Measurement of edge hardness in Project 10-40 has shown that for Grade 36 plate, 12.7 mm ($^1/_2$ in.) thick, cut by oxygen plasma, and Grade 50W plate, 12.7-mm ($^1/_2$ in.) and 19 mm ($^3/_4$ in.) thick, cut by oxygen, air, underwater oxygen, or underwater nitrogen, the maximum edge hardness was below HR_c30 (300 VHN). Even edges that had hardnesses above HR_c35 dropped below this value 0.1 mm (0.004 in.) below the surface in most cases. The exception was the Grade 50 material, 19 mm ($^3/_4$ in.) thick, in which it was 0.3 mm (0.012 in.) before the hardness dropped below HR_c35. This shows that even for free edges, grinding would not be required in practice in many cases in spite of a HR_c35 maximum edge hardness criterion. For those edges that required grinding, removal of 0.5 mm (0.020 in.) from the edge would be adequate. Removal of visible evidence of cutting marks (striations) would be sufficient to remove this amount of material.

Oxygen plasma cutting, in air or under water, produces the lowest edge hardness. Underwater nitrogen plasma cutting is next best, followed by air plasma and nitrogen plasma cutting in air. Therefore, oxygen plasma cutting is recommended to eliminate the need for edge grinding.

7.0 WELDABILITY OF PLASMA-CUT EDGES

Plasma cutting can be used for preparation of both square and bevelled edges. In most instances, the intention will be to cut square edges—either for free edges or for edge preparation of T-butt joints that will subsequently be fillet welded. The plasma-cut mating face of the T-butted portion of the joint can be welded as-cut, and need not be ground, unless this is necessary for fit-up purposes.

The plasma arc cutting process may be used for preparation of edges for joints that are subsequently to be welded, such as groove welds. When the edges of a butt joint are to be welded using flux cored arc welding (FCAW) or submerged arc welding (SAW), the edges do not need to be ground, provided they are acceptable in terms of surface finish, and free of unacceptable notches, etc. Radiographically acceptable welds can be produced without grinding the thermal cut edge (TCE). For welds produced by lower heat input processes such as gas metal arc welding (GMAW) and shielded metal arc welding (SMAW), grinding of the TCE is recommended when the edge has been produced by nitrogen plasma cutting in air.

The best weldability is obtained by cutting with oxygen plasma, followed by air plasma and nitrogen plasma cutting. This is related to the nitriding of the cut edge and the potential for porosity from nitrogen pick-up in the weld metal from the remelted plasma-cut edge. Cutting under water improves the weldability of plate cut by nitrogen plasma cutting. Oxygen plasma cutting also has the widest tolerance of dross-free cutting speeds.

When cutting bevel angles, the cutting speed must be reduced to take account of the increase in effective thickness, compared to that for cutting a square edge in the plate thickness concerned. Bevel angles of up to 45 deg can be produced with standard torch consumables. Larger angles should be cut from the free edge rather than the plate surface for reasons of torch access.

When a plasma-cut edge is to have a single pass and/or low-heat input fillet weld made against it, as in the case of a gusset plate welded to a flange edge (where the flange edge has been plasma cut), it is recommended that the edge be ground locally where the joint is to be made, if the hardness is above HR_c35. This recommendation applies to all plasma cutting processes generating edge hardness above HR_c35 (and should also apply to all oxyfuel-cut edges). The low penetration often associated with this kind of joint will typically be confined to the hardened HAZ of the cut edge, increasing the sensitivity to hydrogen cracking; hence the greater conservatism and the requirement for grinding the edge.

Measurement of surface hardness can be carried out in the field or fabrication plant using an approved portable hardness tester. Prior to testing, the surface should be prepared locally by sanding to remove most of the striations on the cut face, presenting a flat surface for good interpretation of hardness indents. Grinding should not be used since this removes too much material from the surface to get an accurate reading of the edge hardness. Five measurements should be taken on the centerline of the cut face, the highest and lowest discarded, and an average value calculated. If the average hardness level exceeds HR_c35, the test should be repeated on another area of the cut edge. If both averages exceed HR_c35, the edge (and all similarly prepared edges) should be ground to remove 0.5 mm (0.020 in.). Grinding to remove evidence of the cut striations (marks) will be sufficient to remove this amount of material.

8.0 REPAIR OF DEFECTS IN THE CUT EDGE

The requirements for repair of defects in plasma-cut edges, and discontinuities found in the plate material following plasma cutting, shall be the same as described for oxyfuel-cut edges in Section 3.2.3, "Visual Inspection and Repair of Base Metal Cut Edges," in the Bridge Welding Code. This applies to defects in the plate revealed by the cutting process and also to the repair of any notches created by cutting errors. Grinding or welding shall be used to repair any defects according to the requirements in Table 3.1 of the Bridge Welding Code.

9.0 CAUSE AND REMEDY OF COMMON CUTTING DEFECTS

The most common type of problem is dross adherence. This is usually caused by an incorrect cutting speed or worn torch consumables (nozzle and electrode). If the consumables are in good condition, the cutting speed should be increased or decreased depending on the drag angle of the striations on the cut edge. If the striations are inclined significantly away from the direction of cutting, the speed is too high and should be decreased to resolve the dross problem. This may also be associated with an increase in the kerf angle of the cut face, and slowing the travel speed will reduce the angle. If the striations are essentially vertical when dross is present, then the speed should be increased. Table A-1 should be used as a guide for cutting speeds, and the speed appropriate for the particular cutting gas should be selected.

If the torch consumables are worn, the arc shape will be distorted or the arc attachment point on the electrode will be eccentric, resulting in adherent dross and/or a change in kerf angle on the edge of the plate. Worn consumables should be changed as soon as possible. Consumable life is largely related to the number of starts of the cutting cycle as most wear takes place at arc initiation. Electrode life will be highest for nitrogen and nitrogen water injection cutting, lower for air plasma, and lowest for oxygen plasma cutting. Electrode life is related to the oxygen content of the plasma gas and typically ranges between 300 and 400 starts for oxygen plasma cutting.

Top edge rounding on the plate edge is indicative of an excessive voltage caused by the torch-to-work distance being too large. Excessive flash of resolidified metal on the top surface around the cut indicates that the voltage is too low. These conditions are usually avoided by setting the correct standoff recommended for the plate thickness by the equipment manufacturer. Automatic voltage regulation is recommended to ensure consistent torch-to-workpiece distance, and is considered essential if underwater cutting is carried out, because the operator cannot see the working end of the torch.

10.0 INSPECTION OF CUT EDGES

Inspection of plasma-cut edges should be carried out according to the provisions in Section 3, Workmanship, of the Bridge Welding Code D1.5. The edge should be inspected for freedom from cutting defects such as notches, as specified in the Code. The top and bottom edges should be free from dross, preferably in the as-cut condition, but can be scraped or ground to remove any dross. The squareness of the edge should be within 90 ± 5 deg for good fitup, although the Bridge Welding Code does not specify tolerances for thermal cutting.

The corners and edges need not be ground for the purpose of acceptable fatigue life, or to hold paint on free as-cut edges (for edges that will be painted using an inorganic zinc or zinc-rich epoxy primer).

Edges of material 19 mm ($^3/_4$ in.) thick or greater, cut by nitrogen plasma arc cutting in air (not under water), should be ground back by 0.5 mm (0.020 in.) to avoid porosity in subsequent welding operations. This only applies to edges that will be welded.

When a plasma-cut edge is partially melted in an operation, such as welding a thinner gusset to a thicker flange, the hardness of the TCE of the flange material shall be measured as described in Section 7.0 of this guide. If the average hardness is HR_C35 or below, the edge can be welded without further preparation. If the average hardness is above HR_C35, 0.5 mm (0.020 in.) should be removed from the TCE in the region to be welded.

11.0 RECORDING OF CUTTING PROCEDURES

Cutting procedures should be recorded in a manner equivalent to that used for welding procedures. The principle is that recording and subsequent use of parameters producing good cut quality will enable routine production of consistently high quality. The combination of cutting power and material thickness is important, so procedures should be developed for each thickness in common use. The following is a proposed format for the cutting procedure sheet (CPS) or cutting record sheet (CRS):

Material Type/Grade
Material Thickness

Plasma Cutting Type
Equipment Manufacturer (CRS only)
Cutting Machine (if applicable) (CRS only)
Manual, Mechanized, or Automated (CNC)

Plasma Gas Type, Pressure, and Flow Rate
Shielding Gas Type, Pressure, and Flow Rate
Cutting in Air or Under Water

Cutting Current (A)
Operating Voltage (V)
Cutting Travel Speed (mm/min)

Nozzle Orifice Size
Electrode Type
Torch-to-Work Distance
Torch Angle (if beveling)

APPENDIX A-1

TERMS AND DEFINITIONS ASSOCIATED WITH PLASMA CUTTING

KEY TO FIGURE A-1-1
(Terms and definitions associated with plasma cutting.)

Keyhole:	Describes the method of forming a cut. The plasma jet penetrates the full thickness of the plate as in plasma welding, but in the case of plasma cutting, the molten metal is blown out by the high flow rate of gas, thus forming a slot as the torch is traversed across the plate.
Kerf:	The gap or cut produced in the plate, the space between the left- and right-hand edges of the cut.
Kerf Angle:	The angle of deviation from the vertical, between the cut face and the surface of the plate nearest to the cutting torch.
Nozzle:	The nozzle contains the orifice through which the arc passes, causing the arc current to be confined to a small cross section. It produces a well-collimated, intensely hot stream of ionized gas.
Production Part:	The profiled component, either a simple geometric or a more complex shape.
Dross:	The resolidified material usually adhering to the bottom edge of the cut, or occasionally to the face of the cut edge (also called slag).

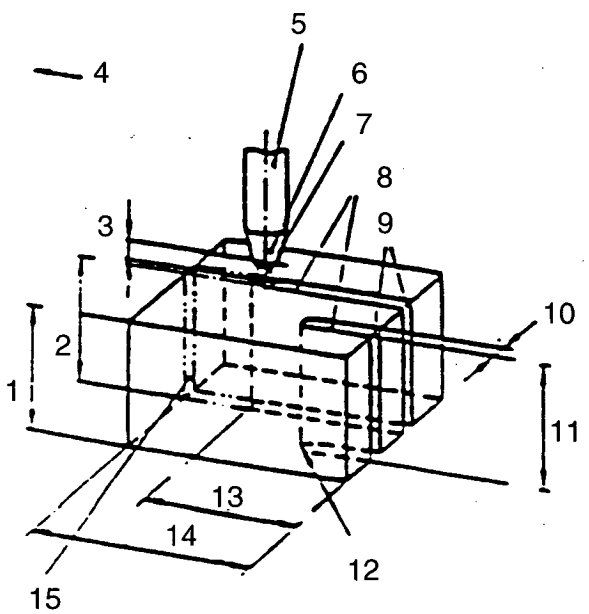

Figure A

Terms on Started Workpiece

1. Workpiece thickness
2. Cutting thickness
3. Nozzle distance
4. Cutting direction
5. Torch
6. Nozzle
7. Cutting jet
8. Cut gap
9. Starting cut
10. Cut gap width
11. Cut thickness
12. End of cut
13. Cut length
14. Cutting length
15. Cutting end

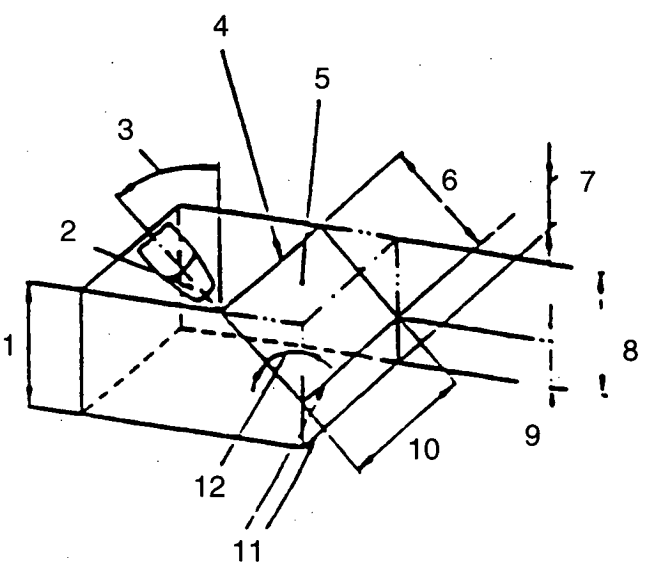

Figure B

Terms on Finished Workpiece

1. Workpiece thickness
2. Nozzle
3. Nozzle setting angle
4. Cut top edge
5. Cut surface
6. Cut thickness
7. Web height
8. Cutting thickness
9. Cut thickness
10. Cut length
11. Cut bottom edge
12. Cut flank angle

Figure A-1-1. Terms and definitions associated with plasma cutting.

APPENDIXES B THROUGH G

UNPUBLISHED MATERIAL

Appendixes B through G contained in the research agency's final report are not published herein. For a limited time, copies of that report, entitled, "Plasma Arc Cutting of Bridge Steels—Appendices B–G," will be available on a loan basis or for purchase ($9.00) on request to NCHRP, Transportation Research Board, Box 289, Washington, D.C., 20055. The available appendixes are titled as follows:

Appendix B: References Used in Literature Review
Appendix C: Survey Forms for Plasma Arc Cutting
Appendix D: Residual Stress Measurements
Appendix E: Fatigue Test Results
Appendix F: Charpy Impact Test Results
Appendix G: Tensile Test Results

THE TRANSPORTATION RESEARCH BOARD is a unit of the National Research Council, which serves the National Academy of Sciences and the National Academy of Engineering. It evolved in 1974 from the Highway Research Board, which was established in 1920. The TRB incorporates all former HRB activities and also performs additional functions under a broader scope involving all modes of transportation and the interactions of transportation with society. The Board's purpose is to stimulate research concerning the nature and performance of transportation systems, to disseminate the information that the research produces, and to encourage the application of appropriate research findings. The Board's program is carried out by more than 400 committees, task forces, and panels composed of more than 4,000 administrators, engineers, social scientists, attorneys, educators, and others concerned with transportation; they serve without compensation. The program is supported by state transportation and highway departments, the modal administrations of the U.S. Department of Transportation, and other organizations and individuals interested in the development of transportation.

The National Academy of Sciences is a private, nonprofit, self-perpetuating society of distinguished scholars engaged in scientific and engineering research, dedicated to the furtherance of science and technology and to their use for the general welfare. Upon the authority of the charter granted to it by the Congress in 1863, the Academy has a mandate that requires it to advise the federal government on scientific and technical matters. Dr. Bruce M. Alberts is president of the National Academy of Sciences.

The National Academy of Engineering was established in 1964, under the charter of the National Academy of Sciences, as a parallel organization of outstanding engineers. It is autonomous in its administration and in the selection of its members, sharing with the National Academy of Sciences the responsibility for advising the federal government. The National Academy of Engineering also sponsors engineering programs aimed at meeting national needs, encourages education and research, and recognizes the superior achievements of engineers. Dr. William A. Wulf is interim president of the National Academy of Engineering.

The Institute of Medicine was established in 1970 by the National Academy of Sciences to secure the services of eminent members of appropriate professions in the examination of policy matters pertaining to the health of the public. The Institute acts under the responsibility given to the National Academy of Sciences by its congressional charter to be an adviser to the federal government and, upon its own initiative, to identify issues of medical care, research, and education. Dr. Kenneth I. Shine is president of the Institute of Medicine.

The National Research Council was organized by the National Academy of Sciences in 1916 to associate the broad community of science and technology with the Academy's purpose of furthering knowledge and advising the federal government. Functioning in accordance with general policies determined by the Academy, the Council has become the principal operating agency of both the National Academy of Sciences and the National Academy of Engineering in providing services to the government, the public, and the scientific and engineering communities. The Council is administered jointly by both Academies and the Institute of Medicine. Dr. Bruce M. Alberts and Dr. William A. Wulf are chairman and interim vice chairman, respectively, of the National Research Council.

Abbreviations used without definitions in TRB publications:

AASHO	American Association of State Highway Officials
AASHTO	American Association of State Highway and Transportation Officials
ASCE	American Society of Civil Engineers
ASME	American Society of Mechanical Engineers
ASTM	American Society for Testing and Materials
FAA	Federal Aviation Administration
FHWA	Federal Highway Administration
FRA	Federal Railroad Administration
FTA	Federal Transit Administration
IEEE	Institute of Electrical and Electronics Engineers
ITE	Institute of Transportation Engineers
NCHRP	National Cooperative Highway Research Program
NCTRP	National Cooperative Transit Research and Development Program
NHTSA	National Highway Traffic Safety Administration
SAE	Society of Automotive Engineers
TCRP	Transit Cooperative Research Program
TRB	Transportation Research Board
U.S.DOT	United States Department of Transportation

TRANSPORTATION RESEARCH BOARD
National Research Council
2101 Constitution Avenue, N.W.
Washington, D.C. 20418

ADDRESS CORRECTION REQUESTED

000021-05
Robert M Smith
Research & Asst Matls Engr
Idaho DOT
P O Box 7129
Boise ID 83707-1129